

2-2021

## **REUSE OF SEWAGE SLUDGE ASH IN PRODUCING SELF COMPACTING CONCRETE**

Siham Saed (Moh'd Saeed) Al Shanti

United Arab Emirates University

College of Engineering

Department of Civil and Environmental Engineering

REUSE OF SEWAGE SLUDGE ASH IN PRODUCING SELF  
COMPACTING CONCRETE

Siham Saed (Moh'd Saeed) Al Shanti

This thesis is submitted in partial fulfilment of the requirements for the degree of  
Master of Science in Civil Engineering

Under the Supervision of Professor Amr S. El-Dieb

February 2021

### Declaration of Original Work

I, Siham Saed (Moh'd Saeed) Al Shanti, the undersigned, a graduate student at the United Arab Emirates University (UAEU), and the author of this thesis entitled "*Reuse of Sewage Sludge Ash in Producing Self Compacting Concrete*", hereby, solemnly declare that this thesis is my own original research work that has been done and prepared by me under the supervision of Professor Amr S. El-Dieb, in the College of Engineering at UAEU. This work has not previously been presented or published, or formed the basis for the award of any academic degree, diploma or a similar title at this or any other university. Any materials borrowed from other sources (whether published or unpublished) and relied upon or included in my thesis have been properly cited and acknowledged in accordance with appropriate academic conventions. I further declare that there is no potential conflict of interest with respect to the research, data collection, authorship, presentation and/or publication of this thesis.

Student's Signature: \_\_\_\_\_

*Siham*

Date: April 14, 2021

Copyright © 2021 Siham Saed (Moh'd Saeed) Al Shanti  
All Rights Reserved

## **Advisory Committee**

1) Advisor: Amr S. El-Dieb

Title: Professor

Department of Civil and Environmental Engineering

College of Engineering

2) Co-advisor: Munjed Maraqa

Title: Professor

Department of Civil and Environmental Engineering

College of Engineering

## Approval of the Master Thesis

This Master Thesis is approved by the following Examining Committee Members:


- 1) Advisor (Committee Chair): Amr S. El-Dieb

Title: Professor

Department of Civil and Environmental Engineering

College of Engineering

Signature \_\_\_\_\_



Date April 14, 2021

- 2) Member: Hilal El-Hassan

Title: Associate Professor

Department of Civil and Environmental Engineering

College of Engineering

Signature \_\_\_\_\_



Date April 14, 2021

- 3) Member (External Examiner): Mohamed T. Bassuoni

Title: Professor

Department of Civil Engineering

Institution: University of Manitoba, Winnipeg R3T 5V6, Canada

on behalf of external examiner

Signature \_\_\_\_\_



Date April 14, 2020

This Master Thesis is accepted by:

Dean of the College of Engineering: Professor James Klausner

Signature James F. Klausner Date 26/5/2021

Dean of the College of Graduate Studies: Professor Ali Al-Marzouqi

Signature Ali Hassan Date 26/5/2021

Copy \_\_\_\_ of \_\_\_\_

## Abstract

Rapid growth of self-compacting concrete (SCC) marks a significant milestone in enhancing the product quality and effectiveness of the construction industry. This special type of concrete is known for its high flowability characteristics and surface finish without the tendency for segregation. To achieve the desired properties, the production of SCC requires high powder content, i.e. higher cement content. Cement production is considered to be an extreme energy intensive process; which is responsible for the emissions of a greenhouse gas such as carbon dioxide (CO<sub>2</sub>). Recently, due to the current innovations and development worldwide, the rate of producing solid waste has increased considerably. Therefore, examining the potential applications for recycling and reusing such waste is a significant step towards sustainable development. Incorporation of solid by-products materials, produced by thermal power plants and metallurgical industries, as partial replacement of Portland cement, played a major role in enhancing the properties of SCC, besides it reduces the cost and heat of hydration. The main aim of this study is to investigate the viability of utilizing sewage sludge ash (SSA) produced from wastewater treatment plants (WWTP) in the mixture composition of SCC. These ashes can lead to serious economic and environmental issues, hence their utilization in the construction sector will be of great benefit in mitigating their negative impact, and will help in reducing the cement content in the SCC, thereby reducing its environmental footprint. This research includes a series of experimental procedures divided into two phases; in the first phase it is essential to burn the organic compounds that comprise a large fraction of the raw sewage sludge. Therefore, the raw sludge was incinerated at different temperatures and for different burning periods, resulting in a powder material what is known as SSA. The morphology, chemical and mineral composition of the produced material of the produced ash were evaluated using scanning electron microscopy (SEM), X-ray fluorescence (XRF), and X-ray diffraction (XRD). Moreover, strength activity index and Frattini tests were conducted to assess the pozzolanic activities of the produced ash. In addition to the effect of SSA as replacement of OPC in terms of workability, workability retention, pore size distribution, and heat of hydration were assessed. In the second phase, SSA was used as a partial replacement of ordinary Portland cement (OPC) at different ratios (0%, 20%, and 40%) to produce SCC



mixtures. Fresh concrete properties, hardened concrete properties, and durability characteristics of the produced SCC were examined. It was concluded that SSA can be used to successfully produce SCC mixtures with minor modification in the mix design to achieve satisfactory fresh properties. SCC mixtures obtained by reusing SSA as OPC replacement exhibited considerable strength gain with age and represented a comparable durability characteristics to control mix. SSA is a promising addition considering its feasibility in producing SCC with acceptable fresh and hardened properties and potential environmental benefits.

**Keywords:** Self-compacting concrete, sewage sludge ash, characterization, durability, recycling.

## Title and Abstract (in Arabic)

### إعادة استخدام رماد حمأة الصرف الصحي في إنتاج الخرسانة المضغوطة ذاتياً

#### الملخص

يمثل النمو السريع للخرسانة ذاتية الدمك (SCC) علامة بارزة في تعزيز جودة المنتج وفعالية صناعة البناء. يُعرف هذا النوع الخاص من الخرسانة بخصائصه العالية في الانسيابية والتشطيب السطحي دون الميل إلى الانفصال الحبيبي. في الآونة الأخيرة، بسبب الابتكارات والتطورات الحالية في جميع أنحاء العالم، ارتفع معدل إنتاج النفايات الصلبة بشكل كبير. لذلك، يعد فحص التطبيقات المحتملة لإعادة التدوير وإعادة استخدام هذه النفايات خطوة مهمة نحو التنمية المستدامة. كان لدمج المواد الثانوية الصلبة، التي تنتجها محطات الطاقة الحرارية والصناعات المعدنية، كبديل جزئي للأسمنت البورتلاندي، دوراً رئيسياً في تعزيز خصائص الخرسانة ذاتية الدمك، إلى جانب تقليل التكلفة وحرارة التفاعل. الهدف الرئيسي من هذه الدراسة هو التحقق من جدوى استخدام رماد حمأة الصرف الصحي (SSA) الناتج من محطات معالجة مياه الصرف الصحي (WWTP) في تركيبة الخليط من الخرسانة ذاتية الدمك. يمكن أن يؤدي هذا الرماد إلى مشاكل اقتصادية وبيئية خطيرة، وبالتالي فإن توظيفهم في قطاع البناء سيكون ذا فائدة كبيرة في التخفيف من أثارها السلبية. يتضمن هذا البحث سلسلة من الاختبارات المعملية مقسمة إلى مرحلتين؛ في المرحلة الأولى، من الضروري حرق المركبات العضوية التي تشكل جزءاً كبيراً من حمأة الصرف الصحي الخام. لذلك، سيتم حرق الحمأة الخام في درجات حرارة مختلفة ولفترات حرق مختلفة، مما نتج عنه مادة مسحوقية تعرف باسم SSA. تم تقييم التركيب البنائي والكيميائي والمعدني للمواد المنتجة من الرماد الناتج باستخدام الفحص المجهر الإلكتروني (SEM) وفلورة الأشعة السينية (XRF) وانحراف الأشعة السينية (XRD). علاوة على ذلك، تم إجراء اختبارات مؤشر نشاط القوة واختبارات فراتيني لتقييم الأنشطة البوزولانية للرماد المنتج. بالإضافة إلى تأثير رماد حمأة الصرف الصحي كبديل للأسمنت البورتلاندي من حيث قابلية التشغيل، واستبقاء قابلية التشغيل، وتوزيع حجم المسام، وحرارة التفاعل. في المرحلة الثانية، تم استخدامه كبديل جزئي للأسمنت البورتلاندي العادي (OPC) بنسب مختلفة لإنتاج خلطات الخرسانة ذاتية الدمك. وتم فحص خصائص الخرسانة الطازجة وخصائص الخرسانة الصلبة وخصائص التحمل مع الزمن الخاصة بالخرسانة ذاتية الدمك. وقد تم التوصل إلى أنه يمكن استخدام رماد حمأة الصرف الصحي لإنتاج خلطات الخرسانة ذاتية الدمك بنجاح مع تعديل طفيف

في تصميم الخلطات لتحقيق خصائص جديدة مرضية. بالإضافة، أظهر استبدال الاسمنت البورتلندي برماد حمأة الصرف الصحي زيادة كبيرة في القوة مع تقدم العمر وكذلك التحمل مع الزمن. ان رماد حمأة الصرف الصحي قد لا تكون من المواد التقليدية المستخدمة في إنتاج الخرسانة ولكنها تعتبر إضافة واعدة مع الأخذ في الاعتبار جودة الخرسانة المنتجة والتي تتميز بخصائص طازجة و متصلة محسنة بالإضافة إلى الفوائد البيئية التابعة لها.

**مفاهيم البحث الرئيسية:** الخرسانة المضغوطة ذاتيا، رماد حمأة الصرف الصحي، التوصيف، المتانة، إعادة التدوير.

## Acknowledgements

At this important junction of my life, it is time to step back and appreciate the contributions of all those who stayed with me, supported me, inspired me and influenced me throughout this challenging yet fascinating journey. I am grateful to all supervisors, colleagues, friends and family members.

In particular, I owe my sincere gratitude and gratefulness to my thesis supervisor, Prof. Amr El Dieb, for his invaluable guidance, encouragement, support academic stimulus and generous help. It was a great privilege and honor to work and study under his guidance. I am extremely grateful for what he has offered me. Prof. Amr El Dieb helped me to clarify my goals, work smarter and communicate better. I will always remember his encouragement “try, ask and learn”. From Prof. Amr El Dieb, I learnt, not only the knowledge of concrete technology, but also the scientific approach and the dedicating spirit for work. He has always infused me with enthusiasm for researching and open mind for different cultures and opinions. Without his incredibly valuable input and constant feedback this project would not have been achievable.

I also would like to thank my co-supervisor Prof. Munjed Maraqa for his time and constructive suggestions. Prof. Munjed Maraqa taught me the methodology to carry out research and to present the research work as clearly as possible. I am very grateful for his critical reviews and continuous feedback.

I would also like to express my sincere thanks to Dr. Hilal El Hassan and Prof. Mohamed T. Bassuoni for their effort as members of my thesis examination committee.

There would never be enough words to appreciate and show gratitude to the contributions of my parents in my well-being and success. I would like to thank my mother for being there for me no matter where I am, for all unconditional support and patience. I would also like to present my sincere thankfulness to my father for being my role model and playing a major role in the path that I have chosen for my future. I would like to express my parents my deepest gratitude for believing in me, sharing their life experience with me, and helping me to overcome the obstacles I have faced. I am truly thankful for their blessing which have always been the source of my motivation in achieving my success in my life.

Particular thanks are due to Eng. Abdelrahman Alsallamin, Eng. Salem Hegazy, and Mr. Faisal Abdulwahab from the civil engineering laboratory at the UAE University, for their help and support throughout the experimental program of this study. I would like to thank them for the friendly environment they have create or me.

Special thanks to my sisters, and auntie for listening, understanding, offering me advices, and supporting me through this entire process. The list of my gratitude cannot be completed without the mention of my friend, and colleague, Eng. Tasneem Bakri who provided stimulating discussions as well as happy distractions to rest my mind outside of my research. I would like to thank her for motivating me towards my MSc. degree, supporting me, and being there all of the time.

This work was financially supported by the UAEU-UPAR2 Research Grant #31N377. Also, the provision of sewage sludge ash for the study by Al Saad WWTP (Abu Dhabi, UAE) is highly appreciated.

As an ACI Middle East Fellowship recipient 2020-2021, I owe my sincere gratitude to the American Concrete Institute (ACI), for their generous financial

assistance. Also, I would like to express my appreciation for the American Society for Testing Materials (ASTM) for offering me ASTM International Project Grant 2019.

## Dedication

*To my advisor, Prof. Amr El Dieb,  
To my Mom, and Dad,  
My family and friends,  
Without whom none of my success would be possible*

## Table of Contents

Title.....	i
Declaration of Original Work.....	ii
Copyright.....	iii
Advisory Committee.....	iv
Approval of the Master Thesis .....	v
Abstract.....	vii
Title and Abstract (in Arabic).....	ix
Acknowledgements .....	xi
Dedication.....	xiv
Table of Contents.....	xv
List of Tables .....	xviii
List of Figures.....	xx
List of Abbreviations .....	xxiii
Chapter 1: Introduction.....	1
1.1 Statement of the Problem.....	1
1.2 Goals and Objectives.....	2
1.3 Methodology and Approach.....	3
1.4 Research Questions .....	3
1.5 Thesis Structure.....	3
Chapter 2: Literature Review .....	5
2.1 Introduction .....	5
2.2 Self-Compacting Concrete .....	5
2.2.1 Background .....	5
2.2.2 Advantages and Disadvantages.....	7
2.2.3 Mix Design Principle .....	8
2.2.4 Mix Design Proportions .....	9
2.3 Supplementary Cementing Materials.....	17
2.4 Studies on Self-Compacting Concrete with Different SCMs .....	22
2.5 Sewage Sludge Ash.....	44
2.5.1 Sewage Sludge Ash Characterization .....	48
2.5.2 Sewage Sludge Ash in Construction Industry.....	59
2.6 Research Significance .....	73
Chapter 3: Investigation Program.....	75
3.1 Materials.....	76
3.1.1 Aggregate .....	76



3.1.2 Cement .....	78
3.1.3 Water .....	79
3.1.4 Sewage Sludge Ash.....	79
3.1.5 Admixtures .....	81
3.2 Methods.....	82
3.2.1 Phase 1: Characterization of SSA .....	82
3.2.2 Phase 2: Reusing Sewage Sludge Ash to Produce SCC .....	94
3.3 Performance Index Approach .....	115
3.3.1 Tests Used for the Performance Index Evaluation in Phase 1 .....	117
3.3.2 Tests Used for the Performance Index Evaluation in Phase 2 .....	118
Chapter 4 : Results and Discussion - Phase 1 : Characterization of SSA .....	119
4.1 Introduction .....	119
4.2 X-Ray Fluorescence (XRF).....	119
4.3 X-Ray Diffraction (XRD) .....	122
4.4 Scanning Electron Microscopy (SEM) .....	126
4.5 Particle Size Analyzer .....	132
4.6 Pozzolanic Activity .....	135
4.6.1 Frattini Test .....	135
4.6.2 Strength Activity Index (SAI).....	138
4.7 Workability and Workability Retention.....	141
4.8 Mercury Intrusion Prosimetry (MIP) .....	143
4.9 Heat of Hydration.....	145
4.10 Toxicity Characteristic Leaching Procedure (TCLP) .....	147
4.11 PI for SSA Selection .....	150
4.12 Concluding Remarks.....	153
Chapter 5: Results and Discussion – Phase 2 : Reusing Sewage Sludge Ash in Producing SCC .....	156
5.1 Introduction .....	156
5.2 Fresh Concrete Tests .....	156
5.2.1 Slump Flow .....	157
5.2.2 J-Ring Test .....	160
5.2.3 V-Funnel Test.....	162
5.2.4 Concluding Remarks .....	164
5.3 Hardened Concrete Properties.....	165
5.3.1 Compressive Strength .....	166
5.3.2 Pore Size Distribution .....	169
5.3.3 Bulk Electrical Resistivity.....	171
5.3.4 Initial Rate of Absorption.....	174
5.3.5 Permeable Pore Percentage .....	176
5.3.6 Water Permeability.....	177
5.3.7 Drying Shrinkage .....	178
5.4 Performance Index for SCC mixtures .....	180

5.5 Concluding Remarks .....	184
Chapter 6: Conclusions and Recommendations .....	188
6.1 General .....	188
6.2 Conclusions .....	189
6.2.1 Sewage Sludge Ash (SSA) Characteristics .....	189
6.2.2 Fresh Concrete Properties .....	191
6.2.3 Hardened Concrete Properties.....	193
6.3 Recommendations .....	196
References .....	197
List of Publications .....	218

## List of Tables

Table 1: Characteristics of commonly used mineral admixtures for concrete.....	19
Table 2: SCC incorporating MK mixture design proportions.....	29
Table 3: The mixture ingredients and proportions of SCC incorporating QLP in kg/m <sup>3</sup> .....	35
Table 4: SCC mixture design with high volume replacement binary, ternary, and quaternary.....	43
Table 5: The physical properties of SSA reported in the literature. ....	50
Table 6: Typical values of oxides and elements present in SSA .....	54
Table 7: Recommended maximum aggregate size.....	77
Table 8: Aggregate sieve analysis.....	78
Table 9: Chemical composition of OPC .....	79
Table 10: Incineration temperature and time for sewage sludge samples .....	80
Table 11: Typical properties of chemical admixtures as obtained from supplier .....	82
Table 12: Mixture design of SCC .....	97
Table 13: SCC fresh properties .....	100
Table 14: Corrosion protection based on concrete resistivity .....	108
Table 15: Typical sorptivity values for concrete obtained by Hall (1977) .....	109
Table 16: XRF analysis for SSA samples .....	121
Table 17: Classification of pozzolans according to ASTM C618 .....	122
Table 18: Particle size analysis of SSA particles .....	134
Table 19: Compressive strength at 7 days and 28 days of curing.....	139
Table 20: Total porosity for pastes at 28 and 56 days.....	145
Table 21: Median pore diameter for pastes at 28 and 56 days .....	145
Table 22: TCLP for SSA pastes at 7 days of curing .....	149
Table 23: TCLP for SSA pastes at 28 days of curing .....	150
Table 24: Performance indices for individual criteria.....	152
Table 25: Performance indices for multifunctional criteria .....	153
Table 26: Slump flow of mixtures with SSA as cement replacement.....	158

Table 27: Classification of slump flow values .....	158
Table 28: T <sub>50</sub> results for mixtures with SSA as cement replacement.....	160
Table 29: J-ring diameter values and passing ability of mixtures with SSA as cement replacement.....	161
Table 30: Viscosity classes .....	163
Table 31: Recorded V-funnel times for mixtures with SSA as cement replacement .....	163
Table 32: COV of compressive strength values for mixtures with SSA as OPC replacement .....	168
Table 33: Average compressive strength for mixtures with SSA as OPC replacement .....	168
Table 34: Total porosity for concrete with SSA as cement replacement .....	171
Table 35: Corrosion protection classification based on concrete resistivity .....	172
Table 36: Resistivity results for mixtures with SSA as OPC replacement. ....	173
Table 37: Metal oxides concentration in OPC and SSA9-2.....	173
Table 38: Initial rate of absorption for mixtures with SSA as OPC replacement. ....	175
Table 39: Permeable pore test results for mixtures with SSA as OPC replacement. ....	177
Table 40: Water permeability test results for mixtures with SSA as OPC replacement. ....	178
Table 41: Selected SCC mixtures for different performance criteria. ....	182
Table 42: Performance indices for individual criteria.....	183
Table 43: Performance indices for multifunctional criteria .....	183
Table 44: Required performance criterion .....	183

## List of Figures

Figure 1: Correlation between strength and absorption for SCC mixtures incorporating FA .....	24
Figure 2: Relation between fly ash content and superplasticizer dosage.....	25
Figure 3: Influence of SSRS replacement on the slump and slump flow.....	27
Figure 4: Filling height, V-funnel and slump flow time for SCC mixtures .....	27
Figure 5: Graphical illustration of MK mixtures .....	30
Figure 6: The effect of NZ on the slump flow and HRWR content .....	32
Figure 7: Workability boxes for determination of self-compactability of concrete mixtures.....	36
Figure 8: Fresh properties of SCC incorporating VP.....	37
Figure 9: Mechanical behavior of SCC mixtures using binary and ternary blends.....	41
Figure 10: Durability characteristics of SCC mixtures using binary and ternary blends.....	42
Figure 11: Deicing salt surface scaling after 50 freezing–thawing cycles.....	44
Figure 12: Conventional sludge treatment procedures .....	47
Figure 13: Particle size distributions.....	52
Figure 14: SEM of SSA sintered at different temperatures .....	57
Figure 15: Pozzolanic reactivity of SSA, FSSA, and PFA .....	58
Figure 16: Ternary plot of SiO <sub>2</sub> , Al <sub>2</sub> O <sub>3</sub> and CaO contents for SSA .....	59
Figure 17: 28-day compressive strengths of mortar test specimens .....	62
Figure 18: Effect of grinding time of SSA.....	63
Figure 19: Relationships between compressive strength and particle sizes for 20% ash–cement mortar.....	65
Figure 20: Drying shrinkage values of mortars containing different amounts of PFA, SSA and FSSA in the binder .....	66
Figure 21: SEM micrographs of the eco-cement clinkers with the addition of different percentages of sewage sludge in the raw meals .....	72
Figure 22: Structure of the experimental program.....	76
Figure 23: Aggregates used in the SCC mixture design .....	78
Figure 24: Incinerated SSA particles before grinding.....	80

Figure 25: SSA grinding .....	81
Figure 26: Diffraction of x-ray crystal planes.....	83
Figure 27: Flow table test.....	90
Figure 28: Isothermal Conduction Calorimetry (ICC) test apparatus .....	92
Figure 29: TCLP test procedures .....	94
Figure 30: J-Ring apparatus .....	103
Figure 31: V-funnel test .....	104
Figure 32: Compressive strength test.....	106
Figure 33: Electrical resistivity test setup .....	108
Figure 34: Sorptivity test.....	111
Figure 35: Drying shrinkage test setup .....	115
Figure 36: XRD patterns for SSA incinerated for 2 hours.....	123
Figure 37: XRD patterns for SSA incinerated for 4 hours.....	124
Figure 38: XRD patterns for SSA incinerated for 6 hours.....	125
Figure 39: SEM images for SSA (X1000).....	127
Figure 40: EDS analysis for SSA particles .....	128
Figure 41: Particle size analyzer for SSA particles.....	135
Figure 42: Frattini test for SSA particles .....	137
Figure 43: Percentage of CaO removal at 28 days of curing.....	138
Figure 44: Strength activity index at 7 days and 28 days.....	140
Figure 45: Workability and workability retention for SSA pastes .....	142
Figure 46: Pore size distribution for pastes containing SSA9-2 at 28 and 56 days .....	144
Figure 47: The effect of SSA on the heat of hydration.....	147
Figure 48: Slump flow results of mixtures with SSA as cement replacement .....	159
Figure 49: Flowability behavior for produced SCC mixtures.....	159
Figure 50: Passing ability of mixtures with SSA as cement replacement .....	161
Figure 51: J-Ring test for SCC mixtures.....	162
Figure 52: V-funnel time for mixtures with SSA as cement replacement .....	164
Figure 53: Compressive strength for mixtures with SSA as OPC replacement .....	169
Figure 54: Percentage gain in compressive strength.....	169
Figure 55: Pore size distribution of concrete mixtures with SSA as cement replacement. ....	171

Figure 56: Bulk resistivity for mixtures with SSA as OPC replacement .....	174
Figure 57: Initial rate of absorption for mixtures with SSA as OPC replacement .....	176
Figure 58: Drying shrinkage strain for mixtures with SSA as OPC replacement .....	180

## List of Abbreviations

A	Cross Sectional Area / Unconfined Compressive Strength of Mortars Specimens Including SSA
ACI	American Concrete Institute
ASTM	American Society for Testing Materials
B	Unconfined Compressive Strength of Control Mortars Specimens
C <sub>2</sub> S	Dicalcium Silicate
C <sub>3</sub> A	Tricalcium Aluminate
C <sub>3</sub> S	Tricalcium Silicate
CH	Calcium Hydroxide
C <sub>i</sub>	Weight Ranking
CO <sub>2</sub>	Carbon Dioxide
COV	Coefficient of Variation
C-S-H	Calcium Silicate Hydrates
CVC	Conventionally Vibrated Concrete
d	Spacing Between the Crystals Planes of a Given Sample
EDTA	Ethylene Diamine Tetra Acetic Acid
EDXA	Energy Dispersive X-ray Analyzer
EFNARC	European Federation of National Associations Representing for Concrete
FA	Fly Ash
F <sub>c</sub>	Compressive Strength
FTS	Flow Table Spread
GGBS	Ground Granulated Blast Furnace Slag



H	Pressure Head
HCL	Hydrochloric Acid
HPC	High Performance Concrete
HRWRA	High Range Water Reducer Admixture
i	Penetration Depth
K	Coefficient of Permeability
L	Length of the Specimen
LP	Limestone Powder
L <sub>14</sub>	Length of the Prism at 14 Days of Age
L <sub>f</sub>	Length of the Prism at Test Day
LF	Limestone Filler
L <sub>0</sub>	Initial Length of the Prism
LOI	Loss on Ignition
MIP	Mercury Intrusion Porosimetry
NZ	Natural Zeolite
OH <sup>-</sup>	Hydroxide Ions
OPC	Ordinary Portland Cement
P	Maximum Compressive Load
PI	Performance Index
Q	Flow Rate of Water
QLP	Quarry Limestone Powder
RH	Relative Humidity
R <sub>i</sub>	Numeric Index
RSS	Raw Sewage Sludge

s	Rate or Absorption
SAI	Strength Activity Index
SCC	Self-Compacting Concrete
SCM	Supplementary Cementing Materials
SEM	Scanning Electron Microscopy
SF	Silica Fume
SP	Superplasticizer
SSA	Sewage Sludge Ash
SSRS	Stainless Steel Reducing Slag
t	Time
TCLP	Toxicity Characteristic Leaching Procedure
$T_v$	V-funnel Time
V	Volume Collected at a Specified Time
VF	Viscosity Classes for V-funnel Time
VMA	Viscosity Enhancing Admixtures
VS	Viscosity Classes for $T_{50}$ cm Time
w/b	Water to Binder Ratio
W/C	Water to Cement Ratio
w/cm	Water to Cementitious Material Ratio
$W_{\text{boiled}}$	Mass of the Specimen After 5 Hours Boiling in Water
$W_{\text{dry}}$	Mass of the Specimen After 24 Hours Drying in the Oven
$W_{\text{submerged}}$	Mass of the Specimen Under Water
$W_{\text{wet}}$	Mass of the Specimen After 48 Hours Immersion in Water
WWTP	Wastewater Treatment Plant

XRD	X-Ray Diffraction
XRF	X-Ray Fluorescence
Z	Impedance (Resistance)
$\gamma$	Water Density
$\Delta W$	Change in Specimen's Weight
$\Theta$	Angle Between the Incident Beam and the Normal to the Reflecting Lattice Plane
$\lambda$	Wave length of X-rays
$\rho$	Resistivity

## **Chapter 1: Introduction**

### **1.1 Statement of the Problem**

Due to the current innovations and development worldwide, the rate of producing solid waste has increased considerably. Many research studies have been directed to investigate the influence of waste materials on the environment and also on examining potential applications for recycling such waste. Improving economic, social and environmental indicators for sustainable development are attractive to the construction industry, which is a globally emerging sector, and an extremely active industry in both developed and developing countries.

Concrete is the most used building material worldwide, and several billions of cubic meters are produced annually. Several types of high performance concrete (HPC) have been developed recently. Self-compacting concrete (SCC) is a type of concrete that is able to flow and compact under its own weight, which means that it is highly flowable and can occupy spaces and form without the need for vibration (Day et al., 2005). The production of a satisfactory SCC requires a high amount of cement paste. Thus, leading to an increase in the cement production and utilization. Cement, which is a main ingredient of concrete, has been among the largest CO<sub>2</sub> emission industries. Studies showed that the manufacturing of one ton of cement generates 0.55 ton of CO<sub>2</sub> and requires 0.39 tons of CO<sub>2</sub> in fuel emissions, accounting for a total of 0.94 tons of CO<sub>2</sub> (Sadek et al., 2014).

Sewage sludge is a by-product produced from the operation of wastewater treatment plants. Sewage sludge ash (SSA) is sometimes disposed to the landfills after incineration. The final disposal of these ashes can lead to serious economic and

environmental issues, hence their utilization in the construction sector will be a great benefit in mitigating their negative impact. It is worth mentioning that the incorporation of solid by-products materials produced from several industries, as partial replacement of Portland cement, played a major role in enhancing the properties of SCC.

It should be noted that, few studies have investigated the use of SSA as cement replacement in conventional vibrated concrete, e.g. (Pinarli, 2000; Cheeseman and Viridi, 2005; Smol et al., 2015). But none of the studies has addressed the inclusion of SSA in SCC.

## **1.2 Goals and Objectives**

Studies are directed nowadays towards contributing positively to the sustainable development of the construction sector. Indeed, the construction industry is increasingly expected to play a major role in achieving the target of zero waste. The main aim of this study is to perform an exploratory examination for the SSA as a replacement of OPC in self-compacting concrete mixtures, the main objectives of this thesis were as follow:

- Investigate the effect of different incineration temperatures and time on the characteristics of the produced SSA. Therefore, it's potential to be used as a partial replacement of cement in making concrete.
- Utilize SS in producing concrete that satisfies all the requirements of SCC
- Investigate the effect of SSA on the fresh and hardened properties of SCC mixtures.

- Identify the optimal content of SSA to be used in SCC mixtures yielding desired fresh and hardened concrete properties.

### **1.3 Methodology and Approach**

To achieve the above mentioned objectives, the work was divided into two main phases. The focus of the first phase was to investigate SSA feasibility to be used as a partial replacement of OPC. This was done by studying the characterization of sewage sludge ash based on different methods and procedures.

In the second phase of this thesis, SSA was used as a partial replacement of OPC at different dosages (0%, 20%, and 40%) to produce SCC. The effect of SSA on SCC mixtures was assessed through the results of several fresh concrete tests, hardened concrete tests and durability tests.

### **1.4 Research Questions**

1. The effect of different incineration temperature and duration on the characteristics of SSA.
2. The optimal incineration temperature and duration that produces SSA with a potential to be used in making concrete.
3. The feasibility of using SSA in producing SCC.
4. Performance evaluation of the produced SCC by reusing SSA as a partial replacement of OPC for different construction applications.

### **1.5 Thesis Structure**

The work done in this thesis is organized into six chapters as follows:

Chapter 1 provides a brief introduction about self-compacting concrete and the problems associated with this unique concrete type. This is followed by the research objectives, significance and organization of the thesis.

Chapter 2 presents a detailed review of the literature on various topics on self-compacting concrete. Topics include background, mix design procedure and principle, different commonly used filler materials, and the use of SSA in construction industry

Chapter 3 provides a detailed description of the material, SSA characterization, methodology, concrete design and mixing processes, along with the conducted fresh and hardened tests in this study.

Chapter 4 presents the results and discussion of sewage sludge ash characteristics.

Chapter 5 presents all the test results of both the fresh and hardened stages and brief discussion of the expected reasons behind the observed trends.

Chapter 6 concludes the study and highlights further research needs in this area.

## **Chapter 2: Literature Review**

### **2.1 Introduction**

The main objective of this study is to examine the effect of reusing sewage sludge ash (SSA) as a partial replacement of cement in producing SCC mixtures. The fresh and hardened characteristics of the produced SCC were evaluated using typical concrete tests. The coming subsections summarize the history, design procedure of SCC, former cement replacement materials used in the literature, and studies on reusing SSA in the construction industry.

### **2.2 Self-Compacting Concrete**

Self-compacting concrete (SCC), also known as self-consolidating concrete, is one of the most widely used concrete types, mainly because of flowability characteristics and strength. Self-compacting concrete (SCC) is defined as a high performance concrete type with a low viscosity and a very high resistance to segregation and bleeding (Day et al., 2005). This type of concrete compacts using its own weight without the need of any kind of mechanical vibration when casting. SCC has several advantages compared to the normal conventional concrete. For that reason, it is considered as an innovative development in the construction field. SCC can flow easily into thin sections, places around closely spaced reinforcements, filling formwork without any compaction and segregation.

#### **2.2.1 Background**

Due to reduction of skilled workers in Japan, the quality of the construction works also reduced. The main identified factor responsible for poor performance of



concrete structure is the lack of uniform and good consolidation. Therefore, the establishment of SCC was connected with the desire to the greater quality concrete pursued in Japan around 1983 (Dehn et al., 2000). The lack of the available means by which full compaction of concrete in a construction site could be achieved, drove the focus of researchers to eliminate the need to compact concrete mixtures by the traditional vibration techniques. This was the primary reason of the development of the first practicable form of SCC. The idea of formulating SCC was first introduced by Prof. Okamura in 1986. However, SCC was first developed in Japan in 1988 by Prof. Ozawa at the University of Tokyo. By 1988, the concept of SCC became ready for the first real scale test (Okamura and Ouchi, 2003; Shi et al., 2015).

The first prototype of SCC was produced by using available materials in the market. The prototype satisfied all the requirements regarding hardening; drying shrinkage, heat of hydration and denseness after hardening. At the beginning, the prototype was known as 'High Performance Concrete'. Professor Aitcin defined High Performance Concrete (HPC) as a concrete with high durability due to low water-cement ratio. Prof. Okamura has modified the name for the newly invented concrete to 'self-compacting high performance concrete' in 1997.

After 1988, European countries started developing SCC. Between 1990 and 2000, researchers were attracted to study SCC and develop specifications and guidelines for producing a satisfactory SCC mix. Furthermore, the first North American Conference on design and use of SCC was organized in November 2002. It included a huge number of research studies conducted to optimize the fluidity of SCC, improve its strength and durability in a cost-effective manner.

This major innovation resulted in producing concrete that is flowable, consistent, and dense concrete with no segregation or bleeding and performing full compaction during the casting process without the need of vibration machines. SCC has more benefits compared to the traditional concrete. Due to its high flowability, it is typically adopted in casting structural members with highly congested reinforcements (Siddique and Kunal, 2015; Ashtiani et al., 2013). SCC is an innovative extension of the already existing concrete technology where generally the same materials as conventional concrete are used. The main difference between SCC and conventional concrete is the performance in their fresh stage. Large quantities of powder materials known generally as fillers or mineral admixtures are used to reduce the frequency of collision between particles and thus enhance the flowability (Siddique and Kunal, 2015).

### **2.2.2 Advantages and Disadvantages**

The production of SCC added many benefits to the construction industry worldwide for their advantages, some of which are:

1. Improves the constructability and structural integrity by flowing into complex forms and providing easier pumping procedures.
2. Reduces skilled labor needs.
3. Bond to reinforcing steel and minimizes voids on highly reinforced areas.
4. Accelerates project schedules.
5. Produces superior surface finishes.
6. Superior strength and durability.
7. Fast placement without vibration or mechanical consolidation.

8. Eliminates the noise of vibration
9. Allows for innovative architectural features.
10. Produces a wider variety of placement techniques (Malherbe, 2015).

Although SCC benefited the construction industry because of its several advantages, a few drawbacks arise with its implementation:

1. Depending upon the ingredients used, SCC mixtures could cost higher than conventional concrete. This issue made SCC mixtures only limited to applications where conventional concrete is not applicable rather than being applied in all construction applications.
2. SCC requires high fluidity in tight joint framework, which might slow down the casting rate.
3. SCC requires a low water-to-cement ratio, due to that plastic shrinkage may occur, yet this can be avoided by proper curing.
4. Using SCC in the work site elaborates testing arrangements required to ensure quality control (Malherbe, 2015).

### **2.2.3 Mix Design Principle**

High fluidity, self-compacting ability, and good segregation resistance in fresh state are notable characteristics of SCC (Corinaldesi and Moriconi, 2011). Moreover, SCC possesses most of benefits of a HPC; low porosity, high compressive strength as well as good durability (Corinaldesi and Moriconi, 2011). The main concept behind modern self-consolidating concrete is to produce a matrix with low yield value and adequate viscosity that can easily be spread without any compaction effort. Unlike conventional concrete, mixture proportion of SCC usually requires a high cement

content, low water–cement (w/c) ratio, and considerably low coarse aggregate volume. In addition, powder component and chemical admixtures are basically higher than that in conventional concrete to provide a homogeneous and cohesiveness for mixture. Indeed, high cement content and the use of chemical admixtures in mixture might increase the cost of SCC. Therefore, replacing them by industrial by-products would be a promising feasibility in construction industries, intended towards reusing waste resources instead of natural materials, reducing environment pollution, as well as enhancing economical profits. Several researchers were attracted to use industrial by-products as fillers in producing SCC. Previous studies reported that Class F fly ash (Khatib, 2008; Şahmaran et al., 2009), blast furnace slag (Boukendakdji et al., 2009), limestone powder (Uysal and Yilmaz, 2011), glass filler, silica fume, or metakaolin (Güneyisi et al., 2009; Uysal and Sumer, 2011) were effective additives to maintain the workability and deformability of SCC mixtures. The incorporation of industrial waste as alternative constituents in concrete industry will reduce the reliance on natural non-renewable ingredients, and hence lower the quick depletion rate of raw minerals. Moreover, it will add value to the by-products of other industries. The use of recycled materials will also help reduce the construction cost. Various industrial by-products have been widely used as less expensive cement substitutes and were proven to enhance the produced concrete properties, both fresh and hardened (Uysal and Yilmaz, 2011).

#### **2.2.4 Mix Design Proportions**

The proportioning of SCC is considered complex since it depends on several factors including grain size distribution, quantity and quality of aggregates, distribution of sizes of aggregates, dosage and quality of admixtures, and cement

content (Hemalatha et al., 2015). The property of SCC to completely fill a formwork and to flow through reinforcement without the need of any further vibration makes it significant to use (Parra et al., 2011). However, to achieve a high flowability of the concrete mixtures, the water-cement ratio should be increased, yet this reduces cohesiveness of the mixture. Due to this reason, segregation of aggregate takes place which results in the blockage of the flow. Due to this interparticle friction, the flowability will be restricted when SCC flows through the congested space between densely reinforced bars. Blockages can be avoided by carefully reducing the interparticle friction among coarse aggregate, sand, and fines through proper proportioning and with the proper dosage of HRWRAs and viscosity enhancing admixtures.

A simple mix design method for SCC was proposed by Su et al. (2001) and it involved nine steps: (1) calculation of coarse and fine aggregate content, (2) calculation of the cement content (for good fresh properties, the binder content should not be too low), (3) calculation of mixing water content required by cement (despite the influence of fine and coarse aggregates, proportions of the ingredients, curing age on compressive strength, the water to binder ratio has the most dominant effect), (4) calculation of binding material other than cement (increased amounts of cement will increase the cost, drying shrinkage, slump loss, and more importantly the yielded compressive strength will be higher than the required in the design), (5) calculation of the mixing water content needed in SCC, (6) calculation of superplasticizer dosage, (7) adjustment of mixing water content needed (based on the moisture content of the aggregates to be used), (8) trial mixes and tests on SCC properties, (9) adjustment of mix proportions (until the properties of the produced SCC mixtures meet with the

specified requirements of the design). Calculations were carried using Fly Ash (FA) and Ground Granular Blast-Furnace Slag (GGBS) as binding materials together with cement.

In addition, significant studies have been done in the recent past to make SCC more robust. Based on the carried research, mix design of SCC was categorized into six classes, namely empirical design method, statistical factorial design method, strength-based design method, rheology of paste method, particle packing method, and Eco-SCC mixture method (Ashish and Verma, 2019). Each method is further explained in the following sub-sections.

#### **2.2.4.1 Empirical Design Method**

The empirical design method is used for the design of SCC using a variety of concrete components. It involves coarse and fine aggregates content, water and cementitious material contents and superplasticizer dosage to determine the initial mixture proportions. Several trial mixes and adjustment are usually done as the best estimates of the mixture proportions for required properties. Okamura and Owaza (1995) developed SCC mix design method with a fixed coarse and fine aggregate content of 50% of solid coarse aggregate volume and 40% of mortar volume, respectively. The water to binder ratio was kept constant between 0.9 – 1.0 in volume, yet to achieve a specific flowability, the final water to binder ratio was determined in the presence of superplasticizer.

In 2003, Edamatsu et al. (2003) improved Okamura's method by setting a specific fine aggregate content, water to binder ratio, and dosage of superplasticizer. Domone (2009) studied the properties of SCC's mortars by using four types of

superplasticizers and different combinations of powders that included ordinary Portland cement (OPC), pulverized fuel ash, GGBS, limestone powder and silica fume. Four different types of superplasticizers (sulfonate naphthalene polymer, acrylate-methacrylate co-polymer, vinyl copolymer and modified polycarboxylic ether) were used. The proportion of sand in mortar was fixed at 0.45 by volume. The water to powder ratio varied; where it was either 0.945 or 1.26 by volume.

In addition, Domone (2009) developed the UCL method for mix of SCC, which is a simple approach of proportioning of trial mixes to tailor specific SCC requirements. In this method, the flow and V-funnel tests were used to calculate the superplasticizer dosage and water to binder ratio of the mortar.

Khaleel and Razak (2014) introduced a mix design method to obtain different properties of concrete; OPC was replaced with metakaolin at replacement levels of 5–20%. Superplasticizers and mineral additives were added to the mix to achieve the required flowability. However, the optimum replacement level of OPC by metakaolin was found to be 10% in terms of workability and compressive strength.

#### **2.2.4.2 Statistical Factorial Method**

Statistical models minimize the number of trial batches by shortening the test practice needed to optimize the mixture properties. They are usually used to identify the relative significance of primary mixture parameters and their effects on related properties of SCC.

Khayat et al. (2000) proposed a statistical factorial approach for the five key parameters including viscosity-enhancing agent (VMA), high range water reducers

(HRWR), water to binder ratio (w/b), cementitious materials content and coarse aggregate volume. Sonebi (2004) developed a factorial design method of SCC with a medium strength ranged from 10-54 MPa by partially replacing OPC with pulverized fuel ash (PFA). However, Ozbay et al. (2009) applied Taguchi method to analyze mix proportions parameters of high strength SCC ranging between 50 – 75 MPa.

Bouziani (2013) used the statistical approach method to study the effect of different types of sand on SCC's properties including river sand, crushed sand, dune sand, and crushed limestone-type gravel and marble powder (MP). Nepomuceno et al. (2012) used this method to design a SCC of binary and ternary blends of powder materials in combination of two cements and four additional fillers including limestone powder (LP), fly ash (FA), granite filler, and micro silica.

#### **2.2.4.3 Strength-Based Design Method**

Based on an overall calculation method, Li et al. (2005) developed a method named semi-empirical and semi-calculation method, which is a method to design concrete to achieve optimum compressive strength that simultaneously meets fresh state requirements of SCC. In this method, the concept of dry mortar surplus coefficient was presented and volume ratio of paste to aggregate was 35:65. Wu et al. (2009) designed a two self-compacting lightweight concrete by general calculation method with fixed fine and coarse aggregate contents of 0.52 and 0.51.

Dinakar (2012) and Dinakar and Manu (2014) recommended an efficiency concept for different percentages of FA and MK to design a SCC mixture. This methodology for SCC evaluates specific strengths for fly ash (FA) and metakaolin contents from 30–80% and 7.5-22.5% of the powder, respectively. It was reported that



with the new design method, high strengths in excess of 90 MPa and 120 MPa can be achieved when FA and metakaolin were used, respectively. In addition to FA, Dinakar et al. (2013) proposed a mix design method using GGBS for designing SCC. It was observed that at replacement levels ranging from 20% to 80%, strengths ranging from 30 to 100 MPa were achieved.

#### **2.2.4.4 Rheology of Paste Method**

In this design method, the SCC is considered as a two-phase material composed of gravel and suspending materials. The flowability of SCC mixture usually dependent on the rheological characteristics of mortar, besides, it also depends on the quantity and physical properties of the used gravel. Saak et al. (2001) proposed a design method to minimize segregation in SCC mixtures. In this study, segregation was minimized in a certain range of yield stress and viscosity, still producing self-compacting material.

The addition of fibers in SCC was proposed by Ferrara et al. (2007) to achieve SCC with good quality and performance. Deeb and Karihaloo (2013) designed two SCC mixtures with and without steel fibers, using an alternative method based on computational simulation of proportioning high and ultra-high performance SCC. In this method, no coarse aggregates were used. For self-compacting high performance concrete, in order to increase the workability, silica fume (SF) was used instead of GGBS and the superplasticizer (SP) dosage was increased. The compressive strength of mixes ranged from 35 MPa to 160 MPa. However, for self-compacting ultra-high performance concrete, a high paste to solids ratio was used.

Wu and An (2014) developed a SCC mix design with pure limestone and without cement content. This model suggested that rheological characteristics

influence the bearing force and movement conditions of gravel particles and affect the flowability and segregation resistance. The water to cement ratio and dosage of superplasticizer was altered to adjust the rheology of SCC. Cepuritis et al. (2016) focused on the sand particle characteristics such as shape, voids content and filler particle distribution to design SCC mixtures. The rheology of SCC was investigated by several experimental trials.

#### **2.2.4.5 Particle Packing Method**

Particle packing improves the density of any proposed concrete mixture. It mainly depends on a number of factors such as the shape of individual particles, surface potential of the solids, the amount of mixing water and the applied energy of compaction.

The interaction between the blocking volume ratio and clear reinforcement spacing to fraction particle diameter ratio was studied by Petersson et al. (2004) as a method to produce SCC mixtures. In this method, the concrete was considered as a solid aggregate phase in a liquid paste phase formed by powder, water and admixtures. Paste fills the voids between aggregates and provides a lubricating coat between particles.

Sedran and Larrard (1999) introduced the compressible packing model. This model optimizes the granular phase of concrete with respect to packing density. Su et al. (2001) proposed an easier SCC mix design method as compared to Japanese Ready-Mixed Concrete Association. In the developed method, the packing factor (PF) was used. The voids of the aggregate framework were filled with the cement paste to attain the required SCC properties. It was reported that the passing ability of SCC mixture

was increased due to the increase in the sand content. Also, as a result of increasing the sand content, binder quantities can be decreased; which saves cost.

Hwang and Tsai (2005) used the densified mixture design algorithm approach to design SCC mixtures. Supplementary cementing materials (SCM) such as fly ash was used to fill the voids between aggregates. Hwang and Hung (2005) used the same approach to design lightweight SCC in accordance with ACI 318 standards, and to combine aggregate packing with lubrication technique.

Brouwers and Radix (2005) introduced the lowest powder contents in their study with the combinations of three types of sands, gravel, SP and slag blended cement. It was concluded that when particles have less voids more water is available which acts as lubricant.

#### **2.2.4.6 Eco-SCC Mixture Design Method**

Eco-SCC is a developed type of sustainable concrete. In Eco-SCC, the maximum powder content is set to  $315 \text{ kg/m}^3$  that includes cement, fly ash, and silica fume and limestone filler. Also, viscosity enhancing admixture (VMA) can be applied to increase the stability/cohesiveness of SCC, thus reducing segregating and bleeding. Since the paste volume is low in Eco-SCC, it is very difficult to attain the required flowability. Therefore, the packing density of the granular skeleton should be high enough to achieve the desired flowability of SCC.

Long et al. (2015) developed sustainable SCC by understanding the interaction between mixture proportion parameters of SCC and environmental impact of SCC. The new method combined by three environmental impact indices included embodied

energy consumption index, embodied CO<sub>2</sub> emission index and embodied resource expenditure index. It was found that using three different mineral admixtures such as FA, GGBS, and limestone powder reduced the three environmental indices by reducing the cement content in SCC mixtures. In addition, Alyamac et al. (2017) consumed maximum amount of marble powder (MP) as mineral admixture in SCC. The response surface methodology and ANOVA were utilized to develop eco-efficient, eco-friendly and workable SCC.

Esmailkhanian et al. (2017) developed a design method to produce low carbon footprint Eco-SCC. The method depended on the optimization of powder composition, sand and coarse aggregates to achieve desired properties of SCC.

### **2.3 Supplementary Cementing Materials**

Unlike conventional concrete, SCC requires a high cement content, low water to cement ratio, and considerably low coarse aggregate content. In addition, powder component; according to the EFNARC (2005) guidelines the particle size of the used powders should be smaller than 0.125 mm and its desirable that 70% pass through the 0.063 mm sieve, is basically higher than conventional concrete to assure a homogeneous and cohesiveness for mixture. Due to the large amount of cement content, SCC is costly, susceptible to be attacked and produces much thermal crack. Therefore, it is necessary to replace cement with other materials. Supplementary cementing materials are often used in SCC mixtures to reduce cement contents, improve workability, increase strength and enhance durability through hydraulic or pozzolanic activity. Utilization of these byproducts in cement/concrete not only

prevents them from being land-filled but also enhances the properties of concrete in the fresh and hardened states.

Supplementary cementitious materials (SCMs) include both pozzolans and hydraulic materials. A pozzolan is defined as a siliceous or siliceous and aluminous material that in itself possesses little or no cementitious value but that will, in finely divided form and in the presence of moisture, chemically react with calcium hydroxide (a hydration product of Portland cement) at ordinary temperatures to form compounds having cementitious properties. However, other SCMs, show hydraulic behavior in that they react with water directly to form hydration products with cementitious properties. Such materials do not require Portland cement to harden and gain strength, but the chemical reactions are greatly accelerated by the presence of Portland cement.

Table 1: Characteristics of commonly used mineral admixtures for concrete (Mehta and Monteiro, 1994; Ramachandran, 1996).

SCM	Type of reaction	Origin	Chemical/Mineral Composition	Particle characteristics
Fly Ash Class C (High-Calcium Content)	Cementitious and pozzolanic reaction	Produced from burning pulverized coal in electric power generating plants	Mostly silicate glass containing calcium, magnesium, aluminum, and alkalis. The small quantity of crystalline matter present generally consists of quartz and C <sub>3</sub> A.	Powder corresponding to 10-15% particles larger than 45µm (usually 300- 400 m <sup>2</sup> /kg Blaine). Most particles are solid spheres less than 20 µm in diameter
Fly Ash Class F (Low-Calcium content)	Pozzolanic reaction	Produced from burning pulverized coal in electric power generating plants	Mostly silica glass containing aluminum, iron, and alkalis.	Powder corresponding to 15-30% particles larger than 45 µm (usually 200- 300 m <sup>2</sup> /kg Blaine). Most particles are solid spheres with average diameter 20 µm.

Table 1: Characteristics of commonly used mineral admixtures for concrete (Mehta and Monteiro, 1994; Ramachandran, 1996) (Continued).

SCM	Type of reaction	Origin	Chemical/Mineral Composition	Particle characteristics
Granulated Ground Blast Furnace Slag (GGBS)	Cementitious reaction	By-product from the blast- furnaces used to make iron	Consists essentially of silicates and alumino-silicates of calcium and other bases.	The average particle diameter of GGBS about 13 $\mu\text{m}$ (between 425 and 470 $\text{m}^2/\text{kg}$ ).
Silica fume	Very high pozzolanic reaction	A byproduct of the smelting process in the silicon and ferro-silicon industry.	Pure silica in non-crystalline form	Silica fume particles are extremely small, with more than 95% of the particles finer than 1 $\mu\text{m}$ . (between 13,000 and 30,000 $\text{m}^2/\text{kg}$ )
Metakaolin	Very high pozzolanic reaction	Dehydroxylated form of the clay mineral kaolinite.	Major constituents are silica oxide and alumina oxide. Other components include ferric oxide, calcium oxide, magnesium oxide, potassium oxide	Particles are extremely small with an average particle size of 3 $\mu\text{m}$ . (less than 30,000 $\text{m}^2/\text{kg}$ )

Many investigators have studied a wide range of artificial and natural SCM and classified them according to pozzolanic and/or cementitious characteristic, as shown in Table 1 (Mehta and Monteiro, 1994; Ramachandran, 1996).

Natural SCMs are experiencing a sort of renaissance. In the US, a new trade group started in 2017, the Natural Pozzolan Association, to represent the interests of this growing industry. Besides, several researchers reviewed emerging SCM sources as the need for new sources of SCMs has never been greater and supplies of traditional SCMs are becoming restricted.

Several natural pozzolans were studied by investigators to test their potential to be used as SCMs including pumice and perlite (Diaz-Loya et al., 2019; Ghafari et al., 2016), vitric ash (Diaz-Loya et al., 2019), and zeolite (Seraj et al., 2016, Burris and Juenger, 2016; Al-Shmaisani et al. 2018; Lv et al., 2019). Moreover, calcined sedimentary materials are considered as an excellent source of natural SCMs. Calcined kaolinite clay, or metakaolin, has a strong history of use as an SCM in concrete (Wang et al., 2018). However, the relatively pure metakaolin that is commonly used as an SCM is also costly because it has limited availability and has value for other industries. Hollanders et al. (2016) reported that illite and hectorite could be dehydroxylated by calcination, they remain inert in cementitious mixtures. On the other hand, calcined smectite, bentonite, or montmorillonite clays, can be pozzolanically reactive (Taylor-Lange et al., 2015; Hollanders et al., 2016; Wang et al., 2018; Danner et al., 2018). Furthermore, Snellings et al. (2017) proposed clay-rich dredged sediments such as ports, harbors, and waterways; which are routinely dredged, de-watered, and stockpiled. It was argued that these sediments might contain clays, so could be calcined and used as SCMs.



The availability of impure clays, their performance as SCMs, and the observed interaction of aluminosiliceous SCMs with limestone additions to form additional reaction products has resulted in the extensive development of a binder system called LC3 (limestone- calcined clay cement). The proportions of components can vary, but the most promising combination is one called LC3-50, which contains 50% clinker, 30% calcined clay, 15% limestone, and 5% gypsum (Scrivener et al., 2018).

Furthermore, by-products materials beyond fly ash and slag were investigated, such as agricultural waste ashes (Aprianti et al., 2015), ashes from biomass used for fuel (Rissanen et al., 2017), municipal waste sludge ash (Joseph et al., 2018), and waste glass (Omran et al., 2018). Different types of slag have been studied as well including steel slag (Hou et al., 2018), ferrous slags (Rahman et al., 2017), and non-ferrous slags (Edwin et al., 2016).

#### **2.4 Studies on Self-Compacting Concrete with Different SCMs**

The usage of FA as cement replacement in SCC played a major role in enhancing the performance of SCC. Thus, investigators were attracted to study the effect of incorporating high volume levels of FA in producing sustainable SCC (Atis, 2002; Xie et al., 2002; Naik et al., 2012; Khatib, 2008; Liu, 2010).

Naik et al. (2012) investigated manufacturing economical high strength SCC containing high-volumes of FA class C. A control SCC mix without the addition of FA, and three other SCC mixes contained Class C fly ash (FA) at 35%, 45%, and 55% of replacement of cement by mass were prepared. It was found that use of high-volumes of Class C fly ash in the manufacturing of SCC reduced the cost of the SCC production by significantly reducing the amount of superplasticizer and viscosity

modifying agent. Besides, by replacing 35% of cement by Class C FA, a high-strength, economical self-consolidating concrete for strength of about 62 MPa at 28 days age could be achieved. At a replacement level of 55% a strength in the range of 48–62 MPa at 28 days age could be manufactured.

In addition, Khatib (2008) studied the influence of including FA on the properties of SCC. Seven SCC mixtures were conducted with a constant w/b ratio of 0.36. Three control mixes (M1, M2, and M3) had different admixture dosages of 0.6, 0.7, and 1% (by mass of binder) respectively. In the other four mixes (M4, M5, M6, and M7), OPC was replaced with 20, 40, 60, and 80% (by mass of binder) of FA respectively with a constant admixture's dosage of 0.7% (by mass of binder). It was found that at 56 days of curing, replacing 40% of OPC with FA resulted in a strength of more than 65 N/mm<sup>2</sup> and using of up to 60% FA as OPC replacement can produce SCC with a strength as high as 40 N/mm<sup>2</sup>. High absorption values were obtained with increasing amount of FA. However, all FA concrete exhibits absorption of less than 2%. Incorporating high amounts of FA in SCC reduced the drying shrinkage. Also, at 80% FA content, the shrinkage at 56 days reduced by two third compared to the control mix. Increasing the admixture content beyond a certain level leads to a reduction in strength and an increase in absorption. As shown in Figure 1, the correlation between strength and absorption indicated that there was a sharp decrease in strength as absorption increased from 1 to 2%. After 2% absorption, the strength was reduced at a much slower rate.

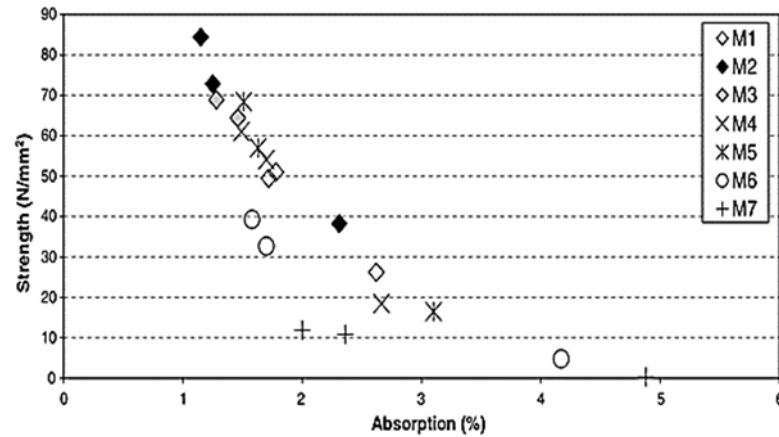


Figure 1: Correlation between strength and absorption for SCC mixtures incorporating FA (Khatib, 2008).

Liu (2010) investigated the fresh and hardened properties of SCC with levels of up to 80% cement replacement by FA. A control mix (0% of FA), and five SCC mixes included varying percentages of OPC replacement (20, 40, 60, 80, and 100%) were made. It was concluded that, all mixes showed satisfactory fresh properties. However, in order to have a constant slump flow of 742–793 mm and a V-funnel time compared to the control mix, replacing cement with FA would require an increase in the water/powder ratio and a reduction in superplasticizer dosage. Similar findings were also reported by Sukumar et al. (2008) as illustrated in Figure 2. The higher the replacement level of fly ash, the higher the reduction in compressive strength, splitting strength, and UPV values. Sorptivity of SCC mixes with up to 40% FA was similar to the control mix. However, at significantly high FA content with a replacement percentage in the range of 60–80%, the sorptivity values increased. Thus, it was reported that the optimal FA content in the mix was at 40%.

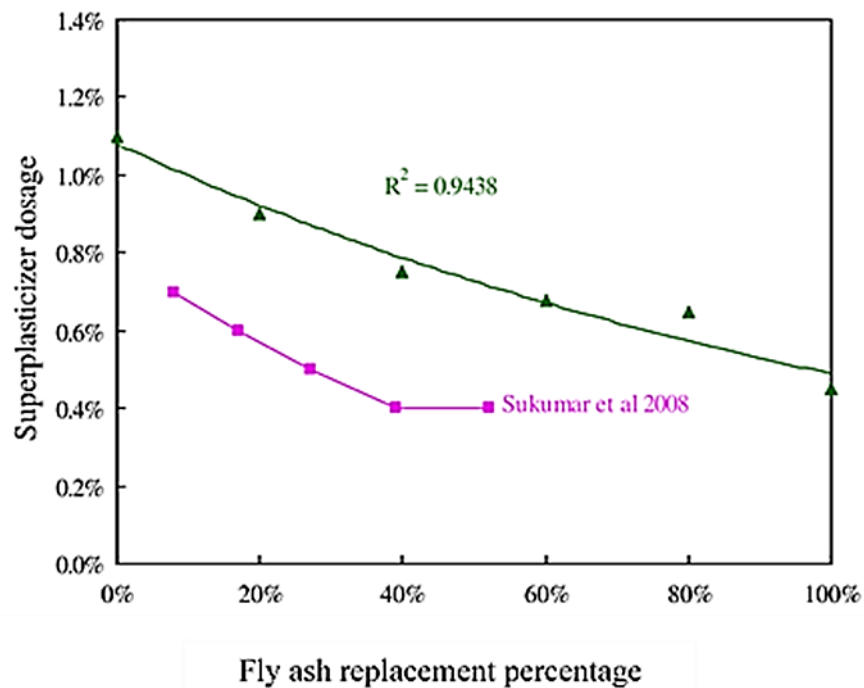


Figure 2: Relation between fly ash content and superplasticizer dosage (Liu, 2010).

In addition, researchers studied different types of slag in making SCC. Boukendakdji et al. (2009) investigated the influence of slag on the properties of fresh and hardened SCC. Five SCC mixtures have been carried out with several slag content replacement levels of 0, 10, 15, 20, and 25% by weight of cement. The binder and water content were constant at  $465 \text{ kg/m}^3$  and  $186 \text{ kg/m}^3$  respectively. Superplasticizer dosage was set at 1.6% of the total binder content. An improvement of workability was observed up to 20% of slag content with an optimum content of 15%. Workability retention of about 60 min with 15% of slag content was obtained. However, a decrease of strength with an increase of slag content was observed. Yet, this decrease of compressive strength is less important at late ages (56 and 90 days after mixing). Similar finding was also reported by Khatib and Hibbert (2005) when slag was incorporated in the conventional concrete.

Sheen et al. (2015) examined SCC mixtures made with stainless steel reducing slag (SSRS). Two types of SSRS with different surface area of 1766 cm<sup>2</sup>/g and 7970 cm<sup>2</sup>/g were used as filler and cement replacement, respectively. Six SCC mixtures were made with various replacement ratios from 0 to 50% (increment 10%) and a water/binder ratio of 0.32. As shown in Figure 3, the slump and slump flow value were found to be higher than the reference mix when the replacement ratio of OPC with SSRS was 20% or less, due to latent characteristic of the mineral admixture. Yet, beyond 20% the slump values were lower than the control mix and tended to gradually decrease as the SSRS replacing OPC increased. As for the T<sub>50</sub> cm, V-funnel time, and box-filling height, all SCC mixtures satisfied the requirement of SCC without the usage of VMA. However, from Figure 4, as the SSRS ratio increased, the V-funnel time was longer and the filling height decreased, indicating a reduction of viscosity, passing ability through densely congested reinforcements and setting time. It was clearly observed that SCC mixture contained 30% SSRS or less satisfied the required 28-day strength of 35 MPa and a UPV measurement of 4500 m/s at 28 days. Yet, the strength and UPV values had a drastic reduction for SCC with a higher SSRS percentage (i.e., 40% and 50%). At 7 days of curing, water absorption of all SCC mixtures met the acceptance range (3–5%) and the resistance to sulfate attack of the 10% SSRS was better than that of control mix. Beyond 10%, the higher SSRS in mixtures the greater weight loss was measured, expressing undesirably inhibiting damage by sodium sulfate attack.

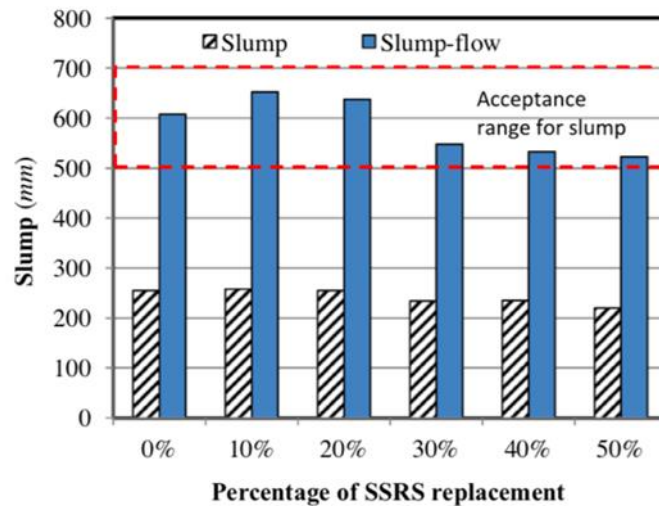


Figure 3: Influence of SSRS replacement on the slump and slump flow (Sheen et al. 2015).

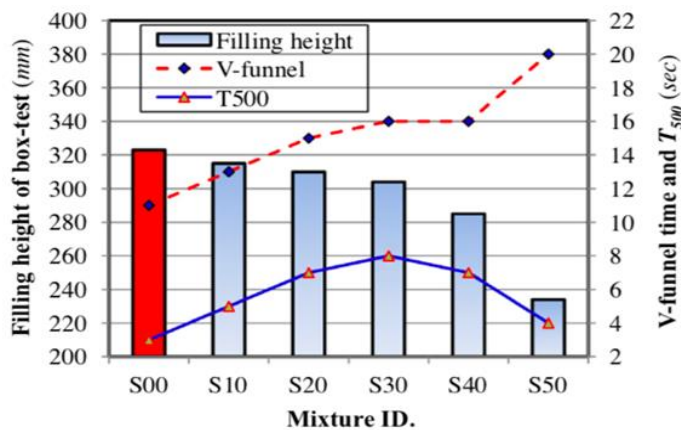


Figure 4: Filling height, V-funnel and slump flow time for SCC mixtures (Sheen et al. 2015).

Mandanoust and Mousavi (2012) evaluated the fresh and hardened properties of SCC containing metakaolin (MK). Totally, fifteen mixes including different MK contents (0–20% by weight of cement) with three water/binder ratios of 0.32, 0.38 and 0.45 were designed. Mixture proportions are shown in Table 2 for SCCL, SCCM, and SCCH varying VMA dosages of 1.31, 1.96, and 2.12 kg/m<sup>3</sup> respectively were added to the mix. It was concluded that SCC containing MK with slump flow values between 660 and 715 mm can be produced by adjusting the high range water reducer dosage.

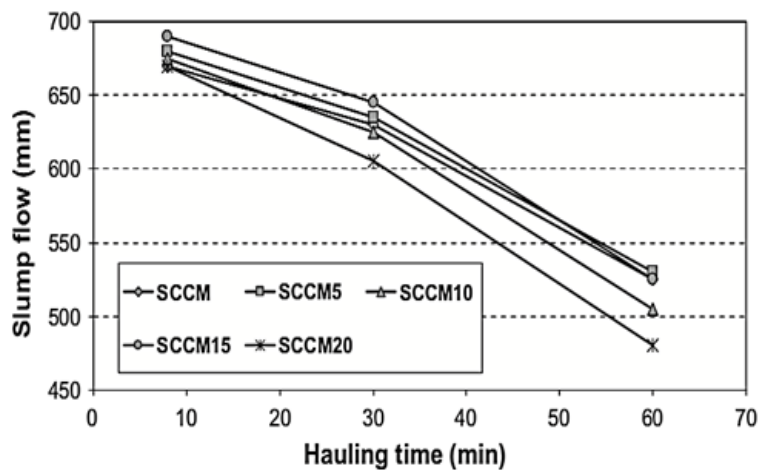
Partially replacement of cement by MK decreases the slump flow retention of the SCC mixtures; workability normally maintains till about 60 min of hauling time for SCC containing up to 15% MK as shown in Figure 5 (a). Both early and later ages compressive strength of SCC was enhanced with the addition of MK. Similar to compressive strength, UPV values and splitting tensile strength was improved. Figure 5 (b, and c) shows splitting tensile strength and UPV patterns. The addition of MK resulted in a decrease in the absorption rate. From Figure 5 (d), all the MK mixes showed a low absorption (below 3% at 30 min) indicating concrete of “good” quality at lower w/b ratios. MK inclusion increased the resistivity of SCC by a maximum of 24%, 26% and 20% for w/b ratios of 0.32, 0.38 and 0.45, respectively as shown in Figure 5 (e).

Sfikas et al. (2014) investigated the effect of replacement of cement or limestone powder (LP) by metakaolin (MK), on the rheology and the mechanical characteristics of the concrete mixtures. It was found that, due to the higher surface area and irregular morphology of MK, the workability was affected for higher MK/OPC or MK/LP replacement levels, resulting in a higher requirement for superplasticizer in order to acquire a similar rheological behavior. Regardless of the replacement level, the viscosity was increased when MK was incorporated in the mixture. On the other hand, an acceleration of the slump-flow spread was observed, though leading to lower slump-flow diameters. Minor blocking issues are raised for higher MK levels for both groups of mixtures, still no bleeding or segregation is evident. Also, the compressive and tensile splitting strength increased for higher MK levels.

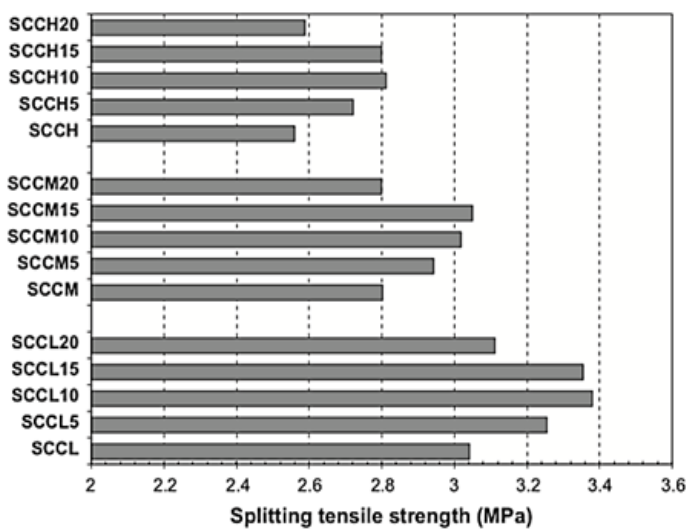
Table 2: SCC incorporating MK mixture design proportions. (Mandanoust and Mousavi, 2012)

<b>Mix. ID.</b>	<b>Cement (kg/m<sup>3</sup>)</b>	<b>MK %</b>	<b>Water (kg/m<sup>3</sup>)</b>	<b>w/b</b>	<b>Sand (kg/m<sup>3</sup>)</b>	<b>Gravel (kg/m<sup>3</sup>)</b>	<b>HRWR (kg/m<sup>3</sup>)</b>
SCCL	490	0	157	0.32	967	817	2.47
SCCL5	466	5	157	0.32	967	815	4.57
SCCL10	441	10	157	0.32	975	805	7.02
SCCL15	417	15	157	0.32	980	800	7.35
SCCL20	392	20	157	0.32	985	795	9.96
SCCM	460	0	175	0.38	940	815	1.73
SCCM5	437	5	175	0.38	947	810	3.31
SCCM10	414	10	175	0.38	958	800	3.60
SCCM15	391	15	175	0.38	964	790	4.89
SCCM20	368	20	175	0.38	970	781	4.89
SCCH	435	0	195	0.45	920	815	1.63
SCCH5	414	5	195	0.45	925	805	1.95
SCCH10	392	10	195	0.45	933	800	2.93
SCCH15	370	15	195	0.45	940	795	3.26
SCCH20	348	20	195	0.45	945	785	3.91

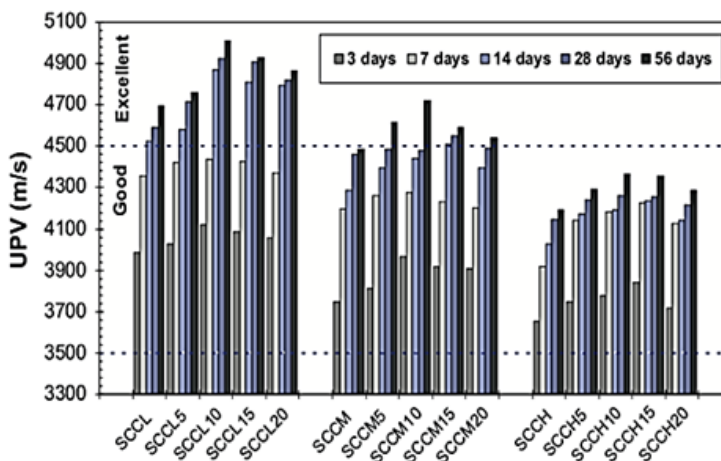




(a)

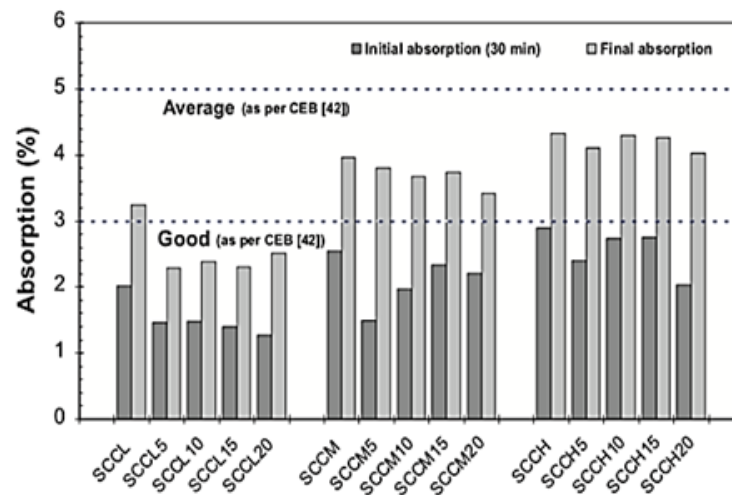


(b)

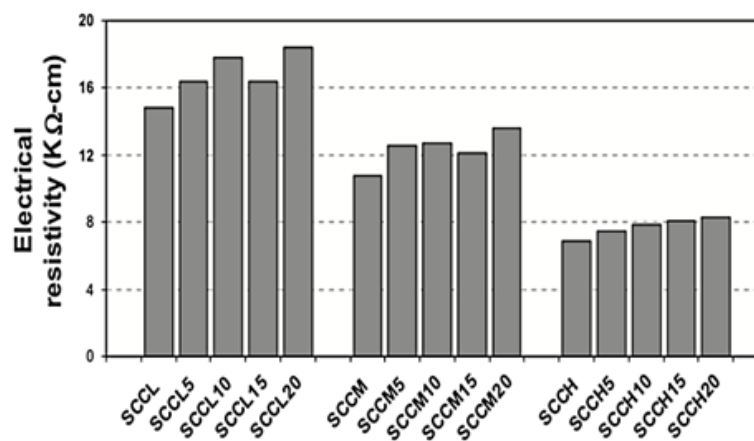


(c)

Figure 5: Graphical illustration of MK mixtures. (a) relationship between slump flow and hauling time, (b) splitting tensile strength, (c) UPV, (d) initial and final absorption, and (e) electrical resistivity (Mandanoust and Mousavi, 2012).



(d)



(e)

Figure 5: Graphical illustration of MK mixtures. (a) relationship between slump flow and hauling time, (b) splitting tensile strength, (c) UPV, (d) initial and final absorption, and (e) electrical resistivity (Mandanoust and Mousavi, 2012) (Continued).

Ranjbar et al. (2013) studied the effect of natural zeolite (NZ) on the fresh and hardened properties of SCC. Regarding the fresh properties, it was found that all concrete mixtures had slump flow within the range of 660–700 mm and were classified as SF2 class by adjusting HRWR dosage. Yet, the higher content of NZ needs higher HRWR dosage to remain in SF2 class as illustrated in Figure 6. Also, increasing NZ content in the formulation of SCC generally resulted in increasing the  $T_{50}$  and V-funnel flow times, therefore, increasing the viscosity of the mix. Besides, NZ showed a good

passing ability with a blocking ratio higher than 0.82. Moving to the hardened properties of SCC containing NZ, it was pointed that the compressive strength of SCC with 10% NZ at w/b ratio of 0.38 was 9% higher than those of control SCC, while using NZ in SCC at w/b ratio of 0.45 leads to decrease in compressive strength. This showed NZ impact for strength increasing is significant at a lower w/b ratio. Additionally, SCC produced with NZ generally performed better in strength development at longer ages than control SCC. Similar trend was observed with the splitting tensile strength. SCC with NZ mostly had UPV values higher than 3500 m/s which can be categorized as good and excellent concrete quality. Moreover, NZ significantly decreases the water absorption of SCC as curing age increases. It was concluded that 10% NZ in SCC can be considered as a suitable replacement regarding to the economic efficiency, fresh and hardened properties of NZ concrete.

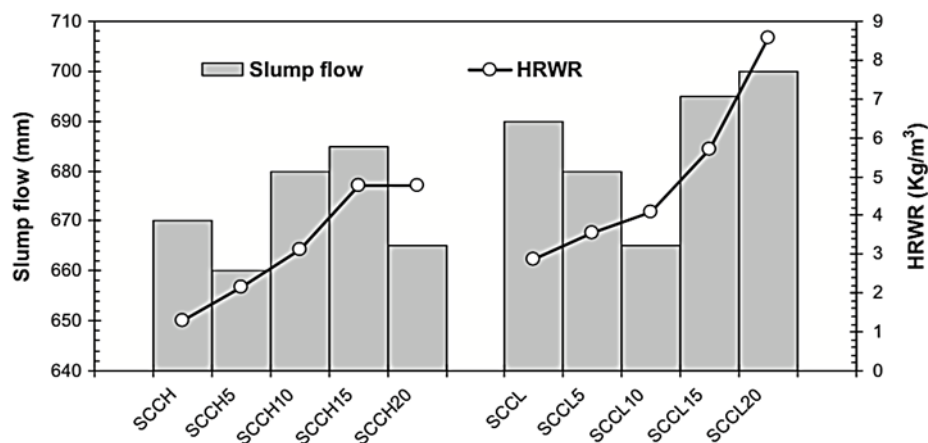


Figure 6: The effect of NZ on the slump flow and HRWR content. (Ranjbar et al. 2013).

Huge quantities of limestone powders are being produced as byproducts of stone crushers in limestone quarries. Considerable amounts of powders are being collected and utilization of this by-product is a big problem from the aspects of disposal, environmental pollution and health hazards. Limestone powder has been

utilized in conventional concrete. Yet, due its high fineness, the introduction of high volumes of limestone to concrete mixes was limited. It participates in increasing the water demand, which has negative effects on the properties of fresh (longer setting times) and hardened concrete (low strength due to increased capillary porosity and loss of interface adhesion between cement paste and aggregate). However, Ho et al. (2002) stated that successful utilization of quarry dust in SCC could turn this material into a valuable resource. Therefore, several researchers studied the effect of adding limestone powder into SCC mixes.

Şahmaran et al. (2009) investigated the effect of limestone powder on the workability of self-compacting concrete mortars. It was found that using limestone powder participated in a significant increase in the workability of these mortars. Therefore, it could reduce the amount of superplasticizer necessary to secure a satisfactory fluidity of SCC (Sonebi, 2004).

High volume of quarry limestone powder (QLP) in SCC was investigated by Felekoglu (2007). Thirteen concrete mixtures incorporating different amounts of QLP and one control mixture without any QLP addition were prepared. The mixture ingredients and proportions were particularly different and are presented in Table 3. The cement content varied from 307 to 470 kg/m<sup>3</sup> and QLP varied from 194 to 292 kg/m<sup>3</sup>. In some mixtures C-type fly ash was also incorporated at small amounts. The aim of changing mixture ingredients was to test the performance of QLP at SCC's with different rheological behavior and strength grades. From Figure 7, it was observed that all SCC mixtures had satisfactory slump flow value and V-funnel time except for C1, C5, and C9. However, modest adjustments of mixture ingredients and in particular superplasticizer dosage were necessary. The superplasticizer requirements of SCCs

incorporating QLP were in the range of 1.29–2.16%. This range was higher than the dosages employed in practical SCC applications (Su et al., 2001; Xie et al., 2002). Normal strength SCC (30 MPa) mixtures that contain approximately 300–310 kg of cement per cubic meter could be successfully prepared by employing high amounts of QLP (C3 and C8). Higher strength classes of SCCs (45–50 MPa) could be achieved but the cement dosage should be increased (C7).

Table 3: The mixture ingredients and proportions of SCC incorporating QLP in kg/m<sup>3</sup>. (Felekoglu, 2007).

Code	Cement	QLP	FA	Water	Fine aggregate	Coarse aggregate	Superplasticizer	Air content (%)	w/b (by weight)	w/p (by volume)
C0	600	0	0	190	754	837	10.5	1.8	0.32	0.99
C1	316	196	36	179	897	718	10	N/A	0.52	0.92
C2	307	288	34	194	882	581	8.7	3.1	0.59	0.86
C3	312	292	35	199	872	574	8.9	1.6	0.59	0.87
C4	316	202	35	191	1010	541	10.0	2.2	0.56	0.98
C5	394	281	0	230	800	543	9.7	N/A	0.58	0.98
C6	412	264	0	2-6	857	558	11.0	2.4	0.50	0.88
C7	470	241	0	180	877	567	10.0	3.3	0.38	0.74
C8	318	228	0	184	962	619	11.8	1.9	0.58	0.97
C9	374	226	0	174	1079	480	9.2	N/A	0.47	0.84
C10	383	244	43	193	951	501	8.5	1.7	0.47	0.81
C11	384	222	43	191	716	774	8.4	2.3	0.46	0.84
C12	386	222	43	181	719	786	12.4	3.5	0.43	0.79
C13	384	255	43	195	700	745	8.5	1.5	0.47	0.81

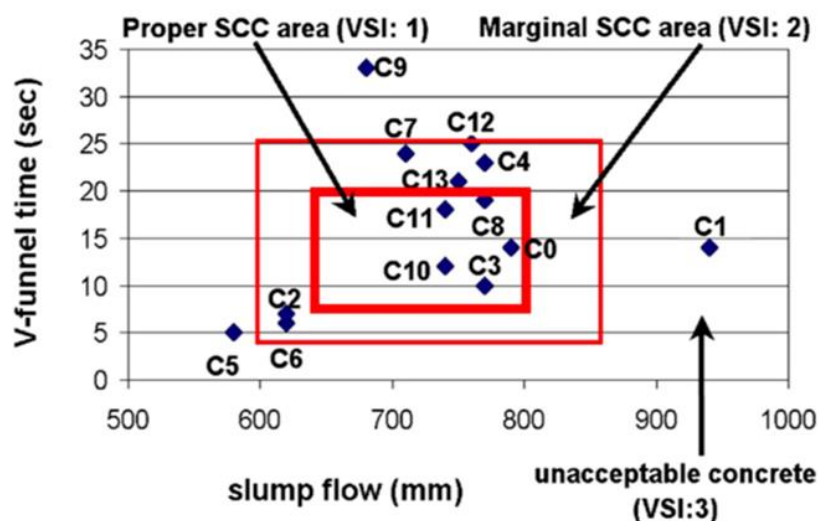


Figure 7: Workability boxes for determination of self-compactability of concrete mixtures. (Felekoglu, 2007).

In 2014, Güneyisi et al. conducted an experimental work to study effect of volcanic pumice powder on the fresh properties of self-compacted concretes with and without silica fume. Eight different SCC mixes were produced. In the first group, SCC without SF was produced with 0, 5, 10, and 20% replacement levels of volcanic powder (VP). However, for the second group, SF was added by a constant SF replacement level of 8%. All mixtures had a constant water/binder ratio (0.37) and with a total binder content of  $520 \text{ kg/m}^3$ . The behavior of all produced SCC mixtures is presented in Figure 8. Increasing the replacement level of VP resulted in increase in the flowability of SCC mixtures, even when SF was incorporated the level of effectiveness of VP seemed to have same trend. A similar trend was also detected in the  $T_{50 \text{ cm}}$  and V-funnel flow times of the SCCs. Also, it was observed that increasing the replacement level of VP resulted in a gradual increase in the L-box height ratio of SCC mixes. The 28-day compressive strengths of SCC mixes were observed to decrease as the amount of VP increased. However, the addition of SF provided an

increase in the compressive strength values of SCC. The percentages of the increases were ranged between 7.6 to 10.2%, depending mainly on the level of VP replacement.

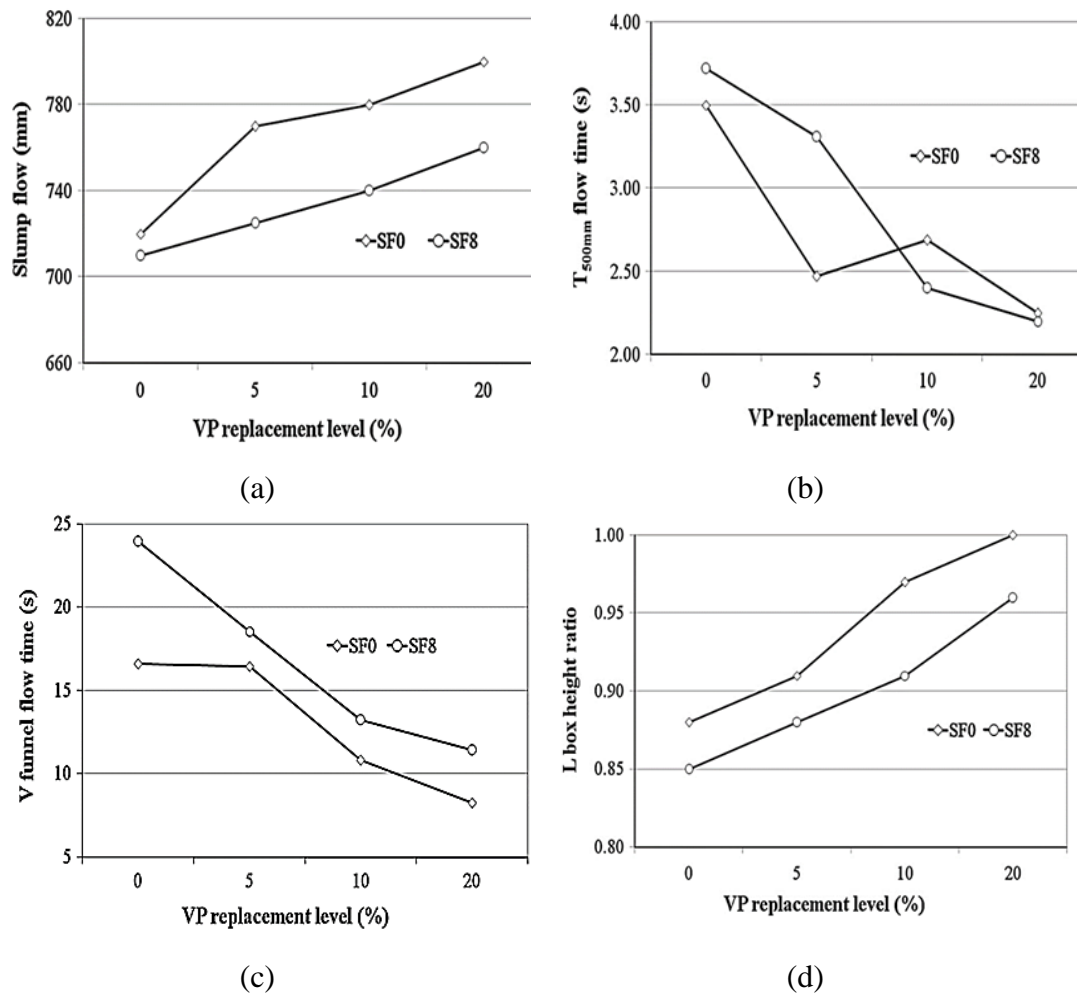


Figure 8: Fresh properties of SCC incorporating VP. (a) Slump flow, (b)  $T_{500\text{mm}}$  flow time, (c) V-funnel flow time, and (d) L-box height ratio (Güneyisi et al., 2014).

Furthermore, Uysal and Sumer (2011) presented an experimental study on the properties of SCC replaced with FA, GGBS, limestone powder (LP), basalt powder (BP) and marble dust (MD) in various proportioning rates. Sixteen series of mix proportions, of which one control and 15 mixtures with mineral admixtures were prepared in different combinations. Cement was replaced at three proportions (20, 40

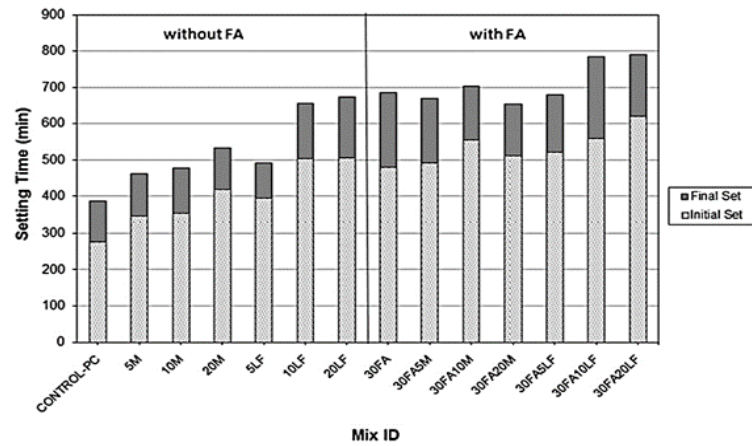


and 60%) with GGBS series. In FA series, cement was replaced at three proportions (15, 25 and 35%) with FA. However, blast powder (BP), marble dust (MD) and limestone powder (LP) were replaced at same proportions (10, 20 and 30%) with cement. The total powder content was fixed to  $550 \text{ kg/m}^3$  and the water–powder ratio (w/p) was selected as 0.33. It was observed that, all the mineral admixtures improved significantly the workability properties of SCC. The workability properties of SCC mixtures as slump flow,  $T_{50}$  time, V-funnel time and L-box ratio for all SCC mixtures remained in the target range. However, in terms of workability, the best performance was detected in FA-replacement series. Also, the addition of mineral admixture in several combinations provided excellent mechanical properties. As pozzolanic materials FA and GGBS increased the late age compressive strengths of SCC mixtures. Replacing 25% of OPC with FA resulted in a strength of more than 105 MPa at 400 days. In addition, filler materials increased the early age compressive strengths of SCC mixtures. Besides, the resistance of SCCs against sulphate attack was improved with the addition of mineral admixtures. Test results indicated that GGBS series presented superior resistance against sulphate attack. Replacing cement with 40% GBFS could reduce magnesium sulphate attack by one third compared to the control mixture. SCC specimens exposed to sulphate solutions and their compressive strength reduction showed that attack by magnesium sulphate was more aggressive in its action on SCC mixtures than sodium sulphate attack.

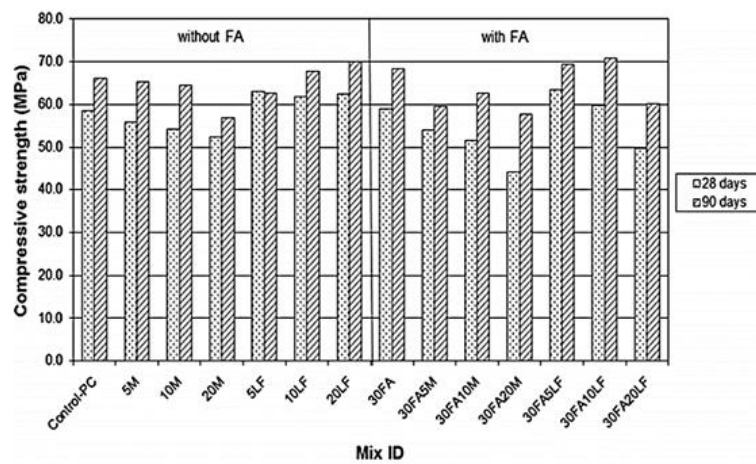
To reduce the negative effect of manufacturing OPC, researches were attracted towards having SCC with low Portland cement composition. Therefore, binary and ternary blended cements were studied by investigators to minimize as much as possible the usage of OPC and to maximize the quality and performance of SCC.

Gesoğlu et al. (2012) investigated the possibility of using marble dust (MD) and limestone filler (LF) in the production of SCCs with and without fly ash. Seven binary and six ternary blends of SCC mixtures apart from a control mixture were designed and cast at a water to binder ratio (w/b) of 0.35. The control concrete was made with only Portland cement (PC) as the binder while the remaining mixtures incorporated binary (PC + FA, PC + M, PC + LF) and ternary (PC + FA + M, PC + FA + LF) blends in which the supplementary materials were replaced by equal amount of cement by weight. A constant replacement level of 30% by total weight of binder content was considered for FA, while the various replacement levels (5, 10, and 20%) were employed for MD and LF. It was stated that the addition of MD or LF increased the dosage of superplasticizer used to keep the target slump flow. However, using FA significantly decreased the amount of SP needed. All SCC mixtures has a slump flow times between 2-5 seconds. Yet, increasing the amount of filler, regardless of the type, resulted in an increase in the  $T_{50}$  cm time. Mixtures incorporated LF showed a lower flow times than that of MD mixtures and that's might be due to the fineness of the filler. Due to the addition of FA, ternary blends of mixtures had relatively short flow times. All of the binary mixes had an L-box height ratio less than 0.8, while all of the ternary mixtures, expect for the mix incorporating 30% FA and 20%, had the blocking ratio between 0.8 and 1.0. Figure 9 and 10 show the mechanical and durability characteristics for the produced SCC mixtures, respectively. The addition of fillers increased the initial and final setting times of SCC in comparison to control and 30% FA reference mixtures. Also, it was observed that 28 and 90 day compressive strength and splitting tensile strength of the binary and ternary mixtures demonstrated a similar tendency. Yet, due to the slow hydration reaction characteristics of FA, 28 day

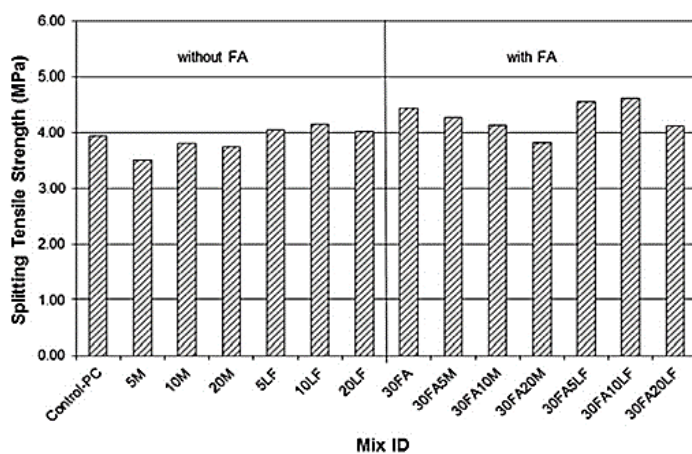
compressive strengths of ternary mixes were lower than those of binary mixtures. Using LF provided greater compressive strength for both series of the mixtures, and the maximum splitting tensile strength values were detected in mixtures containing 10% replacement level of LF. All of the sorptivity coefficient values of SCCs incorporated M or LF, and FA were significantly less than that of the control mix. Besides, the addition of fillers generally improved the chloride penetration resistance of the concretes; all of the binary mixes had low chloride ion penetration characteristics, whereas the ternary mixtures had very low. The lowest electrical resistivity was measured in the control mix. However, incorporation of the fillers and FA exhibited an improvement in electrical resistivity of the SCC. Also, a tendency of increasing electrical resistivity by increasing the amount of the filler was observed.



(a)

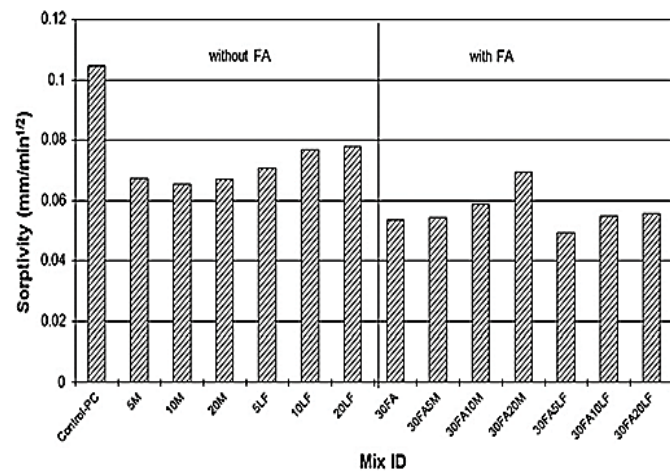


(b)

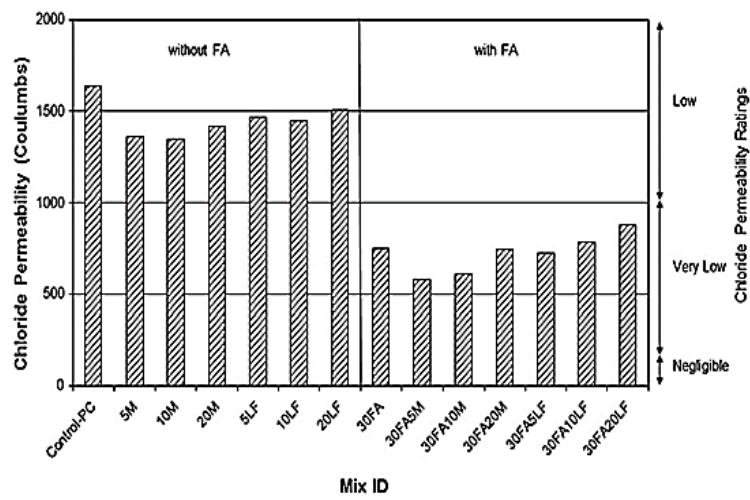


(c)

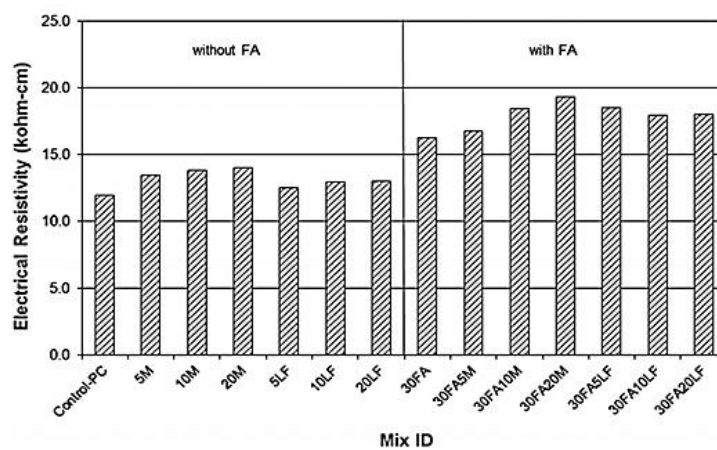
Figure 9: Mechanical behavior of SCC mixtures using binary and ternary blends. (a) setting time, (b) compressive strength, and (c) splitting tensile strength (Gesoglu et al. 2012).



(a)



(b)



(c)

Figure 10: Durability characteristics of SCC mixtures using binary and ternary blends. (a) sorptivity, (b) chloride permeability, and (c) electrical resistivity (Gesoglu et al. 2012).

Additionally, Nehdi et al. (2004) studied the effect of high volume replacement binary, ternary, and quaternary cement blends on SCC's durability. Seven SCC mixtures with a constant water/binder ratio of 0.38 were produced, and mixture proportions are shown in Table 4. Results indicated that high volume replacement of OPC contributed to achieving a satisfactory workability, higher 28, and 91 day strength values, lower chloride ion permeability, and a very low sulphate expansion. However, high volume replacement SCC had poor performance under deicing salt surface scaling in the laboratory, high- volume replacement ternary and quaternary SCC can be designed to achieve comparable deicing salt surface scaling resistance to that of a reference SCC mixture made with 100% OPC, and the use of a VMA seemed to improve its resistance to deicing salt surface scaling. Figure 11 shows the deicing salt surface scaling after 50 freezing–thawing cycles of SCC mixtures.

Table 4: SCC mixture design with high volume replacement binary, ternary, and quaternary. (Nehdi et al. 2004).

<b>Mixture</b>	<b>PC</b>	<b>FA</b>	<b>Slag</b>	<b>RHA</b>	<b>SF</b>	<b>Gravel</b>	<b>Sand</b>	<b>VMA</b>	<b>HR WR</b>
Reference	425	0	0	0	0	900	930	0	1.9
Binary a	215	215	0	0	0	905	925	0	1.5
Binary b	215	215	0	0	0	905	925	0.1	3.3
Ternary a	215	105	105	0	0	905	920	0	1.3
Ternary b	215	105	105	0	0	905	920	0.2	4.9
Quaternary a	215	100	85	0	25	910	915	0	3.0
Quaternary b	215	100	85	25	0	910	915	0	3.2

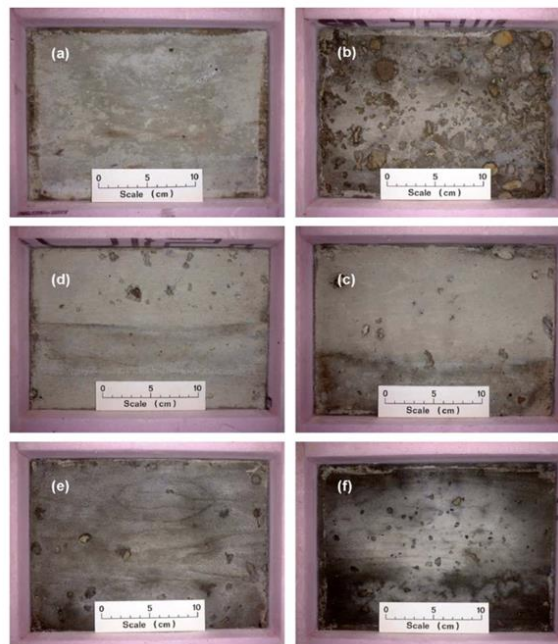


Figure 11: Deicing salt surface scaling after 50 freezing–thawing cycles. a) reference mixture with 100% OPC, (b) 50% OPC–50% fly ash, (c) 50% OPC– 50% fly ash with a VMA, (d) 50% OPC–25% slag–25% fly ash, (e) 50% OPC–24% fly ash–20% slag–6% RHA, and (f) 50% OPC–24% fly ash–20% slag–6% silica fume (Nehdi et al. 2004).

Moreover, Pelisser et al. (2018) evaluated the rheological and mechanical properties with the addition of metakaolin and FA. It was observed that the addition of metakaolin (MK) and FA together presented flow characteristics and resistance to segregation. At 28 days of curing, the compressive strength value of SCC mixture containing metakaolin and FA was higher compared to the control mix.

## 2.5 Sewage Sludge Ash

The vast amount of industry developed and the rapid increase in population resulted in increasing the quantities of wastewater worldwide. Wastewater is mainly a liquid waste including solid materials, produced by humans. It consists of washing water, feces, urine, laundry waste and other material which goes down drains and toilets from households and industry. Discharging of wastewater in huge amounts

without any further treatment causes serious environmental issues (Toumi et al., 2003). Thus, wastewater treatment plants are designed to have distinct water treatment process combinations with varied water treatment facilities depending on the influent's water quality and the effluent discharge standard. The degree of purification of the water achieved by wastewater treatment plants depend on the treatment applied.

The main three treatments in wastewater treatment plants (WWTP) are denominated primary treatment, secondary treatment and tertiary treatment. Once the wastewater is pre-treated and mixed, it enters the WWTP and the primary treatment is then applied. The primary treatment focuses on the removal of readily settleable solids and floatable materials that have not been removed in the pre-treatment stage. Also, it works on minimizing the pollution load on the biological treatment process (Chipasa, 2003). After that, all the wastewater, free of most of the settleable particles flow in the secondary treatment process. It is a biological treatment that uses micro-organisms commonly bacteria (biomass) that works on biodegrading all the organic matter in wastewater (Boulay and Edwards, 2000). There are several types of secondary treatments including activated sludge (Nielsen and Hruday, 1983; Karvelas et al., 2003; Chipasa, 2003), trickling filter (Stones, 1977; Goldstone et al., 1990), high rate algal ponds (Toumi et al., 2003), and new biosorption techniques such as fungal biosorption (Kapoor and Viraraghavan, 1995) or membrane developed in the last years (Aksu, 2005). The secondary treatment is usually considered as a complete process. However, since the environmental guidelines are becoming stricter, the produced sewage from the secondary treatment was no longer a guarantee for discharge. Therefore, tertiary treatment (physico-chemical process) is required for further decreasing the residual constituents in the secondary sewage effluent (Wu et al., 2005).



Due to the high operational costs involved with tertiary treatment, it is only used in developed treatment plants and only if the wastewater is going to be reused in irrigation or some industries.

The end products of WWTP process are millions of tons of dry sludge. With the adoption of the urban wastewater treatment Directive (Council of European Communities (91/271/EEC)), more sludge is produced annually. In the UAE, the growing development resulted in the production of large amounts of sewage sludge. More than one million ton (on a dry-weight basis) of sewage sludge is produced yearly (Alshankiti et al., 2018). However, avoiding the generation of sewage sludge is impossible. Thus, sewage sludge treatment and its disposal are becoming a crucial environmental problem and challenged the development of the industries involved in wastewater treatment (Tyagi and Couillard, 1987; Solis et al., 2002; Fuentes et al., 2004).

Treatment of sludge is frequently influenced by the final disposal option selected. Sludge can have a number of management's options or uses with its own advantages or disadvantages (Tchobanoglous et al., 1991). The conventional procedure of sewage sludge treatment is illustrated in Figure 12 and summarized in the following points.

- Agricultural application is the mostly used disposal method of sewage sludge in the past, since it includes organic matter, nutrients, phosphorus, and full of other plant nutrients that enriched the soil (Fuentes et al., 2004). However, one of the major limitations for agronomic application of sewage sludges is heavy

metals retained in them. These metals are non-biodegradable and pose ecotoxicity in environment (Lester, 1983).

- Landfill: in case high levels of heavy metals are present in sewage sludge, the only suitable method is reclamation of deteriorated and disturbed lands as well as industrial sludge landfills (Chipasa, 2003).
- Incineration in multiple hearth or fluidized bed furnaces: this method is often used before disposing sewage sludge to landfills, and it is the most beneficial method used for sludge treatment, because it provides three main advantages including volume reduction of up to 80–90%, destruction of organic micropollutants and pathogens, and energy recovery (Marani et al., 2003). Incineration temperatures can differ, depending on the type of furnace. However, it usually ranges from around 650°C to 980°C in the incinerator combustion zone. High operating temperatures above 900°C produces ash particles called sewage sludge ash (SSA).

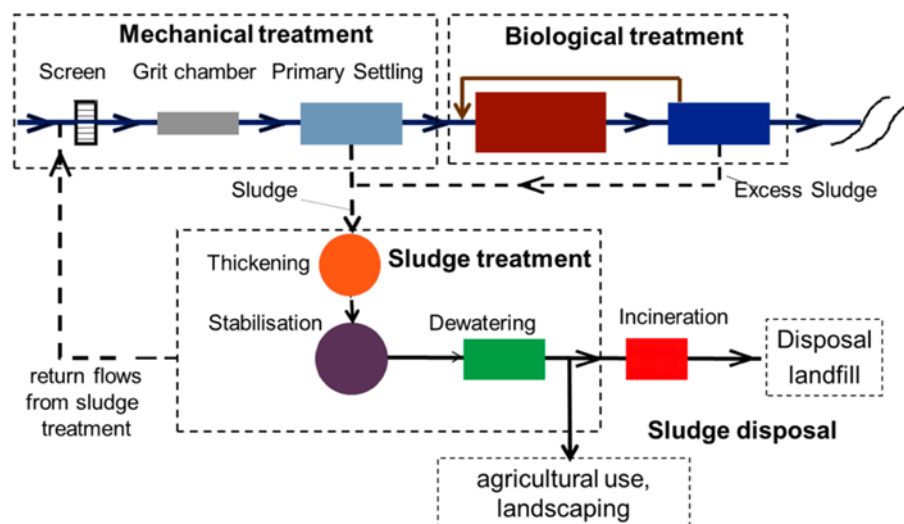


Figure 12: Conventional sludge treatment procedures. (Kroiss et al., 2011).

Although the volume and mass of sewage sludge will be reduced after incineration, SSA still needs to be disposed of in landfills. Therefore, there is an urgent need to investigate the possible application of SSA in construction industry as a solution for the landfilling problem. Besides solving disposal problems, economic and ecological benefits are other advantages of re-using SSA. The following two subsections represent studies investigating the main characteristics of SSA, and their utilization in the construction sector.

### **2.5.1 Sewage Sludge Ash Characterization**

SSA is the by-product of the incineration of dry sewage sludge produced from WWTP. It is primarily a silty material with some sand-size particles (Chen et al., 2013). The specific size range and properties of the sludge ash varies based on the origin of wastewater, the type of incineration system, and the chemical additives introduced in the wastewater treatment process (Bialowiec et al., 2009). However, comprehensive knowledge of the characteristics of SSA is important to investigate its resource recovery potentials. Therefore, in the last decades, investigators were directed to examine incinerated SSA characteristics.

The physical properties of SSA have been reported in the literature and presented in Table 5. The size fraction of SSA particles falls in between the silt and fine sand sizes, with mean diameters ranging from 50-65  $\mu\text{m}$ . Figure 13 shows particle size distributions of as-produced SSA with overall sand limits in concrete (BS 882) and ground SSA with OPC and fly ash. The most part of SSA particles were consistent within the above mean diameter range, showing that SSA could be used as a filler or fine aggregate in concrete. Also, SSA ground for use as a cementitious material can

achieve well graded size distributions compared to Portland cement clinker (PC) and fly ash (class F) (Lynn et al., 2015). However, BET specific surface area and Blaine fineness varied over a wide range from 2500–23,100 m<sup>2</sup>/kg (Pan et al., 2003; Wang et al., 2005) and 500–3900 m<sup>2</sup>/kg (Halliday et al., 2012, Tseng et al., 2000; Lin et al., 2008). The specific gravity of SSA was found to be between 1.8 and 2.9. As the incineration temperature increases, the density increases. However, the rate of increase drops off above 1000°C. The bulk density of SSA was found to be on the average of 805 kg/m<sup>3</sup> (Ai-sharif and Attom, 2014; Donatello and Cheeseman, 2013; Kosior-Kazberuk, 2011; Pinarli and Kaymal, 1994; Tenza-Abril et al., 2015, Yip and Tay, 1990; Tay, 1987).

Table 5: The physical properties of SSA reported in the literature.

Property	Values			
	Wegman and Young (1988)	Khanbiluardi (1994)	Commission (1990)	Gray and Penessis (1972)
4.76 mm	99	100	100	100
2.38 mm	99	98	100	100
2.00 mm	-	-	100	100
0.85 mm	-	-	100	-
0.42 mm	99	73	100	-
0.21mm (No. 80 sieve)	-	-	98	-
0.149 mm (No. 100 sieve)	85	53	83	-
0.074 mm (No. 200 sieve)	66	38	56	47-93
0.0902 mm	11-13	-	-	2-13
0.02 mm	-	-	20	-
0.005 mm	-	-	12	-

Table 5: The physical properties of SSA reported in the literature (Continued).

<b>Property</b>	<b>Value</b>
Loss on Ignition (%)	1.4 (Wegman and Young, 1988)
Moisture Content (% by Total Weight)	0.28 (Khanbiluardi,1994)
Absorption (%)	1.6 (Commission, 1990)
Specific Gravity	2.60 (Wegman and Young, 1988) 2.61 (Commission, 1990) 2.44 - 2.96 (Gray and Penessis, 1972)
Bulk Specific Gravity	1.82 (Khanbiluardi,1994)
Permeability (ASTM D2434 - cm/sec)	$1 \times 10^{-4} - 4 \times 10^{-4}$ (Comission, 1990)

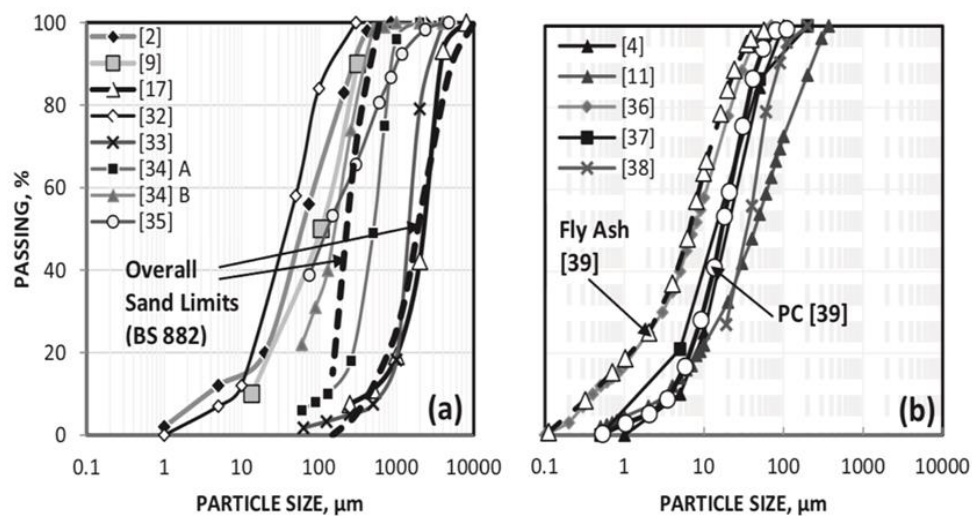


Figure 13: Particle size distributions. (a) as-produced SSA with overall sand limits in concrete (BS 882) and (b) ground SSA with PC and fly ash samples (Lynn et al. 2015).

The main oxides in SSA are  $\text{SiO}_2$ ,  $\text{CaO}$ ,  $\text{Al}_2\text{O}_3$  and  $\text{P}_2\text{O}_5$ . Oxides such as  $\text{Fe}_2\text{O}_3$ ,  $\text{Na}_2\text{O}$ ,  $\text{MgO}$ ,  $\text{P}_2\text{O}$ ,  $\text{SO}_3$  and others are present in lesser amounts (Lynn et al., 2015; Paris et al., 2016). Besides, quartz and hematite have been identified as the most abundant minerals in SSA, whilst other iron oxides, iron phosphates, calcium phosphates and aluminum phosphates have been reported to a smaller degree (Bapat, 2012; Coutand et al., 2006; Cyr et al., 2007; Kjersgaard et al., 2007; Anderson and Skerrat, 2003; Ottosen et al., 2014). The amorphous content of SSA ranged from 35–75%, which indicates that SSA is a reactive material and, when ground sufficiently fine, may have potential as a cement component (Lynn et al., 2015). Sewage sludge was found to include heavy metals (i.e., zinc (Zn), lead (Pb), copper (Cu), cadmium (Cd), chromium (Cr), arsenic (As), and nickel (Ni)) (Lin et al., 2006; Wang et al., 2008). Although these metals are present in very small amounts, leaching of such metals is an important issue if SSA will be considered for use in the construction industry.

Cheeseman et al. (2003) and Shi and Kan (2009) concluded that incinerating sewage sludge into SSA significantly reduced the leaching of heavy metals. However, Cheeseman et al. (2003) found that copper (Cu) and zinc (Zn) in SSA were significantly leached under high acidic conditions ( $\text{pH} < 3$ ). The LOI value of SSA was in the average of 3.5% (Lynn et al., 2015). Yet, high values up to 13% have been reported (Lin and Lin, 2004; Krüger et al., 2014; Tsai et al., 2006; Merino et al., 2005; Baeza et al., 2014). Hence, it is possible for SSA to be generally able to comply with the LOI limit of 5% set for cement in BS EN 197 (2011) and fly ash for concrete in BS EN 450 (2012) (Lynn et al., 2015). Table 6 shows the range of values of oxides and elements present in SSA.



Table 6: Typical values of oxides and elements present in SSA. (Cyr et al., 2007).

<b>Oxide (%)</b>	<b>SiO<sub>2</sub></b>	<b>Al<sub>2</sub>O<sub>3</sub></b>	<b>Fe<sub>2</sub>O<sub>3</sub></b>	<b>CaO</b>	<b>P<sub>2</sub>O<sub>5</sub></b>	<b>SO<sub>3</sub></b>	<b>Na<sub>2</sub>O</b>	<b>K<sub>2</sub>O</b>	<b>TiO<sub>2</sub></b>	<b>MgO</b>	<b>MnO</b>	<b>LOI</b>
Mean	36.1	14.2	9.2	14.8	11.6	2.8	1.0	1.7	0.9	1.9	0.06	5.5
Min	14.4	4.4	2.1	1.1	0.3	0.01	0.01	0.1	0.3	0.02	0.03	0.2
Max	65.0	34.2	30.0	40.1	26.7	12.4	6.8	3.1	1.9	23.4	0.9	41.8
<b>Elements (mg/kg)</b>	<b>As</b>	<b>Ba</b>	<b>Cd</b>	<b>Co</b>	<b>Cr</b>	<b>Cu</b>	<b>Ni</b>	<b>Pb</b>	<b>Sb</b>	<b>Sn</b>	<b>Sr</b>	<b>V</b>
Mean	87	4142	20	39	452	1962	671	600	35	400	539	35
Min	0.4	90	4	19	16	200	79	93	35	183	539	14
Max	726	14600	93	78	2100	5320	2000	2055	35	617	539	66

The morphology of SSA particles was investigated by several researchers. SSA was found to have irregular particles with rough surface textures and a porous microstructure (Payá et al., 2002; Morais et al., 2006; Chiou et al., 2006; Wang et al., 2005). The irregular particles of SSA explained the high absorption and the increase in the water demand of concrete containing SSA; where SSA water absorption values ranged from 8 to 20% (Forth et al., 2006; Halliday et al., 2012), which is considerably high compared to natural sand with a water absorption range of 1–3%.

Few investigators studied the effect of sintering temperature on the characteristics of produced SSA (Lin et al., 2006; Xu et al., 2008; Wang et al., 2008). Lin et al. (2006) and Wang et al. (2008) concluded that increasing the sintering temperature reduced the pore volume, improved the bulk density and reduced the water absorption of produced SSA. The same was also observed when increasing the sintering time (Wang et al., 2008). Figure 14 shows scanning electron microscope (SEM) images of SSA sintered at different temperatures and time. Moreover, it was declared that at temperatures of 1100 and 1150°C, the organic matter is totally destroyed and is responsible for the high porosity of the microstructure (Huang et al., 2007).

Xu et al. (2008) examined the effect of sintering temperature on the characteristics of sludge ceramsite. Dried sewage sludge, clay, and water glass were mixed at proportions of dried sewage sludge/clay = 33% and water glass/clay = 15%. These mixtures were sintered at elevated temperatures: 850, 900, 950, 1000, 1100, and 1200°C to produce sludge ceramsite. It was observed that different heating temperatures resulted in different appearance of the sludge ceramsite since the colors were changing from dark brown to reddish-brown. Furthermore, different elements on

cermasite surface were detected. The contents of Si and Al are higher at a temperature below 1000°C, and those of Fe, Ca, Ti, K, and Na are higher at a temperature above 950°C. Moreover, at temperature below 1000°C, the main crystalline phase was quartz (SiO<sub>2</sub>). However, as the temperature increased to 1000 and 1100°C, the major crystalline phase was Kyanite (Al<sub>2</sub>SiO<sub>5</sub>), and a major portion of crystals is Mullite at 1200°C. A temperature of 1000°C was the optimal temperature for the production of sludge ceramsite and the samples prepared can satisfy the requirements for filter media used for water/wastewater treatment. Results reported by Cheeseman et al. (2003) showed that for samples of SSA pressed into cylindrical specimens and heated in the range of 980–1080°C, maximum sample density, maximum shrinkage and minimum water absorption were achieved after treatment at 1000–1020°C for 1 hour. Heating above this temperature resulted in a decrease of sample density associated with the formation of spherical pores from the decomposition of trace inorganic components in the SSA matrix. Similar studies by Lin et al. (2006) using pressed SSA cylinders concluded that significant sintering of SSA occurred between 900 and 1000°C. Besides, Merino et al. (2005) reported large increases in the density of SSA specimens between 1100 and 1200°C.

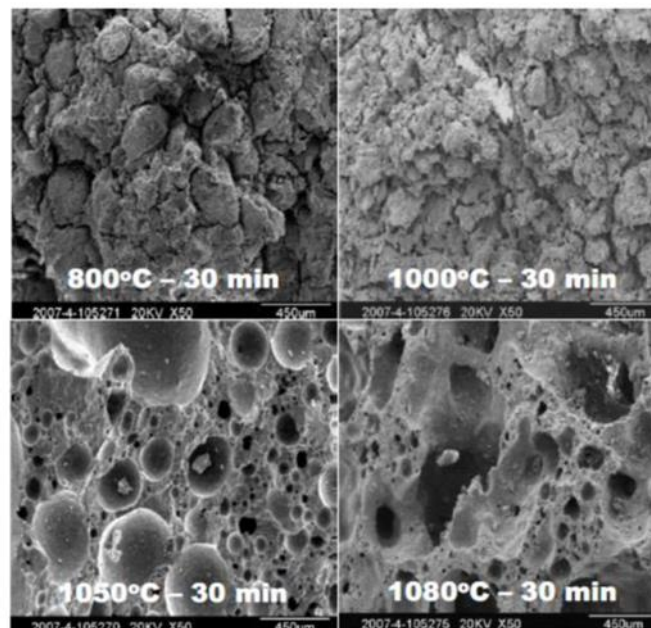


Figure 14: SEM of SSA sintered at different temperatures. (Wang et al., 2008).

Previous work reported that SSA contained pozzolanic components such as  $\text{SiO}_2$ ,  $\text{Al}_2\text{O}_3$  and  $\text{CaO}$  (Franz, 2008; Kosior-Kazberuk, 2011; Tenza-Abril et al., 2015). The requirement of significant  $\text{SiO}_2$  and  $\text{Al}_2\text{O}_3$  content suggested that SSA exhibits pozzolanic activity (Tay, 1987; Tay and Show, 1994; Monzó et al., 1996; Pan et al., 2003). Chen and Poon (2017) examined the pozzolanic activity of SSA, fine sewage sludge ash (FSSA) obtained from grinding SSA, and pulverized fly ash (PFA). It was concluded that under Frattini standards, all three types of SSA exhibited pozzolanic reactivity as illustrated in Figure 15. However, according to strength activity index (SAI) test the PFA can be regarded as a good pozzolan but not the SSA and FSSA using 75% as the reference. However, the test procedures might have distorted the results due to the need for adding more water to achieve the workability requirement due to the porous nature of the SSA. Donatello et al. (2010) reached similar conclusion and reported that using SAI to estimate the pozzolanic activity of a highly water absorbing material such as SSA, would lead to underestimated results.

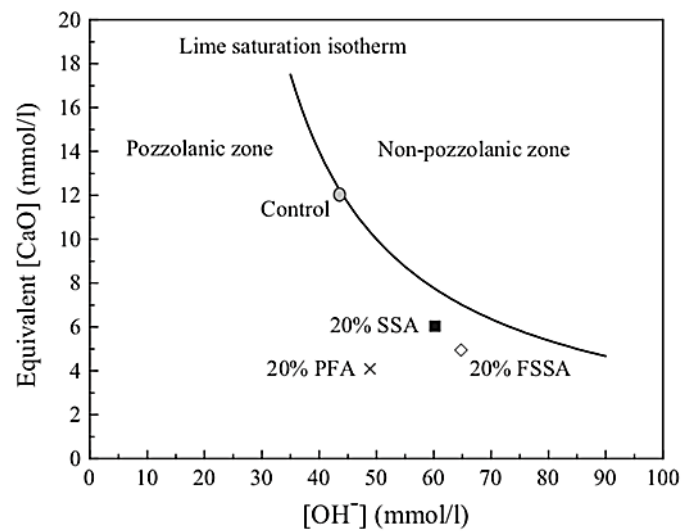


Figure 15: Pozzolanic reactivity of SSA, FSSA, and PFA. (Chen and Poon, 2017).

Milling improved the pozzolanic activity of incinerated SSA according to both the SAI and Frattini tests (Donatello et al., 2010). Figure 16 shows results reported by Lynn et al. (2015) for the pozzolanic activity of 157 samples of SSA. It was found that the majority of results fell around the latent hydraulic and pozzolanic regions, suggesting that SSA could perform as a capable cementitious component and has a potential to be used in construction materials such as concrete mixes. The following subsection will be discussing previous studies done on utilizing SSA in the construction sector.

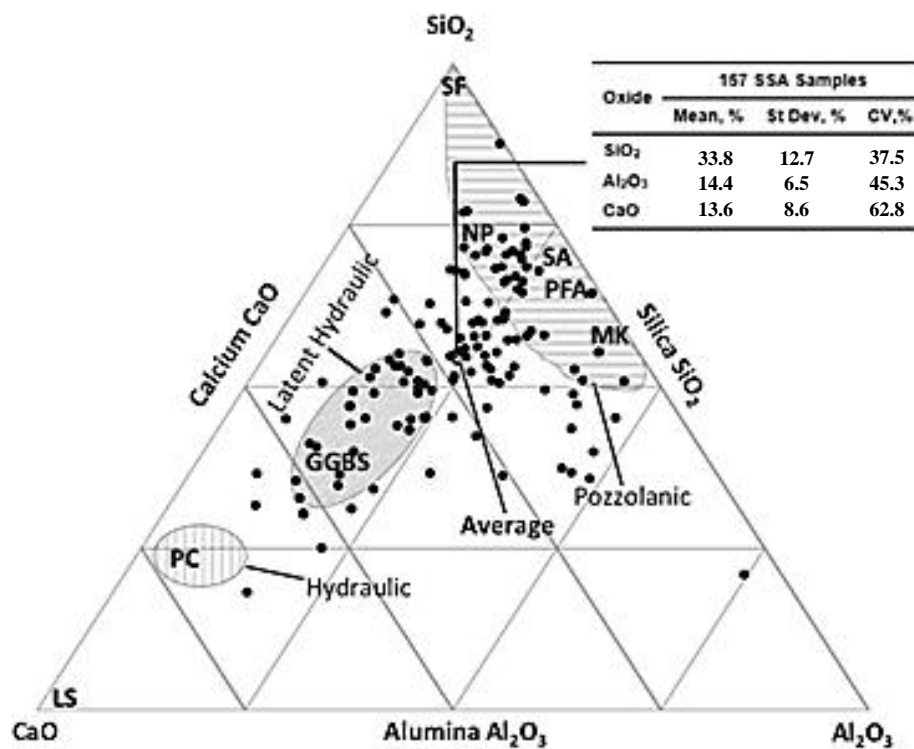


Figure 16: Ternary plot of SiO<sub>2</sub>, Al<sub>2</sub>O<sub>3</sub> and CaO contents for SSA. Note: PC = Portland cement, GGBS = ground granulated blast furnace slag, PFA = pulverised fuel ash, MK = metakaolin, SA = shale ash, NP = natural pozzolan, SF = silica fume and LS = limestone. (Lynn et al., 2015).

### 2.5.2 Sewage Sludge Ash in Construction Industry

Nowadays, the utilization of the industrial waste is becoming one of the most significant challenges in the waste management program (Uyarra and Gee, 2013). Indeed, the construction industry is increasingly expected to play a major role in achieving the target of zero waste and as such, an evaluation of the use of SSA in construction sector can be useful and timely. Several researchers were attracted to investigate the effect of reusing SSA in producing different construction materials and applications.

Previous research studies have revealed that SSA might be used to substitute cement in concrete (Lin and Lin, 2005; Yusuf et al., 2012; Ingunza et al., 2018; Monzó

et al., 1996). Lin and Lin (2005) reported that SSA general elements (silica, iron, calcium, aluminum, magnesium, phosphorus and oxygen) are the same as the major elements presented in the cement. Furthermore, Yusuf et al. (2012) concluded that the hydraulic properties of SSA are relatively the same of cement ones. Monzó et al. (1996) investigated the mechanical behavior of mortars containing SSA and OPC with different tricalcium aluminate content. It was found that partial substitution (15 or 30% by mass) of OPC by SSA does not strongly affect the strength of mortars at 3 to 28 days of curing. Yet, the compressive and flexural strength gain ratio increased with increasing SSA replacement level. There was no clear correlation between compressive strength gain and  $C_3A$  content. However, significant flexural strength gain decreased when the  $C_3A$  content in cement increased. The performance of mortars with the addition of septic tank sludge ash at different replacement ratios (5, 10, 15, 20, 25 and 30%) was examined by Ingunza et al. (2018). The mortar mixes were done using CP-IV-RS-32 cement (equivalent to ASTM IP – Portland Pozzolan Cement), quartz sand and septic tank sludge ash with a calcination temperature of 850°C. It was reported that the addition of SSA in mortars resulted in a reduction of the consistency rates due to the irregular shape of SSA particles that absorbed part of the mixing water. Moreover, there was a reduction in the entrapped air content percentage proportional to the quantity of ash added. Since density varies inversely with the entrapped air content, an increase in bulk density and water retention was observed. Due to the water evaporation during the curing period, the mortar bulk density had a similar performance as in the fresh state but with lower values. It was observed using scanning electron microscopy (SEM), that control mortar has pores with larger diameters than SSA 20% mortar, showing that mortars with SSA addition have less voids and better particle packing, resulting in an increase of the mechanical strengths at 28 and 91 days

of curing. The highest value of compressive strength and flexural strength was obtained when the replacement ratios of cement with SSA were 20% and 15% of SSA, respectively. This indicates that the SSA can replace part of cement in mortar as long as that level is below 20%. The same was also reported by Monzó et al. (1996).

Krejcirikova et al. (2019) investigated the effect of different ratios of cement substitution (0, 10, and 30%) and two pre-treatment methods for ash, i.e. ash grinding and water washing, on the physical properties of mortar. Two different types of SSA were used from Avedøre Wastewater treatment plant (AVE) and from Lynettefællesskabet (LYN). Sorption isotherms showed that the hygroscopic water vapor absorption of the two types of SSA varied. For one of the ashes, the adsorption was less than 1% by mass at 94% RH, despite the pre-treatment method, while the other absorbed more than 7% at the same RH (the ground ash more than the water washed ash). The difference is believed to be due to differences in the fineness of the particles and in the content of hygroscopic salts. Particle size distributions contained larger grain sizes of SSA than that of cement; which clearly increased the porosity of mortar and capillary water absorption coefficient. Moreover, as illustrated in Figure 17, the particle size distribution decreased the compressive strength even at a very low substitution of 10%. However, grinding the ash resulted in increasing the compressive strength compared to pre-treating the ash by water washing.



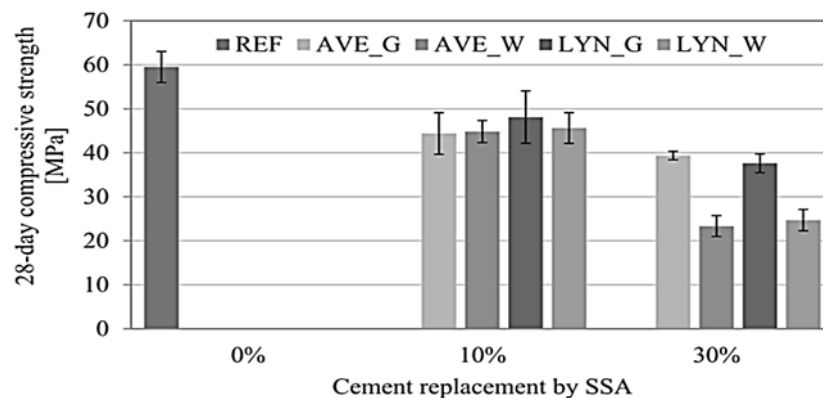
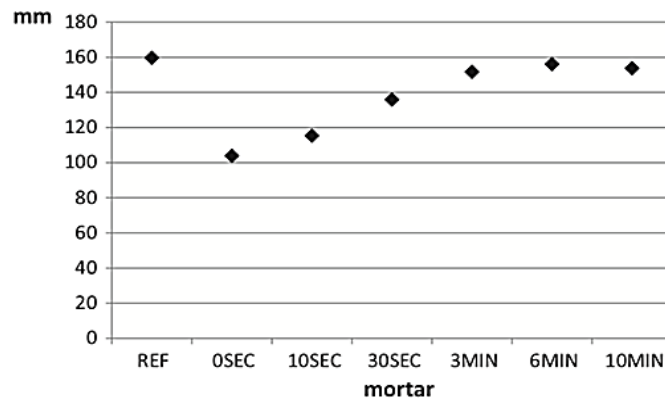


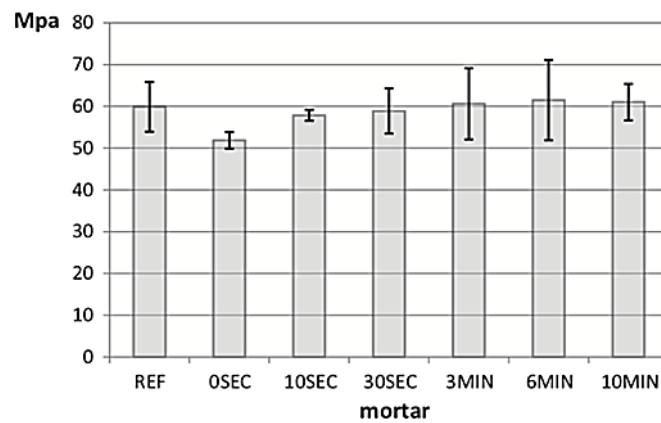
Figure 17: 28-day compressive strengths of mortar test specimens. (Krejcirikova et al., 2019).

The effect of fineness of SSA on the properties of mortars was investigated (Pan et al., 2003; Kappel et al., 2017). Pan et al. (2003) examined the influence of SSA fineness on mortar and paste properties, including workability, time of setting, and compressive strength. SSA was incinerated at 700°C for 3 hours. The grinding time of SSA was selected as 10, 20, 30, 60, 120, 180, and 360 min. six mortars were obtained from each batch, the control mortar batch included 1375 g of graded sand and 500 g of OPC, while for the other batches, 20% of OPC weight was replaced by SSA. It was concluded that the setting time of SSA–cement paste increased with the increase of SSA fineness. Moreover, increasing the grinding duration of SSA altered the morphology of SSA particles from irregular into more spherical-like, which provided additional improvement to SSA mortar workability caused by the reduction of particle interlocking and friction in fresh paste. Due to the improvement of pozzolanic activity caused by grinding and the increase of the outer surface of SSA particles, the compressive strength of SSA mortar increased with the increase of SSA fineness. Figure 18 (a, and b) shows similar conclusions observed by Kappel et al. (2017). In addition, it was noticed that mortar with un-milled SSA was in a grey color with a slightly red tint. However, as the particle size of the SSA decreased due to better

distribution of smaller particles in the matrix, the mortar changed color from grey to reddish.



(a)



(b)

Figure 18: Effect of grinding time of SSA. (a) cement mortar flow value, and (b) 28 days compressive strength (Kappel et al., 2017).

The influence of nanomaterials on the microstructure of sludge cement paste was evaluated by Lin et al. (2008) and Lin and Tsai (2006). Lin et al. (2008) evaluated the effects of nano-SiO<sub>2</sub> on three ash particle sizes in mortars. Mortars were produced by replacing 20% of type 1 Portland cement with three different sludge ash particle sizes, 1, 10, and 75  $\mu\text{m}$  incinerated at 800°C. Moreover, in each ash substitution, 0%, 1%, or 2% of nano-SiO<sub>2</sub> was added to the mix. It was reported that the consistency, setting time and compressive strength have increased as the particle size of the SSA

decreased. However, the addition of nano-SiO<sub>2</sub> resulted in small consistency increase and shortened the setting time. Nano-SiO<sub>2</sub> additives increased the early compressive strength and had a better influence on the compressive strength of mortars with large SSA particle sizes as shown in Figure 19 (a, and b). SEM results showed that a densest mortar structure was observed for specimens with 1 μm particle size, implied that as the fineness of SSA increased and more nano-SiO<sub>2</sub> were added, the densification of the mortars increased. The crystallization components of the mortars vary with different sludge ash particle sizes. Components including Ca(OH)<sub>2</sub>, C-S-H, and C<sub>2</sub>S were observed for mortar with 75 μm ash particles, C<sub>2</sub>S for 10 μm ash particles and Ca(OH)<sub>2</sub> and C-S-H for 1 μm ash particles. These results showed that the initial hydration was slow in mortars as C<sub>2</sub>S was a common component in all the mixes. Nevertheless, after 1% nano-SiO<sub>2</sub> was added, Ca(OH)<sub>2</sub>, C-S-H, and C<sub>2</sub>S were observed for mortar with three different ash particle sizes. Hence, the addition of nano-SiO<sub>2</sub> increased the amounts of original reaction products but couldn't produce new products. Nano-SiO<sub>2</sub> was able to function as a filler material for pores in mortars, resulting in a decrease of mortars pore sizes.

Lin and Tsai (2006) increased the addition of nano-materials up to 3%. Similar to Lin et al. (2008), the higher the amount of nanomaterial were added, the denser cement paste specimens became, leading to a reduction of the total pore volume of the paste. Thus, making it tightly connected together, acting as a single structure. Moreover, it was noticed that the quantities of Ca(OH)<sub>2</sub> increased as more amounts of sludge ash were mixed in the paste and the highest diffraction peak of C-S-H was detected with sludge cement paste with 3% nano-materials added.

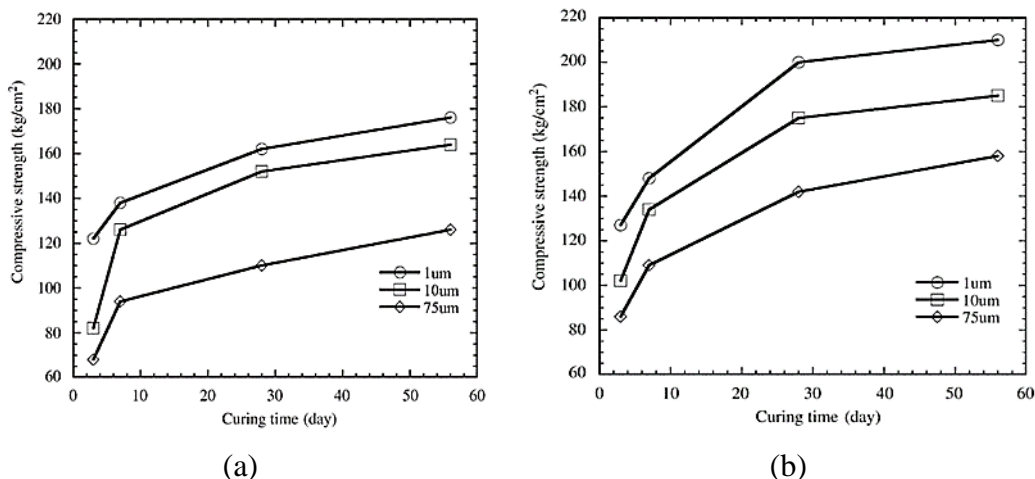


Figure 19: Relationships between compressive strength and particle sizes for 20% ash-cement mortar. (a) 1%, and (b) 2% of nano-SiO<sub>2</sub> added (Lin and Tsai, 2006).

To further investigate the effect of SSA on mortars, a comparative study on the effects of sewage sludge ash and fly ash on cement hydration and properties of cement mortars was done by Chen and Poon (2017). Paste and mortar specimens were prepared in this study with a constant water/binder of 0.484 in all the mixes. Two types of paste specimen were prepared. One type was pure OPC, Pulverized fly ash (PFA), sewage sludge ash (SSA) or fine sewage sludge ash (FSSA) paste. Another type was OPC blended with PFA, SSA or FSSA which were used to replace 5, 10 or 20% of OPC respectively. It was found that SSA promotes early stage cement hydration, while PFA had no effect; which might result in early stage cracking and deformation when SSA is used in large amount. PFA was found to have a stronger pozzolanic activity than SSA. However, at the same replacement level of up to 20%, the compressive and flexural strength of mortars containing PFA, SSA or FSSA were similar. In contrast to common SCMs, SSA and FSSA improve the strength of cement mortars not only through the pozzolanic reaction, but also through a number of interacting factors including lowering the effective w/b ratio, enhancing the rate and degree of cement hydration, providing water for cement hydration by releasing it from their porous

structures, the formation of brushite crystals. As shown in Figure 20, PFA reduced the drying shrinkage of mortar, SSA and FSSA increased the drying shrinkage with FSSA being worse.

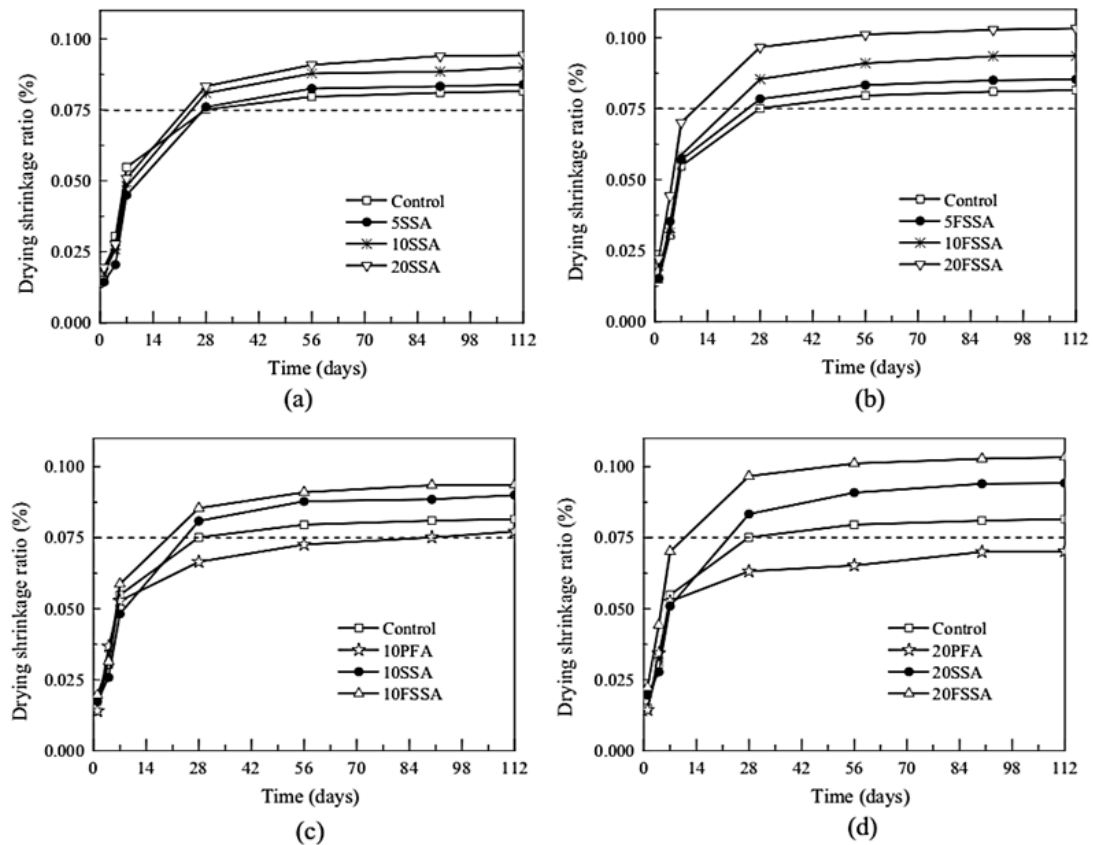


Figure 20: Drying shrinkage values of mortars containing different amounts of PFA, SSA and FSSA in the binder. (Chen and Poon, 2017).

Furthermore, Baeza et al. (2014) examined the binary and ternary combinations of SSA with other solid waste materials including marble dust (MD), fly ash (FA) class F and rice husk ash (RHA) as replacement in Portland cement pastes. It was concluded that an increase of strength by 9%, compared to the control sample was observed when blending SSA, FA and RHA at 30% cement replacement. Whereas, an increase of SSA content resulted in a mechanical strength reduction. It was clear from percentage of fixed portlandite (FP) that all waste materials are showing pozzolanic activity expect for the marble dust (MD). The most pozzolanic material was rice husk ash (RHA) due

to the high silica content in it. FA and SSA had similar fixed portlandite (FP) values and were highly reactive at early ages. The densities of all the mixtures were lower than the control mix and as the SSA replacement percentage increased the density decreased. On the contrary, as the SSA increased, the mortars exhibit a higher water absorption values due to the irregular shape of its particles.

In addition to reusing SSA as SCM in cement mortars, the characteristics of SSA, specifically its fineness, suggested that the material may be suitable for use in concrete as filler or fine aggregate. Previous studies were conducted on reusing SSA as fine aggregate, and lightweight aggregate (Tay and Yip, 1989; Khanbilvard and Afshari, 1995; Chiou et al., 2006; Kosior-Kazberuk, 2011). Tay and Yip (1989) conducted a preliminary investigation to examine the potential of reusing incinerated sludge at elevated temperature as an aggregate to produce lightweight concrete (LWC). Sewage sludge was incinerated at 1050°C for 6 hours and crushed to meet the required grade. Two types of LWC were produced; one mix contained natural sand as fine aggregate, and sludge ash as coarse aggregate, while the other had both fine and coarse aggregate derived from sewage sludge. It was concluded that the aggregates made from sewage sludge are angular, rough textured, and porous (mostly interconnected cells) with an average porosity of 66%. The average water absorption of the aggregate participle was 8.5%.

The workability of the fresh concrete made with sludge ash aggregates is not satisfactory, and segregation tends to occur easily due to the low unit weight of the aggregates. Lightweight concrete made with sludge ash aggregates has low thermal conductivities and high fire resistance and hence, are suitable for application in thermal insulation and fire protection. However, at 28-days, the compressive strength of the

lightweight concrete was similar to those using other lightweight aggregates. On the contrary, Khanbilvardi and Afshari, (1995) found that reusing SSA as fine aggregated dropped the 28-days compressive strength by 20% compared to the control non-ash mix, yet it met the ACI design requirements. The reduction of strength was a result of the clay lumps in SSA, and the tendency of SSA to absorb water, since it is a water-absorbent material. Moreover, there was also no evidence of significant toxic leachate for sludge ash and its concrete product; therefore, sludge ash was environmentally inert and could be used in concrete mix. Kosior-Kazberuk, (2011) applied SSA as a partial replacement of aggregate in concrete. The ash was used as the lightweight aggregate replacing the part of aggregate of size from 0 to 4 mm in concrete. The concrete tested contained 0, 10, 25, 50, or 100% of ash replacement related to aggregate volume. Test results indicated that replacing up to 25% of sludge ash achieved acceptable compressive strength and water absorption. Although the SSA was used as a filler, the latent pozzolanic activity of ash allows developing the concrete strength properties comparable with the strength of concrete containing natural aggregate only.

Few studies investigated the possibility of using SSA in the production of bricks. Baeza-Brotons et al. (2014) examined the potential of using SSA as a raw material in the composition of concrete, with a similar dosage to when it is used to manufacture blocks. SSA was incinerated at 800°C. Portland cement used for concrete was CEM II BM (S-LL)-42.5R. The concrete was produced with additions of 5, 10, 15 and 20% of SSA relative to cement in dry basis. Results indicated that reusing SSA to manufacture blocks provides similar densities and mechanical strengths to the reference sample. However, there was a notable decrease in the water absorption. Thus, to achieve the performance with regards to density, absorption and capillarity, it

is substantial to highlight the behavior of the sample with a 10% replacement of sand by SSA; where a matrix that fills the gaps in a better way is obtained, as a result of the increment of fine particles.

Białecka et al. (2001) studied the physicochemical properties of the bricks produced from raw material for the production of building ceramics containing 10-20% of sewage sludge. It was found that sludge can be used for the production of building materials due to the high proportion of silica and alumina in the ash. Lin and Weng (2001) indicated that the proportion of SSA in the mixture and the incineration temperature are the two parameters that affect the quality of the produced brick. The suggested proportion of using SSA in bricks is 10%, with 24% optimum moisture content, prepared in the molded mixtures and incinerated between 880°C and 960°C to produce a good quality brick.

Moreover, SSA was combined with recycled glass cullet (GC) to produce concrete blocks (Chen et al., 2018). The replacement ratios of SSA were 10, and 20 by mass of OPC, while GC had replacement ratios of 0, 20, and 50% by mass of aggregates. Results indicated that the concrete blocks containing 20% SSA in the binder and 50% GC in the aggregates could achieve compressive strength of not less than 30 MPa at the age of 28 days. However, longer curing time would improve the strength due to the moderate pozzolanic activity of the SSA. The drying shrinkage values of the blocks increased with higher content of SSA in the binder, due to the porous characteristic of the SSA and FSSA particles which took up more water. Yet, the combined use of recycled GC as aggregates could alleviate the detrimental effect due to the much lower water absorption value and the smooth surface of the GC. Furthermore, the addition of SSA or FSSA in the binder could effectively suppress



ASR expansion caused by the reactive glass aggregates. It is recommended that 20% of SSA or FSSA should be added in the binder for assuring the control of ASR expansion if all the aggregates used are GC.

Hamood et al. (2017) investigated the effectiveness of using raw sewage sludge (RSS) as a water replacement in cement mortars mixing containing unprocessed FA. The outcomes of the investigation were encouraging in that cement-based materials containing RSS demonstrated good engineering properties in comparison to the control mixes. The addition of unprocessed-FA significantly reduced flowability; however, developed long-term compressive strength. The highest compressive strength was recorded for the mixes with 10–20% unprocessed-FA replacement.

Additionally, SSA can be used in road construction for creating road pavement and embankments (Merino et al., 2005). Field investigations conducted by Lind et al. (2008) showed that the introduction of the SSA on the road pavement construction (the carrier layer) does not cause environmental risks on the soil or the groundwater by elution of heavy metals. However, SSA need to keep specific parameters, such as resistance to leaching, frost resistance, specified permeability (Lin et al., 2006). Shirodkar et al. (2011) examined the influence of SSA in hot mix asphalt as mineral filler and/or as a fine aggregate substitute. In this study, samples were done by replacing 0% and 20% by aggregate weight with SSA. It was concluded that mix asphalt with 2% SSA shows similar performance in fatigue and rutting compared to the reference mix with 0% SSA. Since the performance of the mix asphalt was not affected with the addition of 2% SSA, future studies could be conducted analyzing the effects of higher percentages of SSA, which could significantly reduce the amount of raw materials required in the construction sector.

A comparison between SSA and FA on the improvement in soft soil was done by Lin et al. (2007). In this study, F-grade FA and SSA incinerated at 800°C were used. Five different FA/Soil and SSA/Soil specimens were prepared corresponding to weight percentages of 0%, 2%, 4%, 8%, and 16%. Test results showed that the addition of FA and SSA reduced the plasticity indices and swelling behavior of the untreated soil, where the volumetric swelling was found to be lower than the allowable safety values for ordinary construction industries. However, SSA was better than FA in mitigating the expansion of the untreated soil. California bearing ratio (CBR), unconfined compressive strength (UCS) and triaxial compression demonstrated that SSA was able to efficiently improve the engineering properties of soft cohesive subgrade soil and the optimum amount of SSA added was found to be 8%.

Moreover, SSA was used as a raw material to manufacture cement. The effects of using dried sewage sludge as additive on cement property in the process of clinker burning were investigated by Lin et al. (2012). The eco-cement samples were prepared by adding 0.50–15.0% of dried sewage sludge to unit raw meal, and then the mixtures were burned at 1450°C for 2 hours. Results showed that the major components detected in the eco-cement clinkers were  $C_3S$ ,  $C_2S$ ,  $C_3A$ ,  $C_4AF$  and that the phase formation of  $Ca_{54}MgAl_2Si_{16}O_{90}$  was identified in all the clinkers. The  $C_2S$  phase formation and peaks increased with increases in sewage sludge, while the  $C_3S$  structures decreased; this conclusion was also verified by SEM investigations. Also, as illustrated in SEM figures (Figure 21), the clinker containing 15.0% sewage sludge was significantly different in that it displayed a larger amount of pore distribution. As the addition of sewage sludge increased in the raw meals, the lower the flexural strength of eco-cement was observed. Yet, there was no significant impact on all the strengths at later

curing ages. The concentrations of Ti, Ba, Zn, Cr, Cu, Ni and Pb in the clinkers increased with the sewage sludge addition into the raw meals, while Mg, Sr obviously decreased, and Al, Fe, Mn slightly decreased.

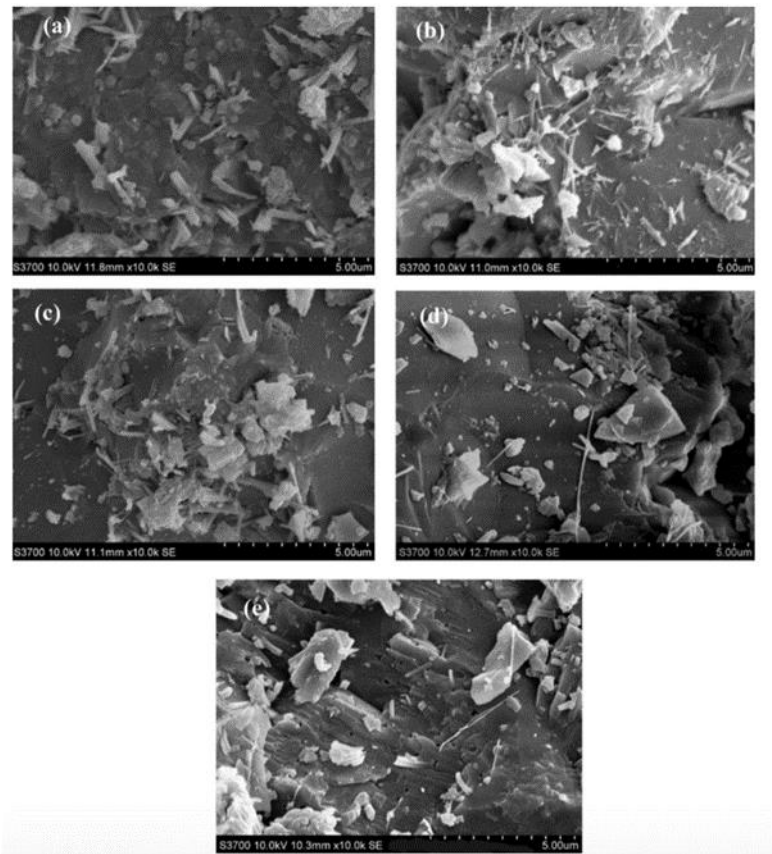


Figure 21: SEM micrographs of the eco-cement clinkers with the addition of different percentages of sewage sludge in the raw meals. (a) 0%, (b) 2.5%, (c) 5.0%, (d) 10.0% and (e) 15.0% (Lin et al., 2012).

Additionally, Rodríguez et al. (2013) evaluated the potential of dried sewage sludge as an alternative fuel in cement clinker production. It was concluded that A calorific value of 8293 J/g (1990 kcal/kg), is sufficient for this material to be considered as a supplementary fuel in cement kilns. SSA cannot be considered as an inert waste and, due to soluble Ni levels, would only qualify for disposal to hazardous waste landfills. This is an important driver in its use as an alternative fuel in the cement industry, where no residual ash is produced, and metals are generally locked into

clinker phases. An increase of stability of belite structure, and a delay in alite crystallisation were due to the phosphorus derived from sewage sludge. Besides, a reduction of free lime contents in clinker was detected. During firing, losses of minor elements ranging from 1 to 40% were noted, the most volatile being Zn.

The behavior of SSA and metakaolin-based geopolymer concrete was assessed by Istuque et al. (2016). It was concluded that the addition of SSA (i.e., up to 20%) to replace metakaolin resulted in slightly lower compressive strength for mortars cured at 65°C compared to mortar without SSA. Mortar with 10% SSA and cured at 25°C showed similar compressive strength compared to a reference mixture without SSA.

SSA has attracted several researchers, yet recent studies pointed out that there still research gaps that need to be filled (Chen and Poon, 2017; Paris et al., 2016; Kappel et al., 2017; Lynn et al., 2015). Recent studies indicated limited published data on the effect of SSA on cement hydration and the relation between pore structure and mechanical properties. Also, the durability and volume stability due to drying shrinkage of concrete including SSA still needs further investigations. Therefore, the proposed research will help understand how incinerating temperature and time of SSA particles introduced as partial replacement of cement in mortars can affect the performance of the mortars, and the potential of reusing SSA in producing SSC. Thus, expanding the areas in which SSA can be effectively utilized.

## **2.6 Research Significance**

SCC is one of the concrete technologies promoting sustainable development through the use of recycled and industrial by-product materials as a partial replacement of cement. The presented research provides an experimental evidence on the potential

of reusing by-products such as sewage sludge ash (SSA) produced from wastewater treatment plants in the development of the construction sector. Moreover, sewage sludge ash characteristics were studied in order to set procedures and guidelines on the production of sewage sludge ash and its possibility to be used in making concrete that satisfy all the requirements and properties of SCC. Therefore, the outcome of this study supports the sustainable development of concrete industry by reducing cement use. Moreover, supporting industries and the global economy by managing the utilization of solid waste materials.

### Chapter 3: Investigation Program

The main objective of this thesis is to examine the feasibility of reusing a solid waste by product, i.e. SSA in the production of SCC. To achieve this goal, the investigation program of this thesis is divided into two main phases.

The structure of the experimental program is illustrated in Figure 22. In the first phase, SSA was characterized based on different methods and procedures. The morphology, chemical and mineral composition, and the particle size distribution of the produced SSA were examined. Moreover, the pozzolanic activity of SSA particles was studied. The effect of incorporating SSA on the workability, workability retention, heat of hydration, and pore size distribution of the cement paste was investigated. The leachability of heavy metals in SSA was investigated as well using the toxicity characteristic leaching procedure (TCLP) test.

In the second phase, several SCC mixtures were designed, cast, and tested. The studied SCC mixtures were tested right after mixing while being still plastic, and this stage of the concrete's lifetime is commonly referred to as the fresh stage. The tests were also extended throughout the hardened stage of concrete at different time intervals (7, 28, and 56 days). SCC differs from conventional concrete in its flowability, viscosity, filling and passing abilities. Therefore, in the fresh stage, SCC was tested for these parameters by slump flow, T<sub>50</sub>, J-ring, and V-funnel. As for the hardened properties, both SCC and CVC are known to be dense and homogeneous sharing the same engineering properties and durability characteristics and hence the same tests are used for evaluation or assessment including compressive strength, bulk resistivity, and initial rate of absorption, permeable pores, water permeability, and

drying shrinkage. Section 3.5 is dedicated for describing the several tests performed to assess the produced SCC and the detailed procedure that was followed.

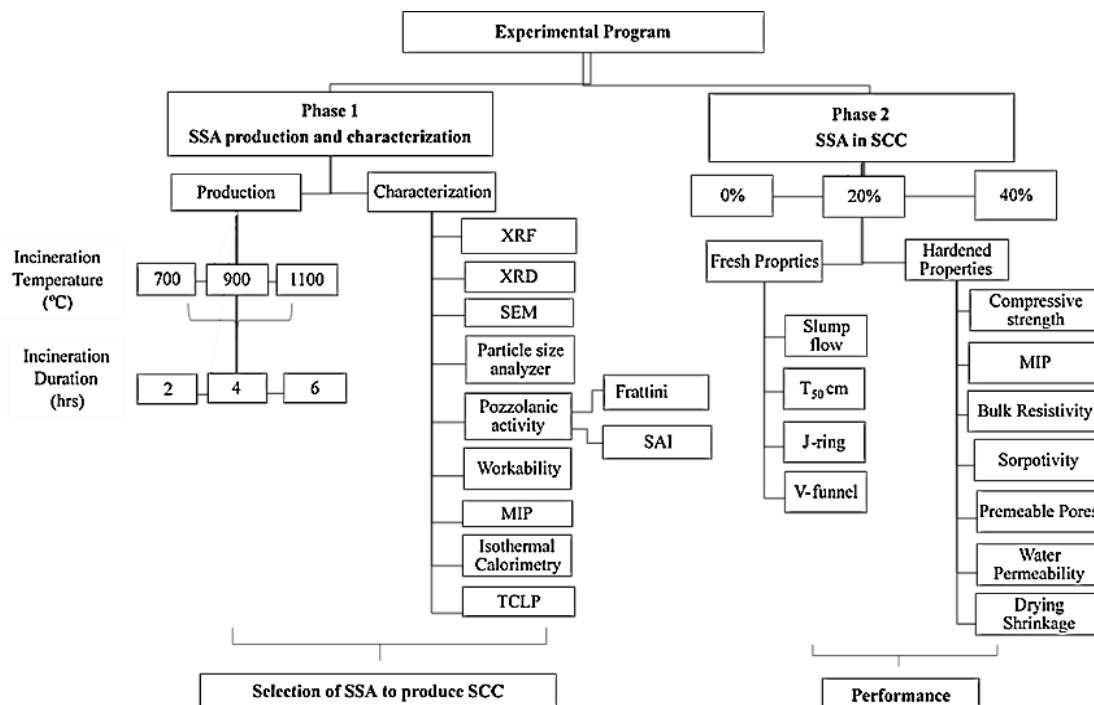


Figure 22: Structure of the experimental program.

### 3.1 Materials

The materials used in the experimental phase of this thesis were the typical concrete ingredients including OPC, aggregates, water, and admixtures. Besides, the addition of SSA as a partial replacement of cement. The properties of the constituent materials are given in the following sections.

#### 3.1.1 Aggregate

The passing ability of SCC mixtures mainly depends on the nominal maximum size of the used aggregates. ACI 237R-07 (2008) recommends that the nominal maximum size of the aggregate must be one size less than that suggested by ACI 301 (1989). Hence, from Table 7, and according to the range of cementitious material

content used for the concrete mixtures in this thesis, the maximum aggregate size to be used was 9.5 mm. The inter-particle friction between the coarse aggregate leads to a reduction in the flowability of the mixture and since SCC mixtures need to be flowable, the ratio of fine to coarse aggregates was increased. According to EFNARC (2005) specifications, the maximum size of coarse aggregate should be less than 12 mm to improve the passing ability of the mixtures by avoiding blocking. Besides, the usage of larger aggregate sizes will decrease the resistance of segregation of the mix, since it can be separated easily from smaller particles and the paste content.

The types of aggregates used in this study are shown in Figure 23. Coarse aggregate was a crushed natural dolomite from Ras Al Khaima (UAE) with nominal size of 9.5 mm (3/8 in.), a specific gravity of 2.67, and water absorption of 0.7%. Two types of fine aggregate were used; crushed natural stone sand from Ras Al Khaima (UAE) with fineness modulus of 3.72 and specific gravity 2.64, and dune sand from Al Ain area (UAE) with fineness modulus of 0.9 and specific gravity 2.63. Sieve analysis was conducted on all aggregates used, and the results are presented in Table 8.

Table 7: Recommended maximum aggregate size (ACI 237R-07).

<b>Nominal maximum size (mm)</b>	<b>Cementitious material content (kg/m<sup>3</sup>)</b>
37.5	280 to 330
25	310 to 360
19	320 to 375
12.5	350 to 405
9.5	360 to 415



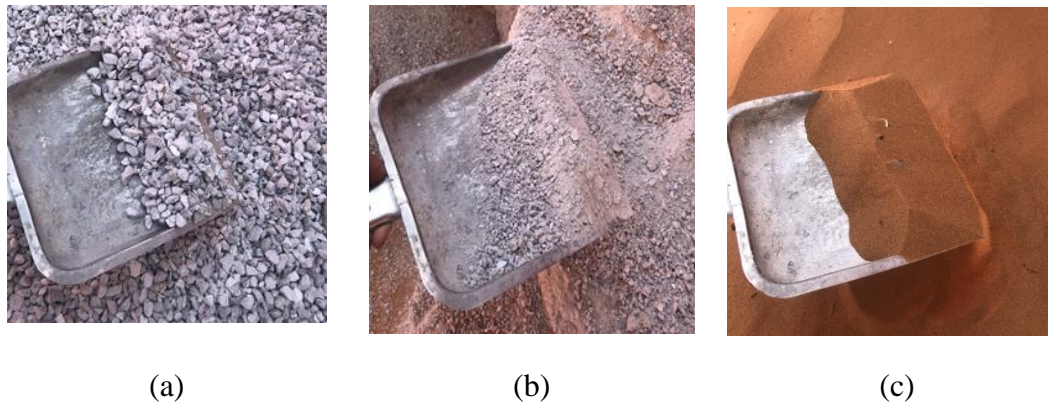


Figure 23: Aggregates used in the SCC mixture design. (a) coarse aggregate (9.5 mm), (b) crushed natural stone sand, and (c) dune sand.

Table 8: Aggregate sieve analysis.

Sieve size (mm)	Cumulative Passing %		
	Coarse Aggregate (10 mm)	Fine Aggregate (Crushed Sand)	Fine Aggregate (Dune Sand)
37.5	100	-	-
19	99.96	-	-
9.5	99.86	-	-
4.75	89.61	95.1	100
2.36	8.12	62	100
1.18	-	35.1	100
0.600	-	19.9	99.7
0.300	-	10.9	99.1
0.150	-	5.1	13.1

### 3.1.2 Cement

Cement is the main ingredient in the mixture design of SCC. OPC which conforms to ASTM C150 (2019) Type 1 and BS EN 197 (2011) CEM I was used. According to the manufacturer data sheet, the cement's specific surface area is 380 m<sup>2</sup>/kg with specific gravity equal to 3.15 as per the manufacturer data sheet. Chemical composition of the used cement is presented in Table 9 as determined by X-ray fluorescence (XRF).

Table 9: Chemical composition of OPC.

<b>Compound</b>	<b>. (%)</b>
CaO	73.08
SiO <sub>2</sub>	15.01
Fe <sub>2</sub> O <sub>3</sub>	4.25
MgO	4.25
SO <sub>3</sub>	4.10
Al <sub>2</sub> O <sub>3</sub>	1.97
Equiv. Na <sub>2</sub> O	0.59
Loss on Ignition	1.60
Insoluble Residue	0.90

### 3.1.3 Water

Potable water confirming to ASTM C1602 (2006) was used in mixing and curing all the SCC mixtures. This is to ensure that the water is reasonably free from such impurities as suspended solids, organic matter and dissolved salts, which may adversely affect the properties of the concrete.

### 3.1.4 Sewage Sludge Ash

Municipal sewage sludge utilized in this study was collected from Al Saad Wastewater Treatment Plant (WWTP) in Al Ain, UAE. Raw sewage sludge was homogenized and stored into labeled containers. The delivered raw sewage sludge had 8.38% moisture content. Sewage sludge was incinerated using a programmable electrical furnace at three different temperatures and for three different periods as summarized in Table 10. As shown in Figure 24, a change in the SSA particles color

was observed when the temperature was raised from 700°C to 1100°C. The produced granular particles of the incinerated SSA particles were ground using a disc-type grinder to reduce particle size and increase its fineness and were placed in tightly sealed containers to prevent contact with any source of moisture. A total of nine samples of finely ground SSA were obtained. After incineration, the SSA water absorption for all the particles was about 60%. Further characterization of SSA will be discussed in detail in Chapter 4. Figure 25 represents the disc-type grinder used for grinding, and the ground SSA particles.

Table 10: Incineration temperature and time for sewage sludge samples.

Sample I.D.	Incineration Temp. (°C)	Incineration Duration (hr)
RSS	Raw sewage sludge	
SSA7-2	700	2
SSA9-2	900	2
SSA11-2	1100	2
SSA7-4	700	4
SSA9-4	900	4
SSA11-4	1100	4
SSA7-6	700	6
SSA9-6	900	6
SSA11-6	1100	6



Figure 24: Incinerated SSA particles before grinding.



(a)

(b)

Figure 25: SSA grinding. (a) Disc-type grinder, and (b) ground SSA.

### 3.1.5 Admixtures

In this thesis, in order to produce a SCC mixture, two types of admixtures were used namely: Superplasticizer (SP) and viscosity modifying admixtures (VMA). Both types were obtained from the chemical company BASF. As recommended, prior of using admixtures in the mixture, the admixtures were mixed with the mixing water. The optimum dosage of these admixtures for yielding the best fresh properties was determined based on trial mixtures. Both types are supplied in the form of a liquid, water soluble compounds. A polycarboxylic ether-based SP (Glenium® sky 504) which conforms to Type G in ASTM C494 (2013) and Type 2 in ASTM C1107 (2012) was used in the study. The amount used varied from 1.6% to 2.4% by weight of the binder content. A high molecular weight synthetic co-polymer VMA (RheoMATRIX® 110) was used in the preparation of the SCC mixtures studied in this thesis. The dosage varied from 0.35% to 0.6% by weight of the binder content. The properties of the used SP and VMA were provided by the manufacturer and are illustrated in Table 11.

Table 11: Typical properties of chemical admixtures as obtained from supplier. (Manufacturer's datasheet).

	<b>Superplasticizer</b>	<b>Viscosity modifying admixture</b>
Appearance	Whitish to straw colored liquid	Brownish liquid
Specific gravity	1.115 at 25°C	1.010 g/cm <sup>3</sup>
Chloride content	“chloride free” to EN 934-2	<0.1%
Alkali content (as NaO equivalent)	0.26%	-

### 3.2 Methods

The experimental procedure in this thesis was divided into two main phases. The first phase included tests to characterize SSA, while the other phase focused on examining the performance of SCC in its fresh and hardened stages. The methods used in this research are explained in detail in the following sub-sections.

#### 3.2.1 Phase 1: Characterization of SSA

The aim of this phase is to study and understand how SSA affects the performance when used in cement paste/mortar, and to relate the effect of SSA content on actual modifications of microstructure and performance.

##### 3.2.1.1 X-Ray Diffraction (XRD)

X-ray diffraction (XRD) analysis is a study of the crystal structure, it is usually used to detect the presence of the crystalline phases in a material and thus reveal the chemical composition information. A beam of X-rays is projected into the sample, and

the way the beam scatters the atoms in the pathway of the X-ray is scrutinized. The scattered X-rays interfere with each other. This interference can be observed by using Bragg's Law to determine different characteristics of the crystal or polycrystalline material (Rajeshkumar et al., 2019). Figure 26 illustrates how diffraction of x-rays by crystal planes allows one to derive lattice spacings by using the Bragg's law as per Equation (1).

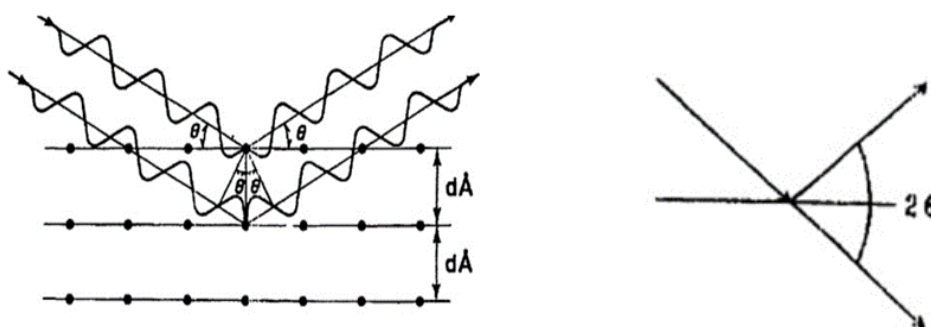


Figure 26: Diffraction of x-ray crystal planes. (Misture and Snyder, 2001).

$$2d \sin \theta = n \lambda \quad (1)$$

Where;  $n$  is an integer called the order of reflection,

$\lambda$  is the wavelength of x-rays (m),

$d$  is the characteristic spacing between the crystal planes of a given specimen (m),

and  $\theta$  is the angle between the incident beam and the normal to the reflecting lattice plane.

In this thesis, XRD analysis was performed on the ground SSA samples incinerated at different temperature and time. XRD analysis was carried out using a

PANalytical X'Pert PRO powder diffractometer equipped with a Cu K $\alpha$  source. The diffractometer was operated at 45 kV and 40 mA, with a copper (Cu) anode ( $\lambda(K\alpha_1) = 1.5406$ ,  $\lambda(K\alpha_2) = 1.5444$ ). Scans were recorded for  $2\theta$  from 20 to 60°C, steps of 10°. Identification of phases is achieved by comparison of the acquired data to that in reference databases.

### **3.2.1.2 X-Ray Fluorescence**

X-ray fluorescence (XRF) is a process whereby electrons are displaced from their atomic orbital positions, releasing a burst of energy that is characteristic of a specific element. This release of energy is then registered by the detector in the XRF instrument, which in turn categorizes the energies by element.

In this thesis, the major oxides of incinerated sewage sludge ash were found by XRF spectrometer on nine powder samples using Shimadzu (model EDX-7000). Before conducting the analysis, the samples were pressed into pellets, thus producing a flat smooth, and dense sample for testing; which gives more accurate results than loose powder samples.

### **3.2.1.3 Scanning Electron Microscopy**

The first commercial scanning electron microscopies (SEMs) became available in the 1960's. SEM and its add-on microanalytical unit, commonly known as the energy dispersive x-ray analyzer (EDXA), do not fall under the domain of any standard procedure. It's a relatively new technique which is yet to be universally accepted by the concrete technologists as an investigative tool. One of the first application of SEM in cement hydration study was done by Gupta, Chatterji, and Jeffery in the early 1970

(Gupta et al., 1970). Following the development of EDXA, Diamond (1976) shed the light on the benefits of this SEM attachment in the microanalysis of concrete. Since then many investigators have practiced and enhanced the technique of concrete examination using SEM-EDXA (Diamond, 1986).

In this thesis, the morphology of incinerated SSA particles was evaluated using SEM (Model – JEOL- JSM-840A). SSA powder samples were prepared by placing the powder on a double-sided tape. Since the samples tend to be nonconductive, they had to be coated with a thin layer of electrically conductive material based on the requirements of the compositional analysis. All samples were placed directly on a carbon tape and gold (Au) coated. The samples were sufficiently dry in order to avoid the evaporation of moisture in the sample under the high vacuum in the microscope, thus deteriorating the vacuum in the SEM column and affecting the efficiency of the electron beam. The morphology of the SSA was recorded with 10-20 kV anode voltage accelerated voltage and X1,000 magnification level. Moreover, the EDXA attached to the SEM device was used to detect the elements associated with the SEM morphology photographs.

#### **3.2.1.4 Pozzolanic Activity**

The pozzolanic activity of a material is a measure of its ability to react with calcium hydroxide. According to Massazza (1998), the total quantity of calcium hydroxide with which pozzolanic material can combine depends on the nature and content of reactive phase in the pozzolan, SiO<sub>2</sub> content of reactive phases, ratio of calcium hydroxide and pozzolan, and duration of curing. Methods for assessing



pozzolanic behavior may be direct or indirect, with the former measuring the consumption of calcium hydroxide and the latter measuring strength development.

Two tests were conducted to evaluate the pozzolanic activity for the incinerated SSA including the Frattini test (BS EN 196-5, 2011) and the strength activity index (SAI) test. In the Frattini test, activity is assessed by monitoring the consumption of calcium hydroxide. On the other hand, SAI test is performed by replacing a standardized proportion of Portland cement with the tested pozzolan and comparing strength development against an equivalent 100% Portland cement mix. Both tests will be explained in detail in the following subsections.

#### **3.2.1.4.1 Frattini Test**

Frattini test is a direct test to investigate the pozzolanic activity of the material. Frattini test was conducted according to the procedures described in BS EN 196-5 (2011) on the incinerated SSA samples to detect any pozzolanic activity it exhibits. The control specimen was prepared with 100% OPC mixed and 100 ml of distilled water. Nine tested specimens were composed of 80% of OPC and 20% of SSA incinerated at different temperature and time mixed with 100 ml of distilled water. Samples were left for 8 days and 28 days in a sealed plastic bottle in an oven at 40°C. Solutions were cooled to ambient temperature and vacuum filtered through a 2.7 $\mu$ m nominal pore size filter paper (Whatman no. 542). The filtrate was analyzed for [OH<sup>-</sup>] by titration against dilute HCl with methyl orange indicator and for [Ca<sup>2+</sup>] by pH adjustment to 12.5, followed by titration with 0.03M EDTA solution using Patton and Reeders indicator. Results are presented as a graph of [Ca<sup>2+</sup>] expressed as equivalent [CaO] in mmol on the y-axis versus [OH<sup>-</sup>] in mmol on the x-axis. The solubility curve

of  $\text{Ca}(\text{OH})_2$  was plotted and compared to the control sample of 100% OPC. Thus, making sure that the results laid on the same saturation curve. Test results lying below this line indicate removal of  $\text{Ca}^{2+}$  from solution which is attributed to pozzolanic activity. Results laying on the line are indicative of zero pozzolanic activity and results laying above the line correspond to no pozzolanic activity. It should be noted that this procedure assumes no other source of soluble calcium is present in the system, as leaching of calcium would invalidate this approach. The theoretical maximum  $[\text{CaO}]$  concentration can be calculated using the formula given in BS EN 196-5 (2011) (Equation (2)) to plot the lime solubility curve:

$$[\text{CaO}] = \frac{350}{[\text{OH}]^{-15}} \quad (2)$$

#### **3.2.1.4.2 Strength Activity Index**

The SAI test is an indirect test used to detect if a material exhibits any pozzolanic activity. The SAI test was carried out on square mortar moulds with internal dimensions of 50 x 50 x 50 mm according to ASTM C311 (2012) standards. Control mortar was prepared by mixing 500 g of OPC, 1375 g of crushed sand sieved on 0.6 mm sieve size and water volume of 242 ml. Test samples were prepared in the same manner, except that 20% of the OPC was replaced with the incinerated SSA. All specimens were demoulded after 24 hours and placed in a water bath at 23°C for 7 and 28 days. They were then removed from the bath, surface dried and tested for 7 and 28 day compressive strength.

Strength results reported are the averages of three tests and are presented as percentage strength relative to the control mortar with the SAI as per Equation (3).

$$SAI = \frac{A}{B} * 100 \quad (3)$$

Where A is the unconfined compressive strength of the mortars containing SSA (MPa), and B is the unconfined compressive strength of the control mortar (MPa).

If the indices at 7 or 28 days are higher than 75%, SSA can be considered as a good pozzolan (ASTM C618, 2012).

### **3.2.1.5 Particle Size Distribution**

Several methods are used to evaluate the fineness of cements or pozzolans such as determining their Blaine surface area, by finding out the amount retaining on 45  $\mu\text{m}$  sieve or by detecting the particle size distribution using laser diffraction. The Blaine air-permeability method might give misleading results especially for porous materials (Ravina, 1980). Also, only the continuous paths throughout the cement contribute to the measured surface area (Neville, 1995). On the other hand, the Blaine-air permeability method provides only a single value and supplies no information on the size of grains smaller than 45  $\mu\text{m}$ , therefore it might be insufficient in examining the fineness of the material. It was concluded that the laser diffraction method is more accurate and informative since it shows the particle size distribution of the material (Mindess et al., 2003).

Laser diffraction measures particle size distributions by measuring the angular variation in intensity of light scattered as a laser beam passes through a dispersed particulate sample. Large particles scatter light at small angles relative to the laser beam and small particles scatter light at large angles. The angular scattering intensity

data is then analyzed to calculate the size of the particles responsible for creating the scattering pattern, using the Mie theory of light scattering. The particle size is reported as a volume equivalent sphere diameter.

In this study, the particle distribution was recorded using Bechman Coulter, LS 13320 XR laser diffraction particle size analyzer. Its measure range of particle sizes is from 0.005 to 2500  $\mu\text{m}$ .

### **3.2.1.6 Workability and Workability Retention**

To have a better understanding of the effects of incorporating SSA on flowability, the workability of a cement paste including SSA was measured using flow table test. Samples were prepared according to ASTM C1437 (2019). Control cement paste was a mix of 500 g of OPC and 165 ml of water. Test pastes contained incinerated SSA replacing 20% of OPC. The test apparatus and procedures of mortar workability, i.e., flow table spread (FTS), conformed to ASTM C230/ASTM C1437 specifications and ASTM C109 (2012) test method, respectively. Cement paste was placed in a conic mold centered on the flow table as shown in Figure 27 (a). Then, the mold was immediately removed (Figure 27 (b)), the table was dropped 25 times in 15 seconds, and the flow spread was measured as in Figure 27 (c) and according to Equation (4).



(a)

(b)

(c)

Figure 27: Flow table test

The FTS of the pastes was calculated as follows (Equation (4))

$$\text{FTS \%} = \text{increase in average base diameter of paste mass} \quad (4)$$

Furthermore, the ability of the cement pastes to preserve its flowability is an important parameter to be measured and it is defined as workability retention. The consistency retention of incinerated sewage sludge ash was examined, and the change of workability for each paste was measured at different time intervals (0, 15, 30, 45, and 60 mins). To avoid initial setting of the pastes, sample was re-mixed before measuring the workability retention at different time intervals.

### 3.2.1.7 Isothermal Conduction Calorimetry Test

When Portland cement is mixed with water, heat is liberated. This heat is called the heat of hydration, the result of the exothermic chemical reaction between cement and water. The heat generated by the cement's hydration raises the temperature of concrete. It is most influenced by the proportion of  $C_3S$  and  $C_3A$  in the cement. Besides, it is influenced by water-cement ratio, fineness and curing temperature. As

each one of these factors is increased, heat of hydration increases. The heat of hydration of cement is directly measured by monitoring the heat flow from the specimen when both the specimen and the surrounding environment are maintained at approximately isothermal conditions. Isothermal Conduction Calorimetry (ICC) was conducted on three samples including a control mix without the addition of SSA (100% OPC), and two OPC samples blended with 20% and 40% of SSA9-2. Test were based on ASTM C1679 (2017) and were conducted by a model Calmetrix, I-cal 2000 HPC. The heat evolution was measured under a constant temperature set at 21°C. Since most heat was generated at the early stages and the peak evolution rate normally occurred within 60 hours, the hydration heat was continuously monitored for a period of 60 hours. Each reported result is the average of measurements from two specimens. Figure 28 shows the ICC test apparatus.

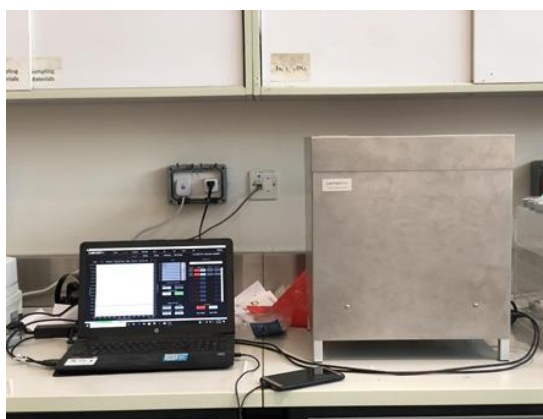


Figure 28: Isothermal Conduction Calorimetry (ICC) test apparatus.

### 3.2.1.8 Mercury Intrusion Porosimetry (MIP)

Mercury intrusion porosimetry (MIP) is a technique used for the calculation of porosity, pore size distribution, and pore volume to characterize a wide variety of porous materials. It employs a pressurized chamber to force a not wetting liquid (i.e. mercury) to intrude into the voids in a porous substrate. As pressure is applied, mercury fills the larger pores first. As pressure increases, the filling proceeds to smaller and smaller pores. Both the inter-particle pores (between the individual particles) and the intra-particle pores (within the particle itself) can be characterized using this technique.

To investigate the effect of SSA on the microstructure development, MIP was conducted on OPC, 20% SSA, and 40% SSA pastes at late ages i.e. 28 and 56 days of curing. The specimens were prepared for performing the test according to BS EN 7591 (1992) Part 1. After reaching the required curing ages, the specimens were cut into small pellets of about 1 cm<sup>3</sup>. These measurements were performed with a pressure of up to 60,000 psi, setting of contact angle of 140 degrees, and a constant surface tension of mercury of 480 dynes/cm. The pore size distribution, total porosity, and median pore diameter of the samples were obtained, and the results were reported as the average of two measurements. Since this method usually underestimates pore size (Diamond, 2000), it was used just for comparative purposes, and not for the absolute determination of pore size distribution.

#### **3.2.1.9 Leachability of Heavy Metals (TCLP)**

Based on the results obtained from the XRD, XRF and SEM tests, that SSA included trace amount of heavy metals. The leaching metals were investigated using toxicity characteristic leaching procedure (TCLP) test according to EPA method 1311 (EPA, 1992). Target metals include Cd, Cr, Pb, As, and Ba as these are the ones with specified permissible limits. If the value of a leached metal is higher than the allowable limits, then the material is considered hazardous.

The TCLP test was conducted at 7 and 28 days of curing for various samples including crushed pastes (0% SSA, 20% SSA, and 40% SSA), incinerated SSA particles at 900°C for 2 hours, and distilled water. Samples were ground to less than 1 mm in size. Then, 1 gram of the ground samples were stirred with 20 ml distilled water for 5 minutes as shown in Figure 29 (a, and b) . Based on EPA method 1311, the



type of fluid to mix the sample with depends on the pH measure. All the samples had a pH value more than 5. Hence, 0.75 ml of HCl was added to the mixture as in Figure 29 (c), and heated at 50°C for 2 mins, then the pH value was measured again. All samples had a pH less than 5. Five grams of each sample was added to 0.01 liters solution that consisted of 5.7 ml of  $\text{CH}_3\text{CH}_2\text{OOH}$  to 1 liter of reagent water. The samples were left for 24 hours to be mixed using a shaker and filtered to test metal's leachability by the geology labs at UAE University.

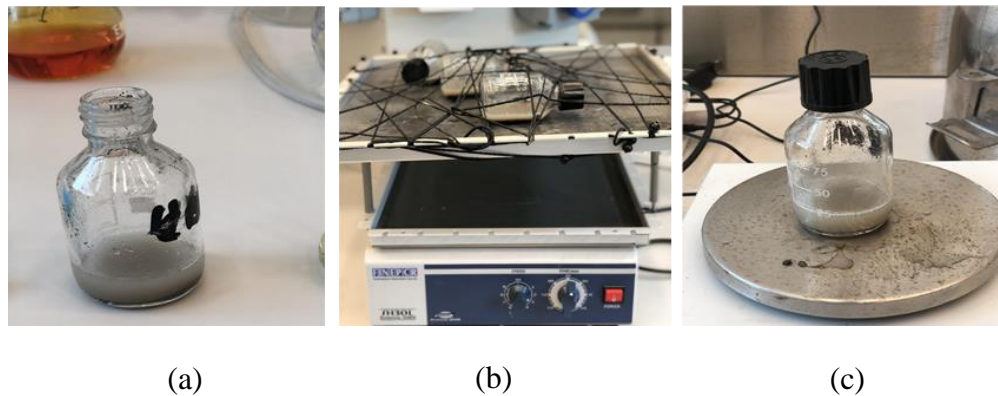


Figure 29: TCLP test procedures.

### 3.2.2 Phase 2: Reusing Sewage Sludge Ash to Produce SCC

#### 3.2.2.1 Mix design Principle and Approach

Based on EFNARC specification, a concrete mixture is defined as SCC by fulfilling three fresh requirements including flowability, passing ability, and segregation resistance. Since self-compactability is largely affected by the characteristics of materials and the mix proportions, it becomes necessary to evolve a procedure for mix design of SCC. Guidelines and specifications to be followed were set on how to adjust a concrete recipe to achieve the desired fresh properties

- The fluidity and viscosity of the produced SCC mixture mainly depend on the type and proportions of cementitious materials used. Hence, paste adjustments should be made to ensure proper fluidity of the mix.
- The water/binder ratio increases the flowability yet increasing the water content would play a major role in reducing the compressive strength of the mixture and increasing the segregation/bleeding potential. Therefore, the addition of admixtures including SPs and VMA compensated the reduction of the water/binder ratio and maintained the flowability and cohesiveness of the mixture.
- For enhancing the fluidity of the SCC mixtures, the friction between the coarse aggregates was reduced. This could be done by increasing the fine to coarse aggregate ratios so that each individual coarse aggregate is fully coated with a layer of mortar for lubrication.

If the previous principles are followed, the produced SCC will differ from the conventional concrete in the following main facts:

- Increased fine to coarse aggregate ratio.
- Increased paste content.
- Low water/ binder ratio.
- Increased SP
- Use of VMAs.

### **3.2.2.2 Concrete Mix Proportions**

In this thesis, SCC mixtures were cast to investigate utilizing SSA as a partial replacement of OPC. Several SCC trials were conducted (R-20T, R-40T1, and R-

40T2). However, a total of three adjusted SCC mixtures were cast (R-0, R-20, and R-40). Mixtures identification ID was R-X, where R stands for replacement. However, for trial mixtures, the ID was R-XT where T stands for trails.

As summarized in Table 12, one control mixture without addition of SSA (R-0) and five SCC mixture with SSA incinerated at 900°C for 2 hours (R-20T, R-20, R-40T1, R-40T2, and R-40) were designed to have a constant w/cm ratio of 0.35 and a total cementitious content of 500 kg/m<sup>3</sup>. These parameters were not altered in this research to eliminate their effects on the results and to inspect the effect of SSA on the performance of the produced SSA. The control mixture contained only OPC whereas the other mixtures incorporated 20% (R-20T, R-20) and 40% (R-40T1, R-40T2, and R40) SSA as a partial replacement of OPC on the total mass basis of the cementitious content. In the control mix (R-0) and trial mix of 20% SSA replacement (R-20T), the fine aggregate-to-total aggregate ratio, by mass, was set at 0.50 and the dune sand-to-total fine aggregate ratio was set at 0.55. Furthermore, the dosage of SP and VMA for these mixtures was set at 1.6% and 0.35% respectively by weight of OPC. However, the necessary workability condition for the trail SCC mix containing 20% SSA as a partial replacement of cement (R-20T) was not achieved. Therefore, SCC mixture (R-20) was modified to have a dune sand -to- total fine aggregate ratio of 0.45. Moreover, the admixtures dosages were increased to 2.0% and 0.5% for both SP and VMA respectively by weight of cementitious content (i.e. OPC + SSA). The first trial mixture of SCC containing 40% SSA (R-40T1) had the same mixture proportions as SCC with 20% replacement of OPC (R-20), except for replacing 40% of OPC with SSA. Yet, the mixture didn't meet the requirements set by EFNARC specifications in terms of flowability. Thus, another trial mix was conducted (R-40T2) where the fine



### 3.2.2.3 Procedure of Mixing

EFNARC recommendations for the order of concrete ingredients to be mixed using a forced action mixer were followed. This includes the addition of aggregates and cement to the mixer together. Followed by major portion of mixing water and SPs. Finally, VMA was added with the remaining mixing water. All mixing was completed within seven minutes (EFNARC guidelines recommend a minimum of four minutes). The mixing time of SCC was longer than the mixing time of the conventional concrete to ensure the full activation of the SP. The detailed steps of the mixing procedure of SCC are as follow:

1. Based on the batch quantities calculated for each SCC mixture, constituent materials were weighed separately.
2. The weighing process of the ingredients for each mixture took place one day before the mixing, except for cement, water, and admixtures that were freshly weighed on the mixing day. Due to the hot weather, the water and admixture were weighted at the end, to prevent evaporation, and thus ensuring the accuracy of their weights.
3. Dry ingredient including both types of aggregates and cementitious materials were first allowed to be mixed for 1 minute before the addition of water.
4. Nearly 70% of the mixing water content was added to the previously mixed dry ingredients.
5. The mixture was mixed for one and a half minute to obtain a uniform mixture with good consistency.
6. SP was added to the remaining mixing water and 20% of the water was added to the mixture. The addition of the remaining amount of mixing water and

admixtures at later stages will increase the consistency to the required level while avoiding “balling”.

7. After 2 and a half minutes, VMA was dispensed with the remaining amount of mixing water. The procedure of adding VMA at a later stage is a preferred practice suggested by EFNARC (2005) guidelines.
8. Ingredients were mixed in the mixer for an additional one and a half minute to ensure all components were efficiently mixed, resulting in a homogeneous fresh concrete.

#### **3.2.2.4 Order of Conducting Fresh Tests**

After mixing, fresh stage tests of slump flow,  $T_{50}$ , J-ring, L-box, and V-funnel were conducted to ensure acceptable flowability, passing ability, and cohesiveness were obtained. The order in which the fresh tests were conducted was maintained throughout all the three mixtures.

1. V-funnel.
2. Slump flow.
3.  $T_{50}$ .
4. J-ring.

#### **3.2.2.5 Fresh Concrete Tests**

The fresh stage of concrete means the wet mix of concrete ingredients before setting. It is the stage where concrete can be cast into any shape of construction. The easiness in casting the concrete mixture highly depends on the rheology and workability of the produced concrete. Rheology is an area of science that is concerned

with the deformation and flow of materials (O'hara et al., 2014). Several models that explain the rheological concrete characteristics exist, and the two most important parameters expressed in these models are: the yield stress; the extent to which a material deforms under a certain force, and the plastic viscosity; the material's internal resistance to flow. Workability is the property determining the effort required to manipulate a freshly mixed quantity of concrete with minimum loss of homogeneity.

The requirements of the SCC were achieved by the properties in its fresh state. The three common properties that characterize SCC mixtures are its filling ability, passing ability and viscosity. In the experimental phase of this thesis, all the fresh properties tests were conducted according to EFNARC specifications, ASTM, and ACI standards. Table 13 summarizes the tests conducted to measure SCC fresh properties, the corresponding parameters evaluated and the recommended values for each parameter. Prior to testing, all used apparatuses were cleaned, and their inner surfaces were dampened.

Table 13: SCC fresh properties. As per EFNARC (2005).

<b>Property</b>	<b>Test</b>	<b>Parameter</b>	<b>Recommended values</b>	
Filling ability	V-funnel	Tv (seconds)	8-12 (seconds)	
	Slump flow	SFD (mm) T50 (seconds)	550-850 (mm) 2-5 (seconds)	
Passing ability	J-ring	JRD (mm)*	0 to 25 mm	No visible blocking
			25 to 50 mm	Minimal to noticeable blocking
			>50mm	Noticeable to extreme blocking
	L-box	H2/H1	0.8 – 1.0	
Viscosity	V-funnel	Tv (seconds)	8-12 (seconds)	

\*The difference between slump flow and J-ring diameters according to ASTM C1621

### 3.2.2.5.1 Filling Ability

The filling ability is defined as the property of the concrete to flow under its own weight without any vibration provided intentionally. Slump flow and  $T_{50}$  tests were conducted to evaluate the filling ability of the produced SCC mixtures in accordance to EFNARC (2005) and ASTM C1611 (2018) standards.

Based on the test method for evaluating the conventional slump, the slump flow was used as a test to assess the horizontal free flow of SCC in the absence of obstructions. The slump flow test is considered to be a simple and a rapid test procedure which can be used easily on the site. To conduct the test, a flat smooth steel square base plate having a minimum diameter of 915 mm and the same truncated slump cone used for determining the slump of conventional vibrated concrete was used. A meter was also needed to measure the two spread diameters perpendicular to each other. To start the test, the plate was put on a leveled ground and dampened, and the cone was positioned centrally on the leveled plate. Then, the concrete was poured into the cone using shovels and scoops. In contrast to the conventional slump test, no tamping was done. The cone was then lifted, avoiding any lateral movements of interference with the flow of concrete. The higher the slump flow values the greater ability of the concrete to fill formwork under its own weight. A value of at least 550 mm is required to satisfactory achieve a SCC mix.

The  $T_{50}$  diameter test is another indication of the filling ability of the mix. The same apparatuses and procedures of the slump flow test were used, in addition to a stopwatch. The stopwatch was immediately started as the cone was raised and stopped when concrete reached the 500 mm circular mark on the plate. The time measured was



designated as  $T_{50}$ . A lower time indicates greater flowability. It is suggested that a time of 2-5 seconds is acceptable for a SCC mix.

### **3.2.2.5.2 Passing Ability**

This property shows the ability of the concrete to maintain its homogeneity. The J-ring test was used to assess this parameter. The test characterizes the passing ability of SCC through restricted spaces reinforcing bars. The J-ring test was performed following ASTM C1621 (2019). In order to conduct the test, the same apparatuses in the slump flow test were used, in addition to a circular steel ring of 300 mm diameter and 100 mm height. During the test, the J-ring flow diameter is measured in a procedure similar to that followed for determining the slump flow diameter. The freshly mixed concrete is poured in the cone oriented centrally inside the ring in an upright position with the aid of shovels and scoops. The cone is then raised maintaining a vertical movement, while the ring is kept in place for the concrete to spread through the steel bars. Figure 30 illustrates the apparatus and J-ring test. After the test, the difference in diameter between J-ring flow diameter and the corresponding slump flow diameter for the same mixture was calculated. According to ASTM C1621 (2019) blocking assessment, SCC mixtures is considered to have a good passing ability if the difference in slump flow to J-ring diameters is less than 25 mm, and a possible blocking if the difference in diameter is between 25 to 50 mm However, a difference of 50 mm indicates that the mixtures exhibited a poor passing ability.

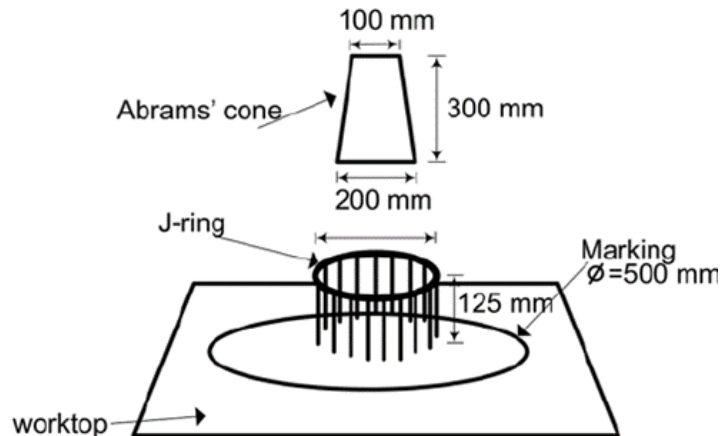


Figure 30: J-ring apparatus. (Nuruddin et al., 2011).

### 3.2.2.5.3 Viscosity

V-funnel test is used to determine the viscosity and the filling ability (flowability) of the concrete with a maximum aggregate size of 20 mm. The test was conducted following EFNARC guidelines. As shown in Figure 31, the test consisted of a V-funnel shape. The funnel is filled with about 12 liters of concrete and the surface was leveled with no tamping or rodding. Then, the time taken for it to flow through the apparatus was measured via stopwatch and denoted as the V-funnel time ( $T_v$ ). The shorter flow time indicates greater flow ability and less viscosity. For SCC a flow time of 8 to 12 seconds is considered appropriate.

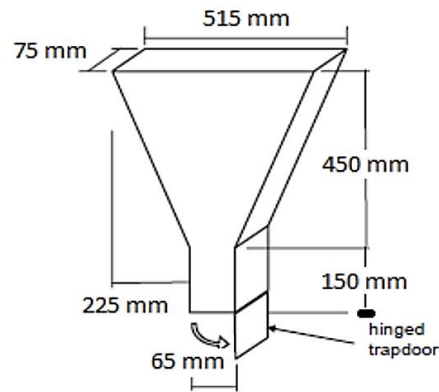


Figure 31: V-funnel test.

### 3.2.2.6 De-Moulding and Curing

After casting the SCC mixtures, the molded specimens were covered with plastic sheets for 24 hours. The control mix was de-molded after 24 hours and then water cured until the testing age. However, mixtures containing SSA didn't achieve enough strength to be demolded after 24 hours, due to the high dosage of VMA compared to the control mix, and therefore, were de-molded after 48 hours, then cured in tap water till the testing date.

### 3.2.2.7 Hardened Concrete Properties

As examining the fresh properties of a concrete mixture is significant for the handling and placing process of concrete; appropriately cured, hardened concrete needs to be strong enough to tolerate the structural and service loads which will be applied to it. Furthermore, it must be able to withstand the external environmental conditions. Hence, testing hardened concrete properties for quality check is an important task in the construction field. In this study, compressive strength and durability tests were conducted to evaluate the effect of incorporating SSA on the

strength and the service life of the produced SCC. These tests are discussed in detail in the following subsections.

### 3.2.2.7.1 Compressive Strength

The compressive strength of concrete is the most common performance measure by engineers in designing buildings and other structures. It is the ability of concrete to withstand the services and structural loads applied to it. The compressive strength of concrete is usually affected by various factors. However, it depends mainly on the w/c ratio, porosity, aggregate grading, texture and size, and the chemical composition of the cementitious materials used (Prajapati and Karanjit, 2019). The compressive strength of the specimen is calculated by dividing the maximum load attained during the test by the cross-sectional area of the specimen as in Equation (5).

$$f_c = \frac{P}{A} \quad (5)$$

Where  $f_c$  is the compressive strength (MPa),

$P$  is the maximum compressive load in N and  $A$  is the cross-sectional area of loaded surface ( $\text{mm}^2$ ).

The compressive strength test was conducted in accordance with BS EN 12390 (2009) standards using WYKEHAM FARRANCE compressive testing machine with a loading capacity of 2000 kN. Prior to casting, cube steel molds with a dimension of 100 mm were prepared by coating the interior faces with oil to avoid adhesion of concrete and for easier de-molding. After 24 hours of mixing, specimens were de-molded and left to cure. For each concrete mixture, three values of compressive

strength were measured at 7, 28, and 56 days of curing and the average was recorded. The compressive strength test is illustrated in Figure 32.



Figure 32: Compressive strength test.

#### **3.2.2.7.2 Durability**

Durability as stated in EFNARC (2005) guidelines is “the capability of a concrete structure to withstand environmental aggressive situations during its design working life without impairing the required performance”. Hence, good quality SCC must tolerate all types of deterioration resulting from either external or internal environment. A durable material helps the environment by conserving resources and reducing wastes and the environmental impacts of repair and replacement. Durability tests in this study were conducted at 28 and 56 days of curing age to examine the behavior of concrete’s durability with time. The durability characteristics of the produced SCC were evaluated using the tests described in the following sub-sections.

### 3.2.2.7.3 Bulk Resistivity

The transport of charged ions through the microstructure of concrete plays an important role in controlling its durability. Concrete's capability to resist the transfer of charged ions is highly dependent upon its electrical resistivity. Electrical resistivity of a material is defined as its ability to resist the transfer of ions subjected to an electrical field and it depends on the properties of concrete's microstructure such as pore size and shape of the interconnections (i.e., tortuosity) (Azarsa and Gupta, 2017). Lower permeability results from a finer pore network with less connectivity and eventually leads to higher electrical resistivity thus higher protection against steel corrosion. Several tests were developed to measure the bulk resistivity of concrete. In this study, Giatec RCON test has been adopted using an electrical resistivity meter. Fully saturated concrete cylinder with a dimension of 200 mm x 100 mm was placed between two conductive plates to which completely soaked sponge were attached. The test setup is presented in Figure 33. After that, the meter measured the resistance by determining the voltage and the applied current, which in turn was used to calculate the resistivity using Equation (6)

$$\rho = \frac{A}{L} * Z \quad (6)$$

Where  $\rho$  is the resistivity (k $\Omega$ .cm),

A is the cross-sectional area of the specimen [cm<sup>2</sup>],

L is the length of the specimen (cm), and

Z is the resistance measured by the device (k $\Omega$ ).

Electrical resistivity values obtained from Equation (6) can be used to judge the corrosion protection for steel bars embedded in concrete. Table 14 presents the interpretation of the resistivity values according to ACI 222R-01 (2010).

Table 14: Corrosion protection based on concrete resistivity. (ACI 222R-01, 2010).

Resistivity ( $k\Omega.cm$ )	Corrosion protection
<5	Low
5 – 10	Moderate – Low
10 – 20	High
>20	Very High



Figure 33: Electrical resistivity test setup.

#### 3.2.2.7.4 Initial Water Absorption (Sorptivity)

Sorptivity defines the ability of concrete to absorb water. Therefore, either the rate of inflow or the depth of water penetration is measured in sorptivity tests when water is allowed to be absorbed unidirectionally by dry concrete under a negligible applied pressure. It was first introduced by Hall in 1977 (Hall, 1977) where he

explained that the cumulative absorbed volume per unit area of the inflow surface ( $\text{m}^3/\text{m}^2$ ), named  $i$ , increases with the square root of the elapsed time ( $t$ ) with a constant of sorptivity ( $s$ ) as in Equation (7). The typical sorptivity values for concrete obtained by Hall (Hall, 1977) is presented in Table 15.

$$i = st^{0.5} \quad (7)$$

Table 15: Typical sorptivity values for concrete obtained by Hall (1977).

W/C	0.4	0.5	0.6
Sorptivity ( $\text{mm}/\text{min}^{0.5}$ )	0.094	0.120	0.170

In this thesis, the sorptivity of SCC mixtures was determined at 28 days and 56 days of curing according to ASTM C1585 (2013). Used specimens were discs from cast cylinders of 100 mm in diameter and approximately 50 mm in thickness. Before conducting the test, the discs were oven dried at  $110 \pm 5^\circ\text{C}$  for about 24 hours. Then the discs were removed from the oven to cool down to room temperature in a desiccator. The tested specimens were sealed with a vinyl electrical tape on their sides and their top surface, to prevent any water movement through the sides during the test, and to avoid water evaporation from the surface. The initial mass of the specimens after sealing was recorded. One surface of the specimens was in contact of water and it was rested on rods to allow free access of water. As soon as the specimens came in contact with water, time was recorded using a digital stopwatch. The water rises through the specimen by capillary rise. Then, the specimen was removed from the container, surface dried with a towel, and the mass was measured at fixed intervals of 1, 5, 10, 15, 20, 30, 60 mins. Then, the measurements were taken every hour, up to 6



hours. Finally, the rate of initial absorption was determined by first calculating the penetration depth from Equation (8) and Equation (9), then plotting the obtained penetration depth against the square root of the elapsed time. The slope of the graph is the sorptivity (i.e. rate of absorption). While the intercept of the graph is considered to be affected by the surface finish that influences the open porosity of the inflow surface and therefore causes these pores to get filled with water at the beginning of the test. The test is illustrated in Figure 34.

$$i = \frac{\Delta W}{\gamma \times A} \quad (8)$$

$$i = B + s\sqrt{t} \quad (9)$$

Where;  $i$  is the penetration depth (mm),

$\Delta W$  is the change in the specimen's weight (g),

$\gamma$  is the water density ( $\text{g}/\text{mm}^3$ ), and

$A$  is the cross-sectional area ( $\text{mm}^2$ ).

$B$  is the equation positive intercept,

$s$  is the rate of absorption (i.e. sorptivity) ( $\text{mm}/\text{min}^{0.5}$ ), and  $t$  is the exposure time (min).

As per ASTM C1585 (2013), the regression coefficient of Equation (9) shall not be less than 0.98, or else the test must be repeated as then the relation is not strongly linear.



Figure 34: Sorptivity test.

### 3.2.2.7.5 Permeable Pores

The connectivity of pores and the percentage of voids in the concrete is considered to be an important indicator of concrete's durability. An interconnected pore system with high porosity allows fluids to transport through the concrete; thus, contributing to the permeability of the concrete which will allow the ingress of the different aggressive species. The ingress of these species will result in concrete deterioration which in turn will reduce the service life of concrete. Therefore, a proper curing, sufficient cement, and proper compaction could minimize the percentage of permeable pores. In this study, the percentage of permeable voids in the produced SCC was measured according to ASTM C642 (2013). The permeable pore test was conducted on concrete discs (100 mm diameter and 50 mm thick) at 28 and 56 days of curing. The volume of the specimens conformed to ASTM C642 (2013). At the test age, the specimens were oven dried for 24 hours at a temperature of 110°C and then left to cool down using a desiccator till they reach room temperature (25°C). The dry mass of the specimens was recorded and denoted as  $W_{dry}$ . After that, the specimens were immersed in water at approximately 21°C for not less than 48 hours. Surface moisture were removed with a towel and the mass was determined and designated as

$W_{wet}$ . The surface dried specimens were then placed in a suitable receptacle covered with tap water and boiled for 5 hours. Specimens were allowed to cool by natural loss of heat for 24 hours to reach a final temperature of 25°C. Again, the surface moisture was removed using a towel and the mass after boiling was measured and recorded as  $W_{boiled}$ . Finally, to determine  $W_{submerged}$ , the specimens were suspended by a wire and the apparent mass in water was measured. The percentage of permeable pore spaces was calculated as per Equation (10).

$$\% \text{ of permeable pores} = \frac{W_{boiled} - W_{dry}}{W_{boiled} - W_{submerged}} \times 100 \quad (10)$$

#### **3.2.2.7.6 Water Permeability**

Water is common to most of the durability problems in concrete. The presence of water, or its involvement in the reactions is necessary for the problems to occur. Thus, the durability of concrete is intrinsically related to its water tightness, or permeability. Although the permeability of concrete is not a direct measure of its durability, yet a high permeable concrete indicates that the concrete is unable to withstand the ingress of materials, thus it is not classified as a durable concrete.

The permeability of concrete is a function of the permeability of the cement paste, of the aggregate, and of the interfacial transition zone. Theoretically, permeability of these components is in turn related to the porosity. However, it is important to note that porosity and permeability need not be directly related, but the interconnectivity of pores is generally responsible for a high permeability.

The water permeability test was conducted for all SCC mixtures at 28 and 56 days of curing. Discs with 100 mm in diameter and 50 mm in thickness were cut from

SCC cylinders. Prior to testing, each disc was sealed within the permeameter cell, thus ensuring the flow of water is in one direction. The test was conducted using a water permeability machine. The apparatus was completely filled with water and a constant pressure head of 35 bar was applied. The volume of water collected at a specified time was recorded and the permeability coefficient was determined as per Equation (11) and Equation (12).

$$Q = \frac{V}{t} \quad (11)$$

$$k = \frac{QL}{AH} \quad (12)$$

Where;

V: Volume of water collected at a specified time (m<sup>3</sup>).

t: Time (sec).

k: coefficient of permeability (m/s).

Q: Flow rate of water (m<sup>3</sup>/sec).

L: length of the specimen (m).

A: Cross-sectional area of the specimen (m<sup>2</sup>).

H: Pressure head (m).

### 3.2.2.7.7 Drying Shrinkage

Drying shrinkage of concrete often induces cracking in reinforced concrete members, which may result in deterioration of durability in concrete structures. The amount of drying shrinkage is influenced mainly by the amount and type of aggregate and the water content of the mix. The greater the amount of aggregate is, the smaller is the amount of shrinkage. The higher the stiffness of the aggregate is, the more effective it is in reducing the shrinkage of the concrete.

In order to enhance the longevity of structures, it is very important quantitatively to estimate shrinkage in concrete as well as to control cracking at the design stage. The drying shrinkage was evaluated in this thesis according to ASTM C157 (2006). For each mixture, two concrete prisms with square cross-sectional area were cast having dimensions of 80 x 80 x 243 mm. Prior to casting, two steel studs were tightened into the end plates of the used steel molds. These studs act as the anchorage points where the hardened concrete prisms were fixed in the measuring device. The measured shrinkage was the linear shrinkage in the direction of the longitudinal dimension of the prism. SCC mixtures were cast in these prisms, demoulded after 24 hours, and left to cure. After 14 days of curing, the length change between the two steel studs was measured using a length comparator. During the measurement, the specimens were placed in the length comparator and gently spun until three readings were recorded and the average was calculated. The measurements were documented till 110 days (almost 18 weeks) at different time intervals (every two to three days for a week, then the interval was increased to a week until four weeks and then once a month). Ambient conditions in the lab during the test period ranged

from 40% to 60% for the relative humidity and 25-35°C for the temperature. Test setup is shown in Figure 35. The shrinkage strain was calculated using Equation (13).

$$\text{Shrinkage Strain} = \left[ \frac{L_f - L_{14}}{L_o} \right] \quad (13)$$

Where;  $L_o$  = the initial length of the prism (243 mm),

$L_f$  = the length at test day,

and  $L_{14}$  = the length of the prism at 14 days of age (when drying started).



Figure 35: Drying shrinkage test setup.

### 3.3 Performance Index Approach

The performance index (PI) is a management tool that allows multiple sets of information to be compiled into an overall measure. The philosophy behind using

performance indices is simple; the method condenses a great deal of information into just one number (Jordan et al., 2001). The performance index method is adopted to facilitate the selection process of the incineration temperature and duration to produce the most suitable SSA to be used in making concrete, and the best suitable SCC mixture. For each individual criterion, a weight ranking ( $W_i$ ) is calculated in such a way that the mixture achieving the best test value (i.e. highest value) in a certain criterion scores 1.00, and the rest of the mixtures' test values are proportioned to that best value, thus their weight ranking will be  $\leq 1.00$ . Equation (14) represents the calculation of the weight ranking. However, for specific criteria; where the lowest value is the best value, then weight ranking ( $W_i$ ) is calculated as shown in Equation (15).

$$W_i = \frac{\text{Measured performance for each mixture}}{\text{Best measured performance}} \quad (\text{Larger is better}) \quad (14)$$

$$W_i = \frac{\text{Best measured performance}}{\text{Measured performance for each mixture}} \quad (\text{Smaller is better}) \quad (15)$$

The second step toward the completion of the PI approach is the computation of a numeric index ( $R_i$ ). The highest numeric index used in this study is set to 5.00. For each individual incinerated SSA, the corresponding numeric index is the product of the previously calculated weight ranking  $W_i$  and 5.00 as presented in Equation (16).

$$R_i = 5W_i \quad (16)$$

Finally, based on the required performance criteria ( $n$ ), the related  $R_i$  are multiplied to calculate a single index ( $S_n$ ) as per Equation (17) for each SSA produced

and SCC concrete including SSA replacement. The PI is calculated for each SSA sample/ SCC mixture as the percentage of the sample / mixture index ( $S_n$ ) with respect to the highest index of all SSA samples / SCC mixtures ( $S_{nmax}$ ) as per Equation (18). SSA incinerated at different temperature and duration, and SCC mixture achieving a PI of 100% is designated as the optimal SSA selection with respect to incineration temperature and duration, and the optimal content of SSA to produce SCC in terms of the corresponding required multiple criteria.

$$S_n = R_1 * R_2 * R_3 * \dots \dots R_n \quad (17)$$

$$PI = \frac{S_n}{S_{nmax}} * 100 \quad (18)$$

This approach can be used to select the optimal incineration temperature and duration to produce SSA that can be used as a partial replacement of OPC in making SCC. Also, this approach was used in phase 2 to identify SCC mixtures with different performance criteria in the fresh state or hardened state or both.

### 3.3.1 Tests Used for the Performance Index Evaluation in Phase 1

Performance index evaluation was performed to select the optimum incineration temperature and duration of SSA. The criteria used for the selection process were based on the pozzolanic reactivity, workability, and energy consumption of SSA. The sum of  $\text{SiO}_2$ ,  $\text{Al}_2\text{O}_3$ , and  $\text{Fe}_2\text{O}_3$  detected in the XRD analysis, SAI, and CH were used to judge SSA pozzolanic activity. The flow table spread test results were used to judge the workability and workability retention (60 mins) of cement pastes containing SSA. The energy consumption of the incineration process at different temperature and duration was calculated based on the model and type of the used



furnace (Nabertherm, muffle furnace L 3/12). It is worth mentioning here, that the lower energy consumption value was selected to have a score of 1.0.

### **3.3.2 Tests Used for the Performance Index Evaluation in Phase 2**

The criteria used for the selection process were the flowability (i.e., slump flow), viscosity (i.e., V-funnel), the 28 days compressive strength and the 28 days electrical resistivity. The flowability and viscosity were used to judge the concrete in its fresh state. The higher slump flow value was used to judge the flowability of fresh concrete. The higher viscosity value was selected to have a score of 1.0 since it leads to a better cohesiveness of the mix, thus lower segregation ability. The 28 days compressive strength was used to judge the mechanical property of the hardened concrete. The 28 days electrical resistivity was used to judge the hardened concrete durability. From the durability tests conducted in this study, the electrical resistivity was chosen to judge the durability since the test was simple and easy to conduct.

## **Chapter 4 : Results and Discussion - Phase 1 : Characterization of SSA**

### **4.1 Introduction**

The feasibility of using SSA in making SCC mixtures was studied by evaluating the characteristics of SSA incinerated at different temperature and time, and their effects on mortars strength, workability, workability retention, heat of hydration, and pore size distributions. Besides, the leachability of heavy metals from SCC made with SSA was assessed.

During this phase, raw sewage sludge was incinerated at different temperatures of 700°C, 900°C and 1100°C for 2, 4, and 6 hours. Then, the chemical, mineral compositions and morphology were measured using X-ray fluorescence (XRF), X-ray diffraction (XRD), and scanning electron microscopy (SEM), respectively. The pozzolanic activity of SSA particles was evaluated using Frattini and strength activity index (SAI) tests. The particle size distribution was measured using particle size analyzer. The effect of incorporating SSA as a partial replacement on mortars properties was examined by evaluating the workability, workability retention, heat of hydration and pore size distribution. Regarding the leachability of heavy metals when subjected to severe conditions, toxicity characteristic leaching procedure (TCLP) was conducted. The following sections show the results obtained from each test.

### **4.2 X-Ray Fluorescence (XRF)**

Several aspects of mortar casting, such as hydration degree and its rate, workability, or compressive strength will be affected by the existence of specific chemical compounds in cement or SSA (Krejcirikova et al., 2019).

Table 16 summaries the XRF analysis results obtained for incinerated SSA at different temperature and time.

The major constituents in all SSA samples were  $\text{SiO}_2$  (11.4–31.2%),  $\text{CaO}$  (10.6–23.5%), and  $\text{P}_2\text{O}_5$  (9.2–21.3%). The next most abundant components were  $\text{Al}_2\text{O}_3$  (4.2–9.7%),  $\text{Fe}_2\text{O}_3$  (3.5–6.4%),  $\text{MgO}$  (3.41–7.2%),  $\text{SO}_3$  (0.3 – 5.6%), and  $\text{K}_2\text{O}$  (0.5–1.3%), which are also major components of ordinary cement. Similar composition was also reported by Donatello et al. (2010). It is well known that pozzolanic activity is directly related to the chemical composition of the materials, since siliceous or siliceous-aluminous materials, if such compounds are present in amorphous state, react chemically with calcium hydroxide at room temperature, forming compounds that possess cementitious properties (Malhotra and Mehta, 1996).

Furthermore, it is notable that increasing the incineration temperature will result in a higher  $\text{SiO}_2$  content, since the highest  $\text{SiO}_2$  content (31.2%) was found when SSA was incinerated at 1100°C for 4 hours followed by SSA incinerated at 1100°C for 2 hours. Cyr et al. (2007) reported that the  $\text{CaO}$  content in SSA ranges from 1.1% to 40.1%, so all the SSA samples examined here were within the average range of other SSAs.  $\text{CaO}$  content in SSA could provide some hydraulic properties to the ash, while the presence of  $\text{SiO}_2$  and  $\text{Al}_2\text{O}_3$  could be responsible for some pozzolanic properties, hence supporting the feasibility to be used as a partial substitute of cement (Pekmezci and Akyüz, 2004). Hewlett and Liska (2019) stated that  $\text{P}_2\text{O}_5$  is occasionally present in small amounts in the raw materials of cement manufacture and in such case, it passes into the clinker. If present in quantities of 1–2% in Portland cement clinker it slows the rate of hardening of the cement. Since  $\text{P}_2\text{O}_5$  is one of the main components of SSA, the addition of SSA to the concrete may attribute to the increase of its setting time,

hardening and so may reduce its compressive strength. Furthermore, the total percent of SiO<sub>2</sub>, Al<sub>2</sub>O<sub>3</sub>, and Fe<sub>2</sub>O<sub>3</sub> and the percent of SO<sub>3</sub> could classify SSA as Class C type of pozzolan according to ASTM C618 (2012) classification of pozzolans shown in Table 17.

Table 16: XRF analysis for SSA samples.

<b>Oxide (%)</b>	<b>RSS</b>	<b>SSA 7-2</b>	<b>SSA 9-2</b>	<b>SSA 11-2</b>	<b>SSA 7-4</b>	<b>SSA 9-4</b>	<b>SSA 11-4</b>	<b>SSA 7-6</b>	<b>SSA 9-6</b>	<b>SSA 11-6</b>
SiO <sub>2</sub>	11.4	26.6	25.2	30.5	29.2	27.7	31.2	26.9	28.0	26.6
CaO	10.6	22.7	23.5	23.2	21.8	22.8	23.0	22.5	22.6	23.1
P <sub>2</sub> O <sub>5</sub>	9.3	20.3	21.3	20.0	19.1	20.2	19.8	20.2	20.2	20.3
Al <sub>2</sub> O <sub>3</sub>	4.2	9.3	9.6	9.7	9.1	9.54	9.5	9.3	9.4	9.1
Fe <sub>2</sub> O <sub>3</sub>	3.5	6.2	6.2	6.4	5.9	6.0	6.4	6.2	5.9	6.4
MgO	3.4	7.1	7.0	7.1	7.1	6.9	7.2	7.1	7.1	7.1
SO <sub>3</sub>	5.6	4.0	4.5	0.47	4.9	4.2	0.3	5.1	4.1	4.5
K <sub>2</sub> O	0.5	1.2	1.2	1.2	1.2	1.2	1.1	1.3	1.3	1.3
Sum of SiO <sub>2</sub> , Al <sub>2</sub> O <sub>3</sub> and Fe <sub>2</sub> O <sub>3</sub>	19.2	42.0	40.9	46.7	44.3	43.2	47.1	42.4	43.2	42.1

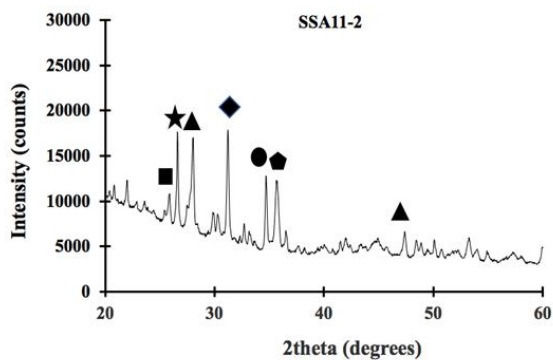
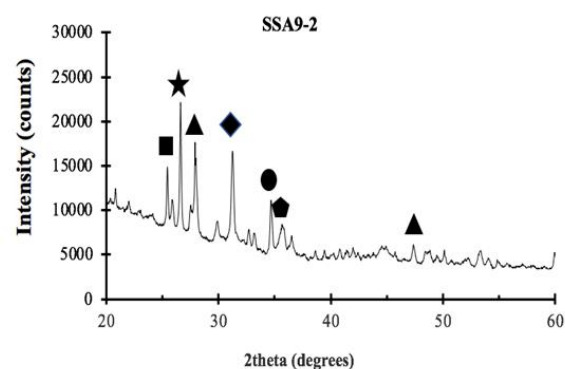
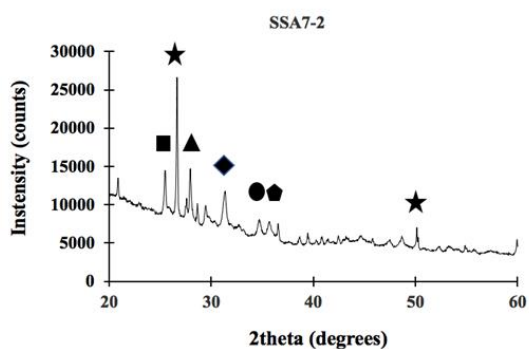
Table 17: Classification of pozzolans according to ASTM C618.

Description		N Class	F Class	C Class
SiO <sub>2</sub>	min (%)		54.90	39.90
SiO <sub>2</sub> + Al <sub>2</sub> O <sub>3</sub> + Fe <sub>2</sub> O <sub>3</sub>	min (%)	70.0	70.0	50.0
SO <sub>3</sub>	max (%)	4.0	5.0	5.0
Water content	max (%)	3.0	3.0	3.0
Incandescent lost	max (%)	10.0	12.0	6.0
Alkali as Na <sub>2</sub> O	max (%)	1.5	1.5	1.5
Pozzolan activity with 7 days	min (psi)	800	800	-
	min (kg/cm <sup>2</sup> )	56.25	56.25	-

### 4.3 X-Ray Diffraction (XRD)

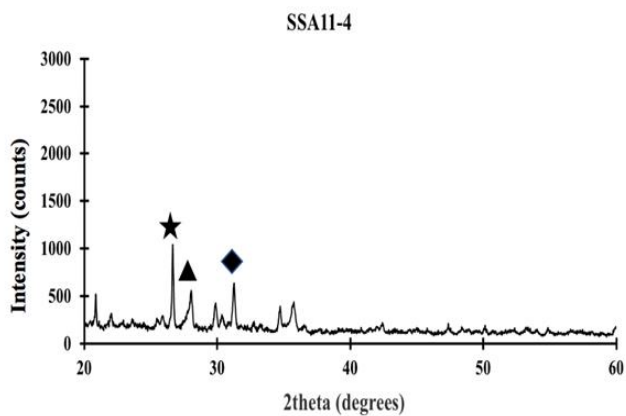
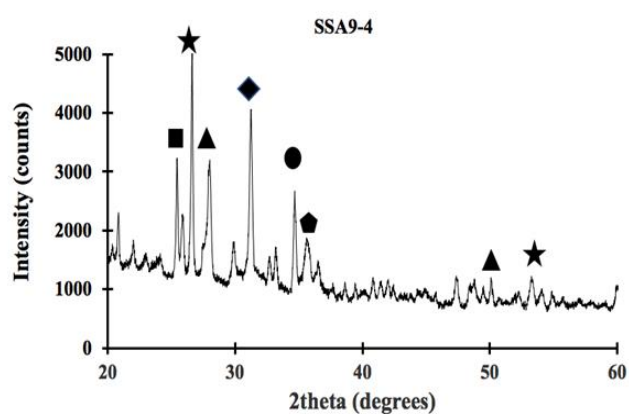
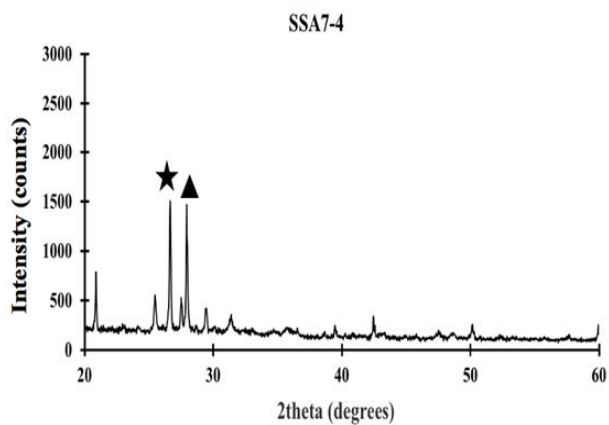
The mineralogical configuration of incinerated SSA was investigated using XRD analysis. The XRD results of all the samples are illustrated in Figure 36, 37 and 38. The predominant crystalline constituents of all SSA samples are identically quartz (SiO<sub>2</sub>) at 2 $\theta$  of 26.5°. This verified the obtained results of XRF that revealed the silicon oxide constituted the greatest percentage in the SSA particles composition. Other minerals were detected including mullite (Al<sub>1.272</sub>Si<sub>9.728</sub>O<sub>4.864</sub>), CaF<sub>2</sub>, calcite (CaCO<sub>3</sub>), whitlockite (Ca<sub>7</sub>Mg<sub>2</sub>P<sub>6</sub>O<sub>24</sub>) and dolomite (CaMgCO<sub>3</sub>). Cyr et al. (2007) reported that the amount of CaO and P<sub>2</sub>O<sub>5</sub> in SSA is high compared to classical mineral admixtures such as fly ash, silica fume or metakaolin and these elements are combined to form about 26% of whitlockite mineral observed in the XRD analysis. No other crystalline phases matched sufficient peaks to be positively identified. Additionally, the presence

of humps in the range between  $2\Theta$  values of 20 and  $30^\circ$  as well as the unlevelled graph trend from  $2\Theta$  values between 0 to  $40^\circ$  indicated the occurrence of some amorphous phases in SSA which will play a major role in increasing the tendency of SSA to exhibit pozzolanic activities and the potential of SSA to be used as a partial substitute of cement.



■ Mullite ★ Quartz ▲ CaF<sub>2</sub> ◆ Calcite ♥ Whitlockite ● Dolomite ◆ Fluorspar

Figure 36: XRD patterns for SSA incinerated for 2 hours.



■ Mullite ★ Quartz ▲ CaF<sub>2</sub> ♠ Calcite ♥ Whitlockite ● Dolomite ◆ Fluorspar

Figure 37: XRD patterns for SSA incinerated for 4 hours.

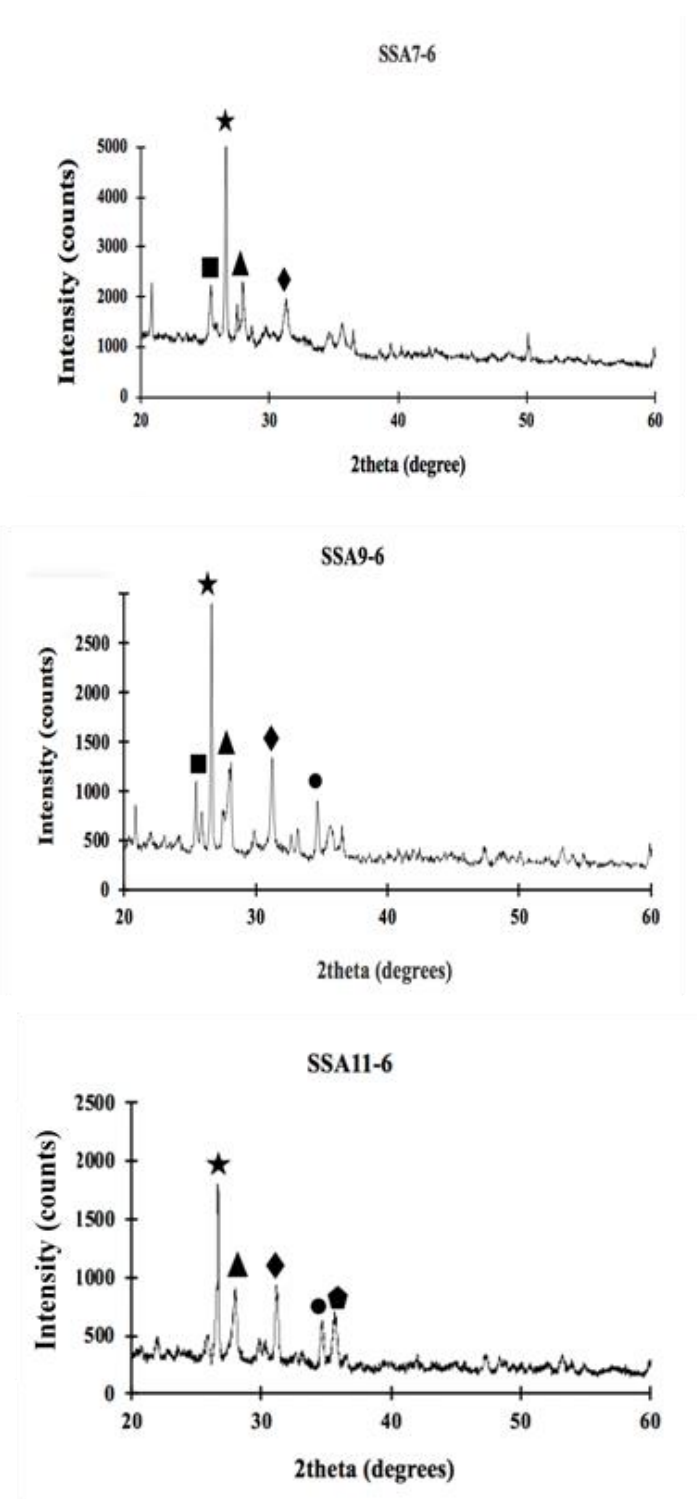


Figure 38: XRD patterns for SSA incinerated for 6 hours.



#### 4.4 Scanning Electron Microscopy (SEM)

The morphology of the incinerated SSA at different temperature and durations was investigated using scanning electron microscopy (SEM). Figure 39 shows the microstructure of incinerated SSA. It is observable that SSA particles were irregular with rough surfaces confirming the previous report by Donatello and Cheeseman, (2013). The irregular morphology of SSA particles might contribute to the reduction of workability of the concrete mixtures. Moreover, Figure 39 clearly showed that the pore structure of the particles became more compact as a result of increasing the incineration temperature from 700°C to 1100°C. This might be due to expansion or bloating of materials at high temperature and this is thought to be due to gas evolving decomposition. Also, it was noticeable from Figure 39 (e) that the shape of SSA contained some spherical like-particles and smoothed the particle's surface. Also, many finer grains peeled off from SSA particles. This phenomenon was possibly due to the compaction and agglomeration of fractured particles and peeled grains in the grinding process. To further understand the composition of the formed fracture surfaces, an EDS analysis was carried out. The EDS analysis presented in Figure 40 indicated the presences of silica (Si) and calcium (Ca); which showed the same mineral and chemical composition obtained from XRF and XRD analyses respectively, with similar concentration. In addition, heavy metals were detected in the ash particles, including copper (Cu), nickel (Ni), chromium (Cr), manganese (Mn), cobalt (Co), iron (Fe), titanium (Ti), and scandium (Sc). Thus, utilizing SSA in making concrete might participate in the leachability of these heavy metals, further investigation of the heavy metal's leachability is explained in this chapter.

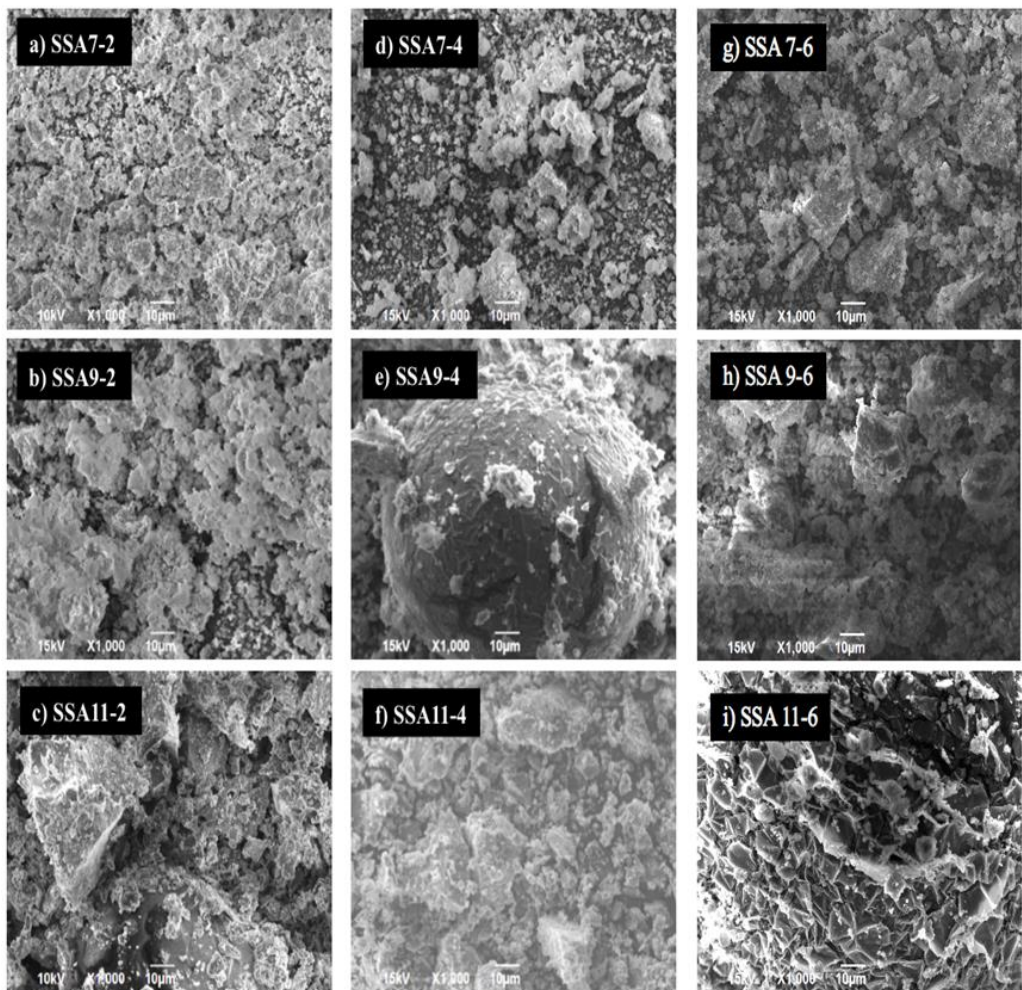
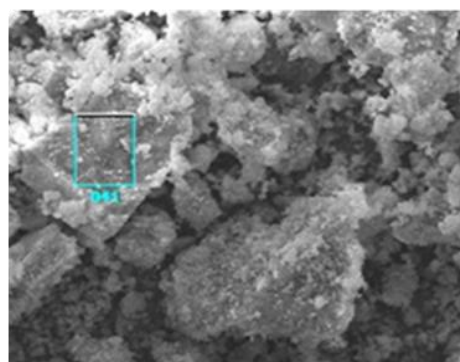
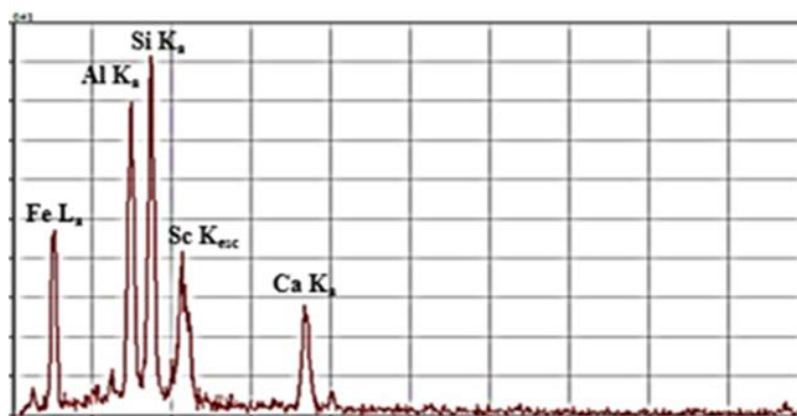


Figure 39: SEM images for SSA (X1000).

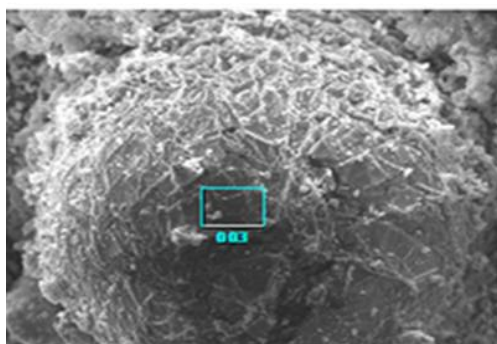
## SSA7-6



Element	%
Si	33.11
Ca	27.25
Al	22.2
Fe	2.28
Mg	1.65
Ni	1.60



## SSA9-2



Element	%
Ca	33.58
Al	2.08
Sc	11.44
Co	6.28
Mg	5.84

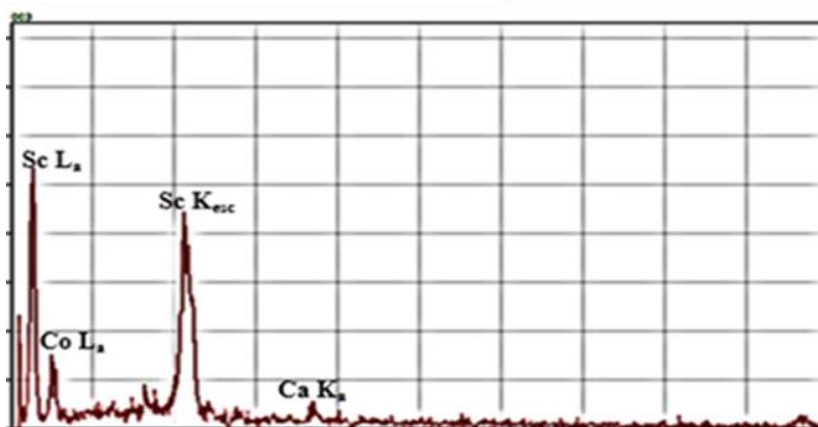
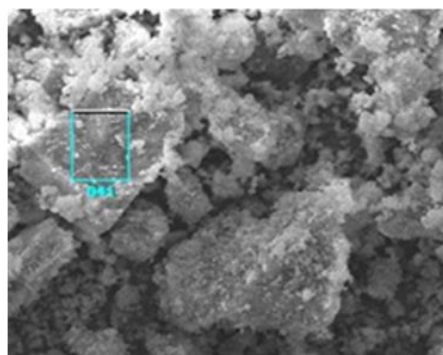
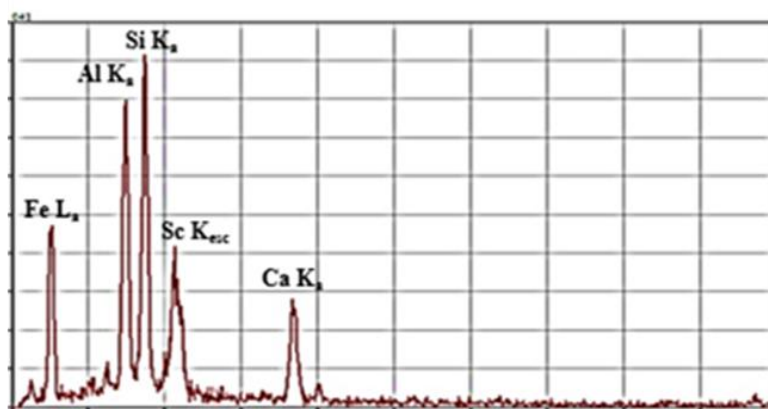


Figure 40: EDS analysis for SSA particles.

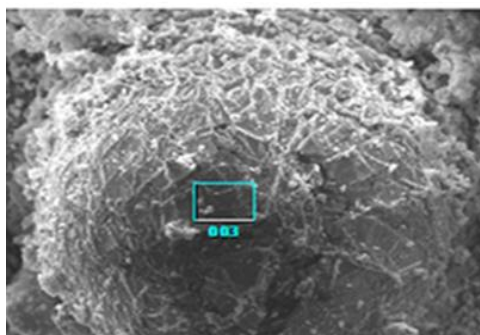
## SSA7-6



Element	%
Si	33.11
Ca	27.25
Al	22.2
Fe	2.28
Mg	1.65
Ni	1.60



## SSA9-2



Element	%
Ca	33.58
Al	2.08
Sc	11.44
Co	6.28
Mg	5.84

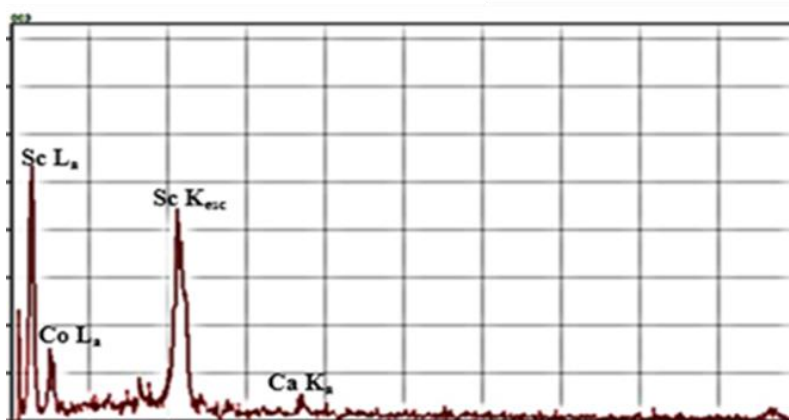
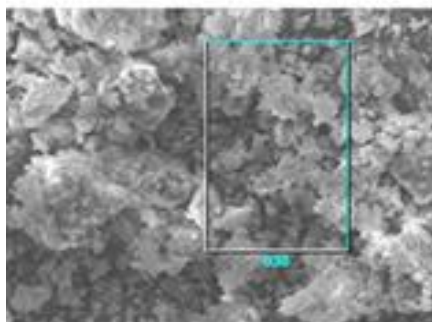
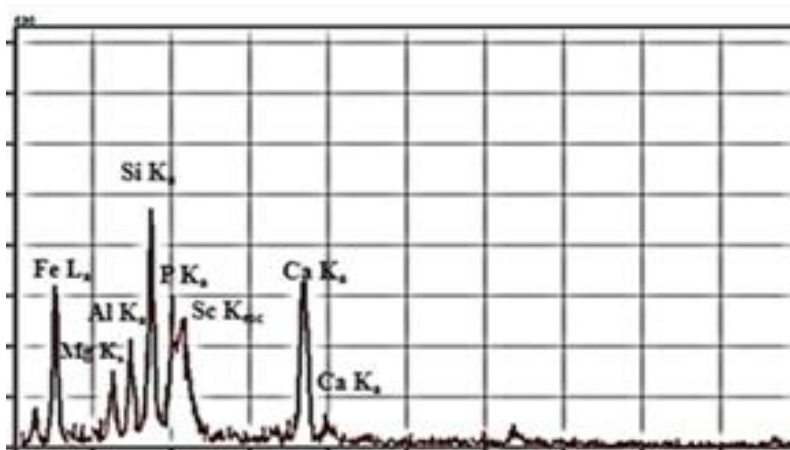


Figure 40: EDS analysis for SSA particles (Continued).

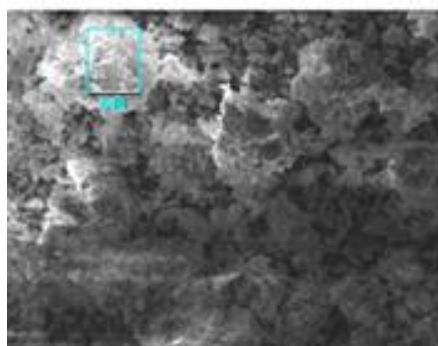
## SSA9-4



Element	%
Ca	33.58
Si	2.08
Fe	11.44
Al	6.18
Co	6.06
Mg	3.72



## SSA9-6



Element	%
Ca	37.82
Si	23.3
Al	8.7
Fe	5.4
Mg	4.10
Pb	4.01
Sc	2.23

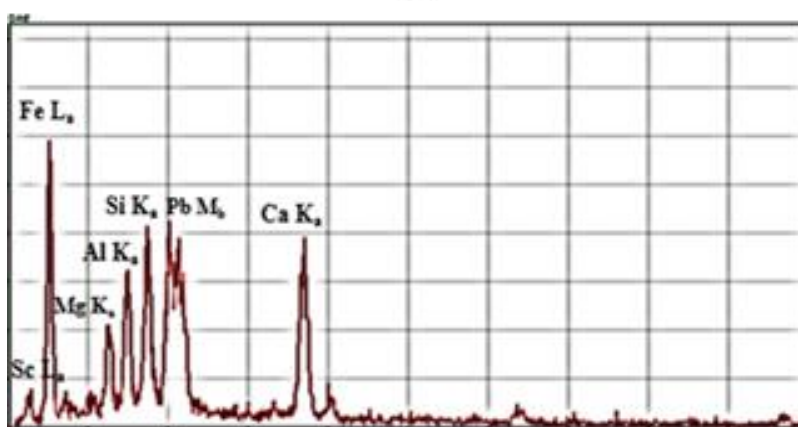
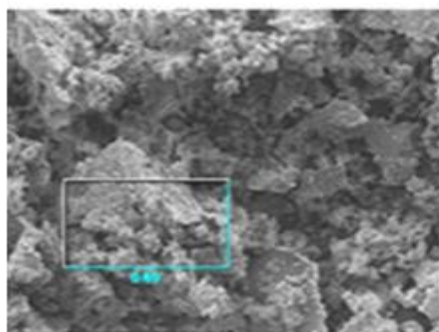


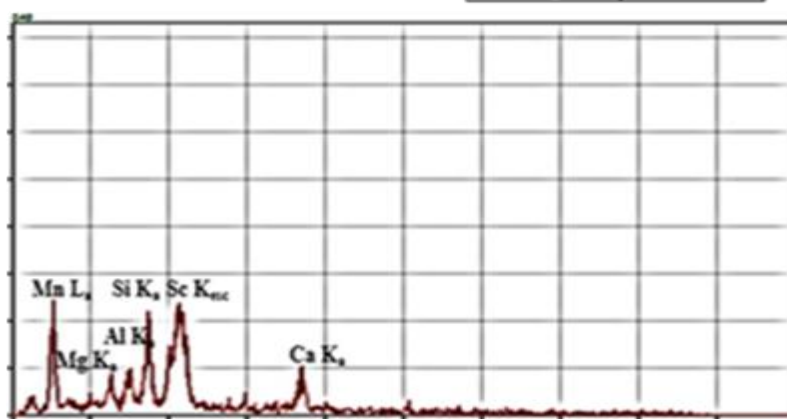
Figure 40: EDS analysis for SSA particles (Continued).



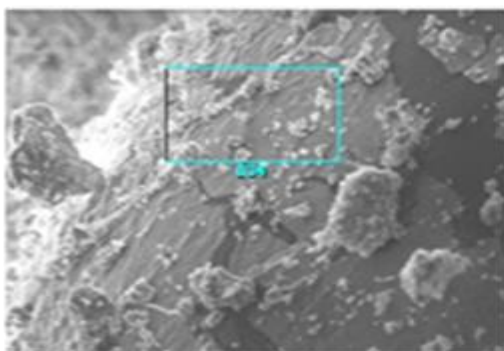
## SSA11-2



Element	%
Ca	28.24
Si	24.25
Mn	7.44
Co	5.52
Al	5.12
Cr	4.14
Sc	3.48
Cu	3.11
Mg	3.025



## SSA11-4



Element	%
Ca	31.14
Si	20.06
Sc	11.37
Fe	8.82
Al	7.58
Mg	5.23
Ti	2.23
Cr	2.03

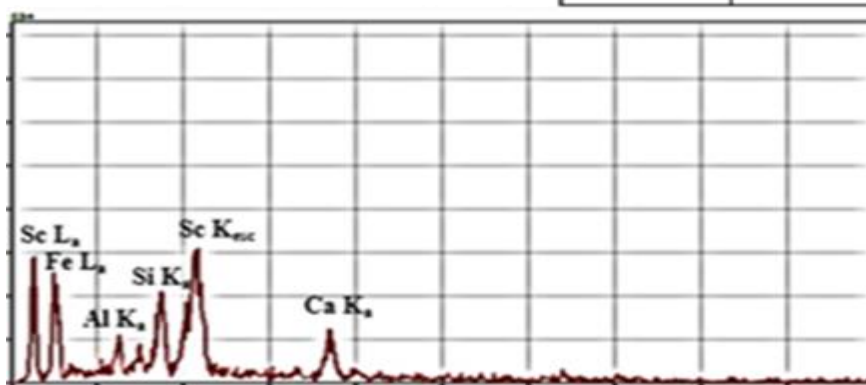


Figure 40: EDS analysis for SSA particles (Continued).

## SSA11-6

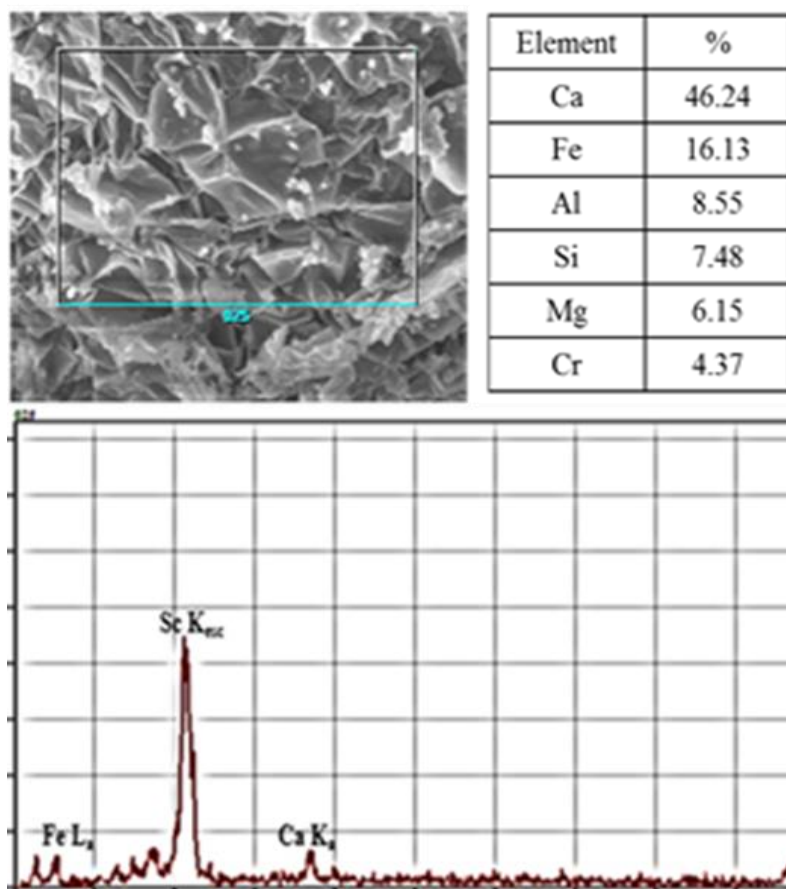


Figure 40: EDS analysis for SSA particles (Continued).

#### 4.5 Particle Size Analyzer

The particle size distribution of a material can be important in understanding its physical and chemical properties. Increasing the fineness of cement or cementitious materials affects its reactivity with water. Generally, the finer the binder, the more rapidly it will react (Mamlouk and Zaniewski, 2006). However, the cost of grinding and the heat evolved on hydration set some limits on fineness. It was reported in the study that the rate of reactivity and the strength development can be enhanced by finer grinding of binders. Hu et al. (2014) concluded that cement fineness and water-to-cement ratio (W/C) affected the heat of hydration and set times. The initial and final

set times of coarser cement were found to be late compared to finer cement. Additionally, the decreased surface area of coarser cement delayed the rate of hydration.

The particle size distribution of all ground SSA samples was examined to ensure the consistency of sewage sludge's grinding and that the properties of SCC were not affected by the particle size distribution. Figure 41 and Table 18 show the particle size analysis results of OPC, and incinerated SSA particles at different temperatures and durations. It can be observed that all SSA particles had a similar average particle size compared to OPC  $\sim 156 \mu\text{m}$ . This conclusion was also obtained by Lynn et al. (2015) showing that the above grain size distributions correspond to the range of particle size that characterizes silt ( $2.5\text{--}62.5 \mu\text{m}$ ) and fine sand ( $62.5\text{--}250 \mu\text{m}$ ). Furthermore, the specific surface area (BET) of SSA particles was very close to that of OPC ( $1.0491 \text{ m}^2/\text{g}$ ) falling in the range of  $0.7$  to  $1.2 \text{ m}^2/\text{g}$ ; indicating suitability for use as a supplementary cementing material, possibly with minor modifications.

Furthermore,  $D_{50}$  showed that 50% of OPC and SSA9-4 particles had diameters less than  $23$  and  $27 \mu\text{m}$ , respectively, while for the other SSA samples 50% of the particles had a larger diameter ranging from  $55 \mu\text{m}$  to  $80 \mu\text{m}$ ; showing that SSA might be slightly coarser than OPC. Previous work reported that the particle size distribution and morphology of cement and ash grains have a considerable impact on the heat of hydration, the progress of hydration and consequently on mortar porosity and its compressive strength (Frigione and Marra, 1976; Monzó et al. 1996). Hence, the consistency of grinding incinerated SSA particles using disc-type grinder, would greatly help in ensuring that the fineness of SSA particles was a constant factor

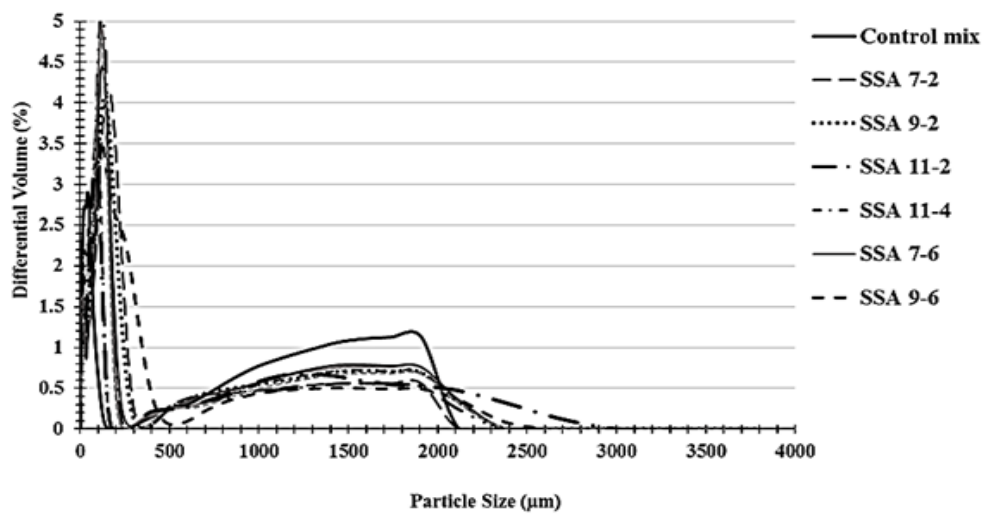


throughout the study, and would help in investigating the effect of SSA addition on the properties of the produced mortars.

Table 18: Particle size analysis of SSA particles.

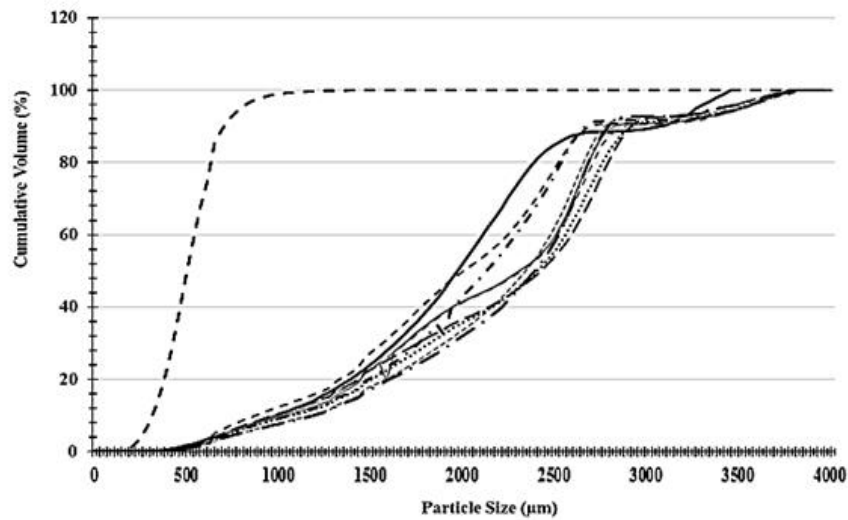
	OPC	SSA 7-2	SSA 9-2	SSA 11-2	SSA 7-4	SSA 9-4	SSA 11-4	SSA 7-6	SSA 9-6	SSA 11-6
Mean ( $\mu\text{m}$ )	162.4	156	170	145.9	168.1	146	141	163	166	152
D10 ( $\mu\text{m}$ )	2.1	1.9	2.3	3.1	1.9	1.5	2.3	2.1	3.0	2.9
D50 ( $\mu\text{m}$ )	23	73	69	67	56	27	36	55	80	60
D90 ( $\mu\text{m}$ )	662	237	241	175	220	141	132	191	292	168
Specific Surface Area ( $\text{m}^2/\text{g}$ )	1.049	0.9	0.89	0.777	0.997	1.20	0.93	0.97	0.78	0.80

\*D10/D50/D90 – 10%/50%/90% of particles have diameters smaller than the mean ( $\mu\text{m}$ ).



(a)

Figure 41: Particle size analyzer for SSA particles. (a) differential volume (%), and (b) cumulative volume (%).



(b)

Figure 41: Particle size analyzer for SSA particles. (a) differential volume (%), and (b) cumulative volume (%) (Continued).

## 4.6 Pozzolanic Activity

As mentioned earlier, the pozzolanic activity of incinerated SSA was detected by two different tests including Frattini and strength activity index tests. The results and discussion of both tests are illustrated in the subsections below.

### 4.6.1 Frattini Test

The pozzolanic activities of the incinerated SSA samples were evaluated by the Frattini test and results are presented in Figure 42. The  $[Ca^{+2}]$  was expressed as equivalent  $[CaO]$ . According to the BS EN 196-5 (2011), a material is regarded as pozzolanic when the test result lies beneath the lime saturation isotherm at 40°C. However, a result lying on or above the lime saturation isotherm indicates no pozzolanic reaction. The test was conducted at 8 days and at 28 days of curing. It was obvious from Figure 42 that most of the samples did not exhibit any pozzolanic activity

at 8 days, except for SSA7-4 and SSA9-6. On the contrary, at 28 days, all SSA samples lied below the lime saturation isotherm, except for SSA7-2; indicating that ground SSA incinerated at different temperature and periods could meet the criterion to be a pozzolan according to the Frattini standard, but at late age.

The pozzolanic activity can also be assessed by checking the degree of reduction of the [CaO]. The percentage of CaO removal was detected at 8 and 28 days, and results are illustrated in Figure 43. CaO removal percentage at 8 days was negative and normalized to 0% removal; showing that there was no pozzolanic reaction at early age. However, all SSA samples had a considerable percentage of CaO removal at 28 days. The highest degree of [CaO] reduction was revealed for SSA9-2 followed by SSA11-6. The high percentage of CaO removal detected in SSA9-2 could be interpreted by the humps observed in its XRD pattern which indicated higher amorphous phase than other SSA samples. Thus, it can be concluded from the Frattini test results that all samples of SSA exhibited late pozzolanic activity and this modest pozzolanic activity will contribute to strength at late ages.

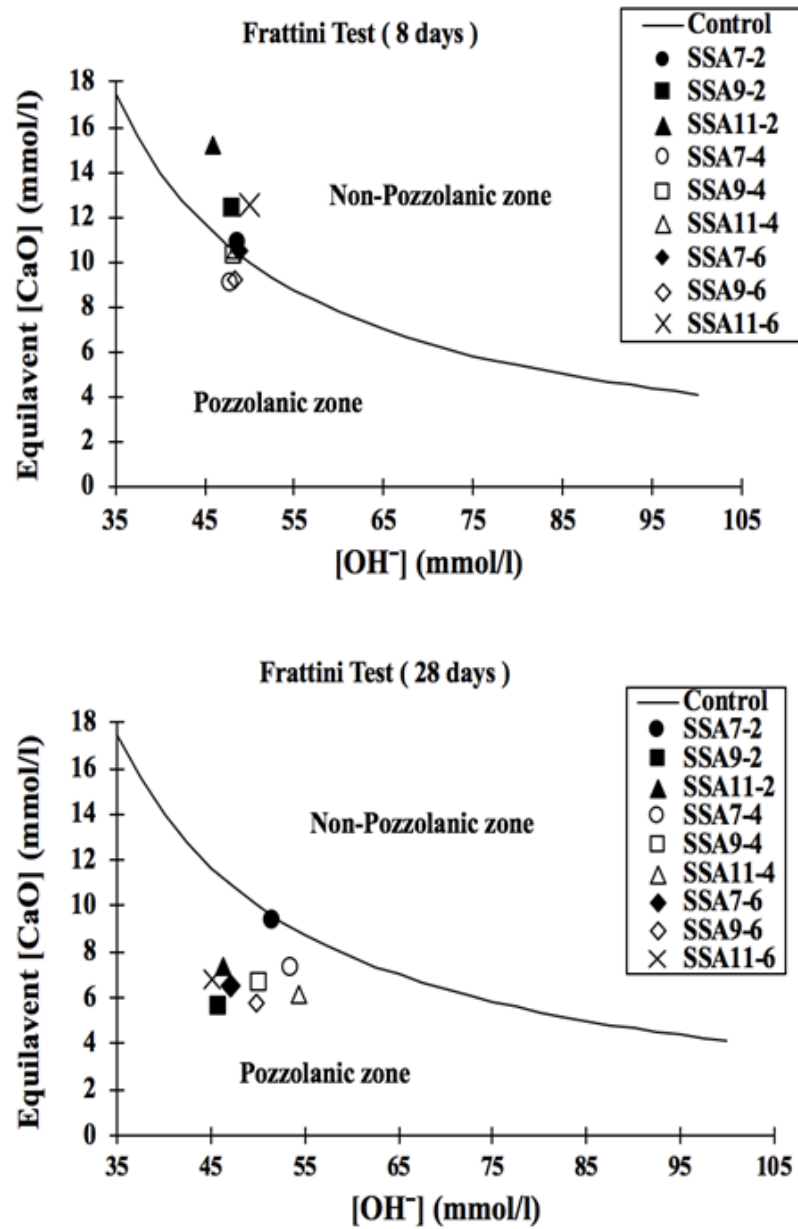


Figure 42: Frattini test for SSA particles.

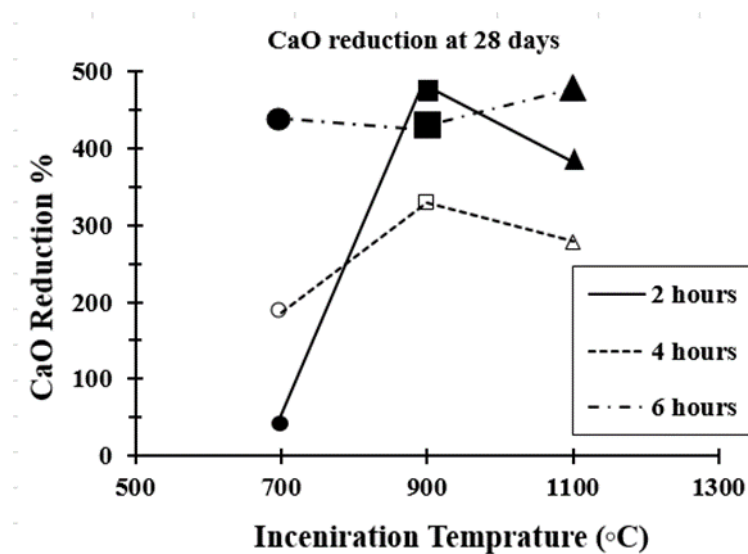


Figure 43: Percentage of CaO removal at 28 days of curing.

#### 4.6.2 Strength Activity Index (SAI)

The mean values of the compressive strength ( $F_c$ ) of hardened SSA mortars including 20% SSA cement replacement, and control mortar at 7 and 28 days of curing was measured, and results are summarized in Table 19 and Figure 44. The compressive strength of all mortar specimens increased when curing age extended from 7 to 28 days. All SSA mortars had a lower compressive strength compared to the control mix. The highest reduction of compressive strength was observed in SSA particles incinerated at 1100°C, which indicated that increasing the incineration temperature above 900°C might reduce the compressive strength of SSA mortars. Test results of the SAI at 7 and 28 days of curing for the different SSA mixes are shown in Figure 44. At 7 and 28 days, the SAI for all SSA samples incinerated for 6 hours was lower than 75%; which indicated that SSA had very low pozzolanic activity (i.e., should be higher than 75% as per ASTM C618 (2012)). Also, SSA incinerated for 2 hours had higher SAI values than those incinerated for 4 hours; concluding that as the incineration

duration increases the SAI decreases. However, the SAI value for SSA mortars including SSA particles incinerated at 700 and 900°C for 2 and 4 hours exceeded 75% with values between 77.1% and 95.6%, which indicated that SSA could be considered as good pozzolan material at those incineration temperatures and durations, and that is mainly due the high peaks of quartz (SiO<sub>2</sub>) observed in the XRD analysis. Therefore, SSA can potentially be used in concrete or mortar to partially replace Portland cement; as confirmed by Frattini test results, SSA exhibited pozzolanic reactivity at late ages. However, previous work revealed that the pozzolanic activity of SSA is lower than that of some common pozzolans such as fly ash. Tay and Show (1994) found that the strength activity index (SAI) of SSA with Portland cement was between 57.6% and 67.2%. While the SAI value of fly ash class F was between 96% and 134% (Pan et al., 2002; Bhatta and Reid, 1989). Thus, the effectiveness of using SSA in the mortar was lesser than that of fly ash. Also, on using SSA, one should not expect pozzolanic activity at an early age.

Table 19: Compressive strength at 7 days and 28 days of curing.

Mortar Sample	Compressive strength (MPa)*	
	7 days	28 days
Control mix	13.9 (0.04)	18.7 (0.04)
SSA7-2	14.1 (0.02)	17.9 (0.02)
SSA9-2	11.5 (0.01)	14.7 (0.03)
SSA11-2	9.20 (0.06)	11.6 (0.11)
SSA7-4	11.4 (0.07)	16.6 (0.11)
SSA9-4	10.6 (0.05)	14.4 (0.07)
SSA11-4	9.8 (0.03)	13.2 (0.05)
SSA7-6	8.9 (0.04)	12.2 (0.02)
SSA9-6	7.4 (0.02)	12.4 (0.04)
SSA11-6	5.8 (0.05)	8.9 (0.09)

\* Values in parenthesis are the standard deviation in MPa

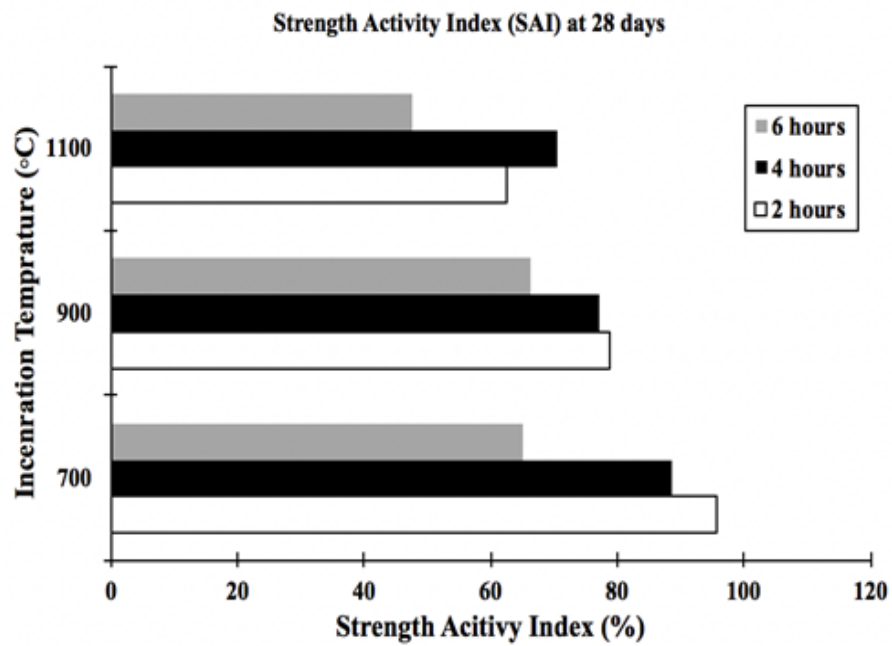
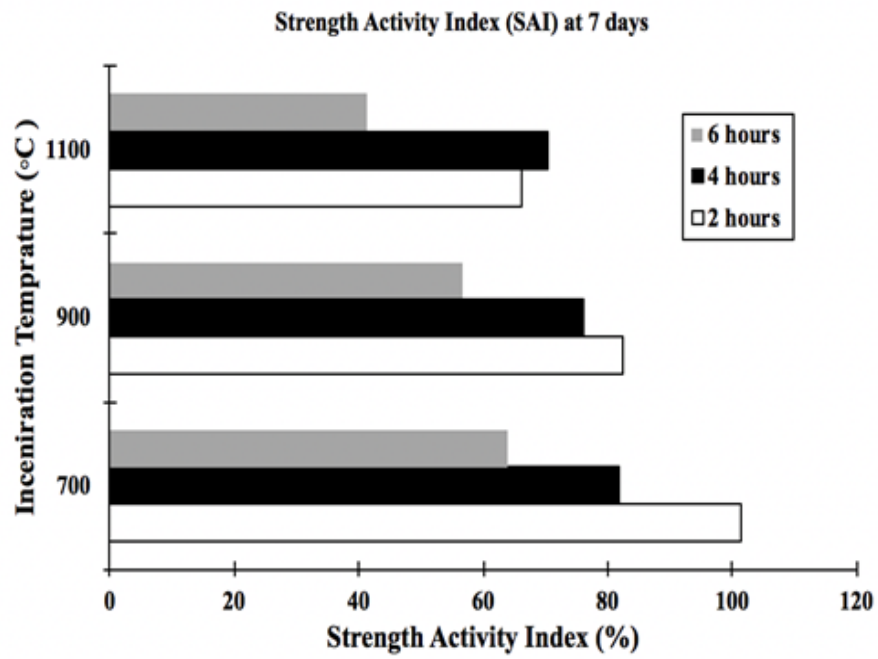


Figure 44: Strength activity index at 7 days and 28 days.

#### **4.7 Workability and Workability Retention**

The main aim of this thesis is to reuse SSA to produce SCC that achieves a desired workability. Therefore, testing the effect of SSA on the workability of the pastes would provide an indication of the feasibility of incorporating SSA in producing high workable concrete such as SCC. Without adding additional water, concrete producers suffer to consistently deliver expected performance attributes. Yet, hydration of Portland cement leads to a change in fresh concrete properties immediately after batching, most notably with respect to workability. Workability loss may lead to retempering of the concrete or implementation of other measures to counteract the expected loss in workability (Daczko, 2019). Therefore, another important property to test for producing SCC is the workability retention. Workability retention is a cost-effective means of maintaining consistency between loads of concrete with respect to slump, workability and air content.

The effect of SSA on the workability of cement pastes was studied by the flow table test. Results are presented in Figure 45 as the percentage increase of average base diameter (i.e., flow table spread (FTS) %). It can be seen that the addition of SSA resulted in a reduction in consistency rates for almost all cement pastes containing SSA compared to the control mix. This occurred due to the high water absorption of SSA (about 60%). Furthermore, the porosity, and irregular morphology of SSA particles as shown in the SEM images, played a major role in adsorbing part of the mixing water, lowering the workability and changing the consistency of the mortar (Monzó et al., 1996). Thus, in order to preserve the consistency of mortars, it is necessary to increase the water content or use workability improving admixtures for mortars containing SSA as a cement replacement (Tay, 1987; Monzó et al., 1999, 2003). The highest



workability was achieved when SSA particles were incinerated at 1100°C. This improvement is due to the low D<sub>50</sub> and mean diameter of SSA particles incinerated at 1100°C compared to the other SSA particles (as shown in Table 18). Another reason of this enhancement in workability might be due to the expansion or bloating of materials at high temperature, resulting in a smoother surface, and a more compacted pore structure.

Okah and Godwin (2016) reported that much of the loss of mortar workability takes place in the first 1 hour. However, SSA did not show a notable decrease in consistency in the first hour expect for SSA particles incinerated at 1100°C for 6 hours. Insignificant decrease of the pastes workability with time could be due to the loss of the water being utilized by the cement hydration or evaporation. In conclusion, the produced SSA showed good workability retention.

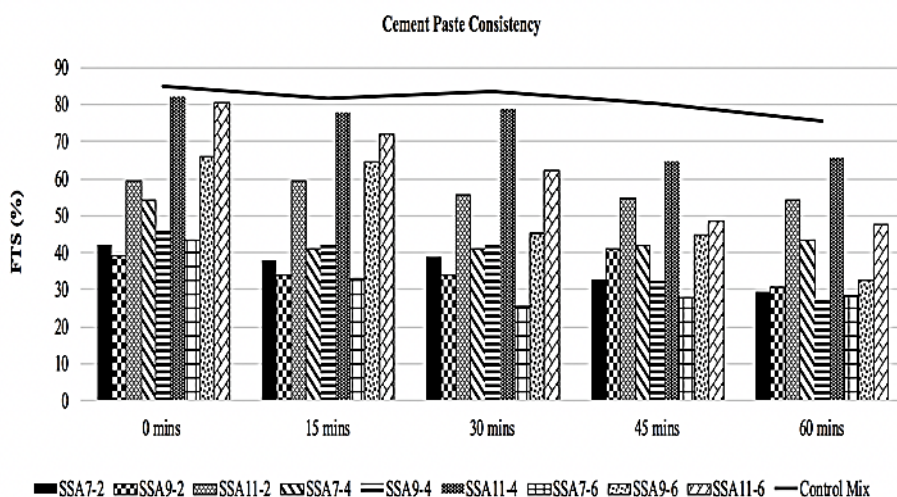


Figure 45: Workability and workability retention for SSA pastes.

#### 4.8 Mercury Intrusion Prosimetry (MIP)

The porosity and the pore size distribution are the main factors which affect the service life of concrete. The discontinuity of pores would reduce the ionic mobility and therefore would increase the concrete resistivity and corrosion protection. The results of the MIP analyses of the paste specimens prepared with 0, 20, and 40% of SSA cured for 28 and 56 days are shown in Figure 46 and Table 20, and 21. Results of previous studies indicated that the longer the curing time; the finer the pore structure and the less interconnection between the capillary pores by continuous curing in water (Marsh, 2003). In this study, at 28 days of curing, both mortars containing SSA increased the total porosity of the paste compared to the control. However, at late ages (i.e. 56 days) adding 20% of SSA (R-20) resulted in the lowest porosity, and therefore, improved the microstructure of the paste;

Additionally, it can be observed that despite the porous nature of SSA particles, incorporating SSA didn't affect the median pore size of the paste; where the median pore diameter for all samples ranged from 2.51 to 2.73  $\mu\text{m}$ . However, the highest pore diameter was found when pastes incorporated 40% of SSA. Incorporating 20% of SSA in cement paste slightly reduced (about 5%) the pore size diameter compared to the control mix. Yet, previous work conducted by Krejcirikova et al. (2019) stated that an increase in porosity by more than 20% was found compared to reference mix, but when only 10% of the cement was replaced, there was no significant changes in the porous structure of the material. It should be noticed that the small capillary pores (i.e. mesopores) do not affect the mechanical properties but have a critical influence on the drying shrinkage of concrete (Collins and Sanjayan, 2000). Therefore, it can be concluded from the obtained results that replacing 20% of OPC with SSA would

achieve the required performance in terms of service life. Yet, reusing 40% of SSA in producing concrete could still be acceptable, since the pores in SSA might serve as a place to accommodate hydration products for late age improvement in durability (Zhou et al., 2010).

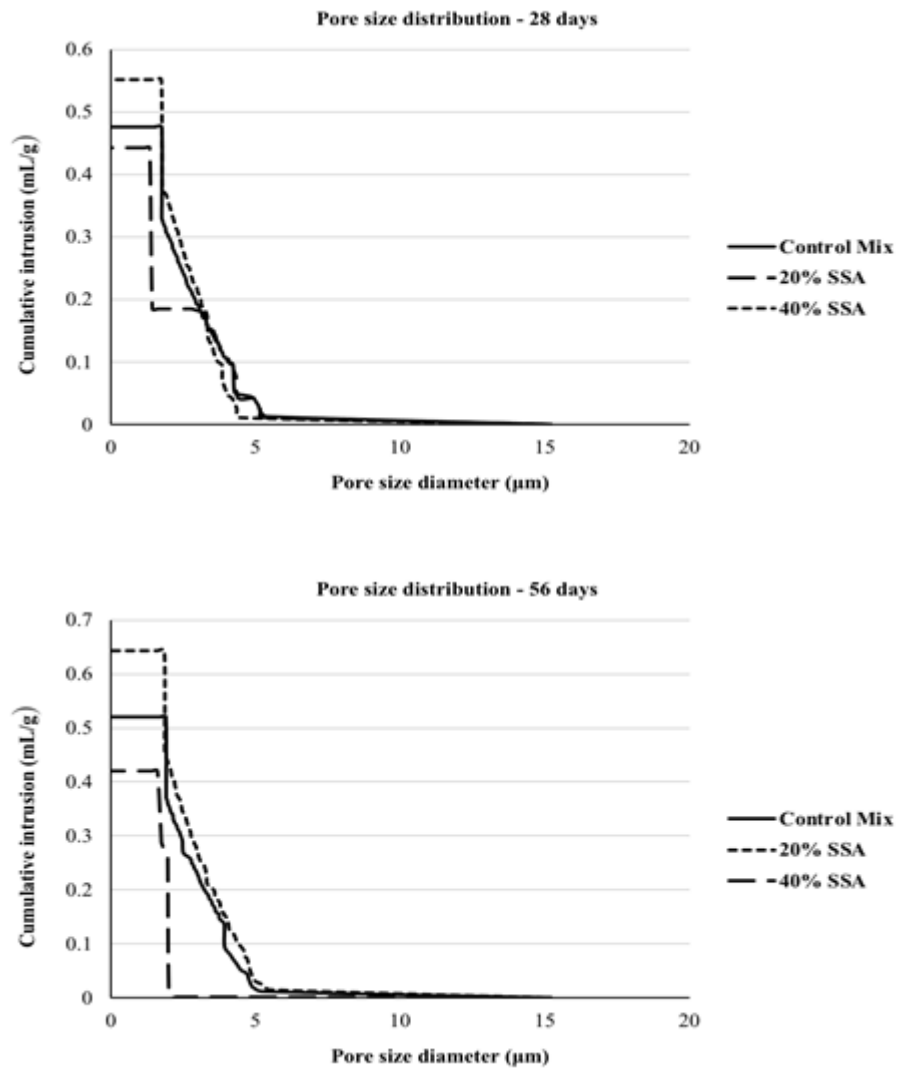


Figure 46: Pore size distribution for pastes containing SSA9-2 at 28 and 56 days.

Table 20: Total porosity for pastes at 28 and 56 days.

Paste	Total porosity (%)	
	28 days	56 days
Control mix	27.90	30.46
R-20	37.17	28.97
R-40	32.355	33.69

Table 21: Median pore diameter for pastes at 28 and 56 days.

Paste	Median pore diameter ( $\mu\text{m}$ )	
	28 days	56 days
Control mix	2.70	2.55
R-20	2.65	2.56
R-40	2.73	2.51

#### 4.9 Heat of Hydration

Mixing Portland cement with water results in heat liberation. This heat is called heat of hydration and it is an exothermic reaction which raises the temperature of concrete. The mass concrete may then attain high internal temperatures, especially during hot weather construction, or if high cement contents are used. Elevated heat of hydration may lead to major cracks in concrete. Therefore, controlling the heat of hydration of concrete is essential especially when dealing with mass concrete.

The effect of reusing SSA on the heat of hydration was evaluated in this study. Samples containing 100% OPC, 20% SSA, and 40% SSA was evaluated by isothermal calorimetry conduction (ICC). Figure 47 presents the heat of hydration in power (Watt) per mass (gram) of cementitious materials during the first 60 hours. It can be observed that increasing the replacement ratio of OPC by SSA, decreased the heat of hydration.

It can be seen that there was no significant effect of SSA in the initial reaction of hydration between 0-40 minutes. During the induction period (i.e. up to 30 mins); before the initial set of cement, increasing the replacement ratio resulted in a slight increase of the heat of hydration. However, when the reaction started to accelerate, the reaction was highly exothermal due to the generation of hydration products such as C-S-H, yet the sample contained 100% OPC exhibited greater heat of hydration than the samples with SSA. Replacing 20% and 40% of OPC by SSA reduced the heat of hydration by 10.87% and 31.5%, respectively. Therefore, replacing part of OPC with SSA resulted in increasing the setting time approximately from 11 hours for R-0 to 12 and 13 hours for R-20 and R-40 respectively. Similar findings were reported by others where the use of SCM in cement reduces the heat released during hydration (De Rojas et al., 1993; De Rojas and Frías, 1996; Frías et al., 2000).

Furthermore, according to the study of Stumm (1992), particles with larger surface areas provide more nucleating sites and allow more hydraulic reaction to proceed, since the nucleation effect on cement hydration induced by very fine powder substitutes is due to the interfacial energy between two solids being smaller than that between a solid and a solution. Therefore, the coarser particle size and smaller surface area of SSA compared to OPC, provided less nucleation sites for hydration product precipitation and thus slowed down cement hydration.

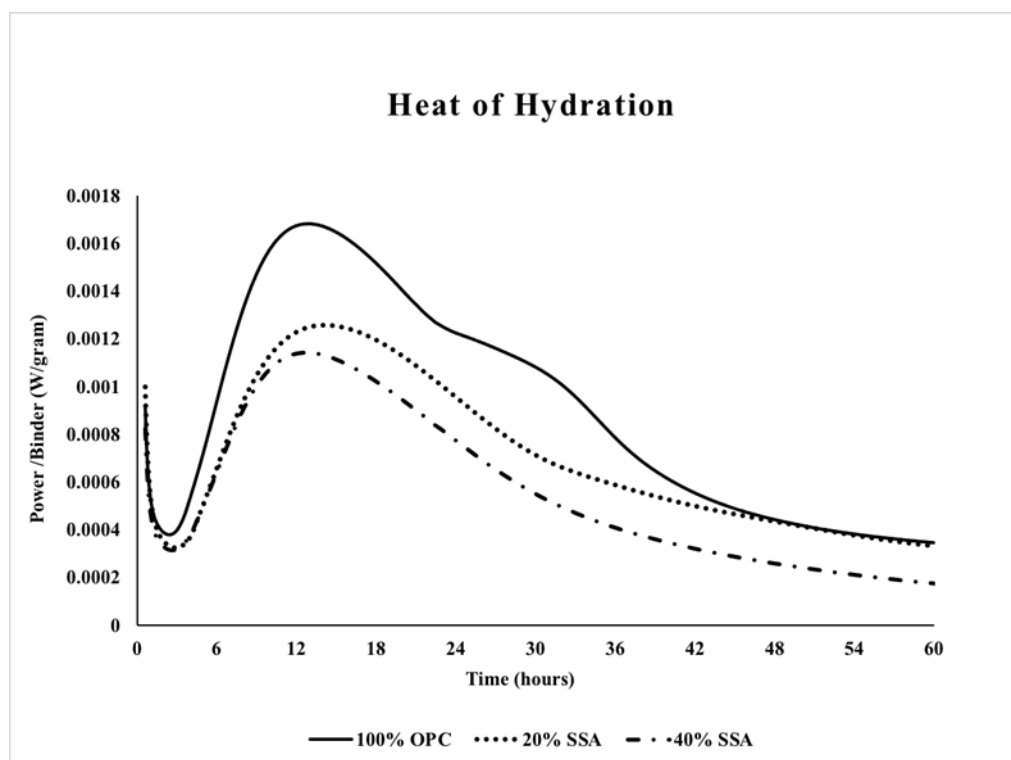


Figure 47: The effect of SSA on the heat of hydration.

#### 4.10 Toxicity Characteristic Leaching Procedure (TCLP)

Based on the conducted XRF analysis, SSA was found to include some heavy metals. These metals can be leached when subjected to severe environmental conditions causing serious environmental issues. Therefore, the leachability of toxic heavy metals in SSA particles should be investigated when SSA is to be used in making concrete. However, it was reported that using cement could encapsulate certain waste materials (Felix et al., 1997). Meanwhile, Katsioti et al. (2008) reported that SSA containing trace metals such as Cu, Zn, and Pb could be stabilized by using cement.

The leaching test was conducted according to toxicity characteristic leaching procedure (TCLP) at 7 and 28 days of curing. Results and concentration of heavy metals in SSA, control mix, 20% SSA, and 40% SSA are listed in Tables 22 and 23.

Detected metals were Aluminum (Al), Copper (Cu), Iron (Fe), Magnesium (Mg), Manganese (Mn), Strontium (Sr), Vanadium (V), and Zinc (Zn). Additionally, five other metals with established limits were targeted including Cadmium (Cd), Chromium (Cr), Lead (Pb), Arsenic (As), and Barium (Ba) as these are the ones that have specified permissible limits. According to EPA (1992), if the value of the leached metal is higher than the allowable limit then the material is considered hazardous. By comparing the obtained results with the TCLP regulated limits, it can be reported that there was no toxicity issue associated with the produced material. At 7 days of curing, it was found that the leachability of Arsenic (As) was the highest in the control mix, followed by 40% SSA and 20% SSA. Chen et al. (2006) obtained similar concentration of (As) leachability with a value of 0.023 mg/l for ground SSA. For all samples, the leachability concentration of Barium (Ba) and Strontium (Sr) increased with respect to age. Also, the concentration of Magnesium (Mg) was significantly high up to 122.2 mg/l for ground SSA, yet when SSA was blended with cement a sharp decrease was noted; that was mainly due to the chemical reaction taking place with OPC, which will promote the absorption of free lime and also increase the formation of  $C_3S$  and  $C_4A_3S$ . Therefore, the increment of Ba and Sr ions observed with age could be explained by the ion exchange process of Ba and Sr ions with Mg ions; where Mg ions formed a stronger bond with the constituents in the paste sample than Ba and Sr, which lead to the release of these ions. The low concentration of Mg ions at 28 days, indicates that all the magnesium (Mg) ions were bonded, therefore, no more Ba or Sr ions will be leached with age. Nakic (2018) reported a barium leaching concentration of 0.47 mg/l when only 10% of OPC was replaced by SSA. Both Lead (Pb) and Cadmium (Cd) had a low detect concentration values, and therefore was adopted to the limit of detection (LOD) of 0.003 and 0.011 respectively. This conclusion was also found by Nakic

(2018) and Chen et al. (2006). However, it should be noted here that lead leachability was relatively higher than paste samples including ground SSA by 80%. Yet, it is within the established limits according to EPA (1992).

To minimize the leachability of heavy metals in SSA, it was found that the addition of fly ash to sewage sludge may be considered as an interesting alternative sludge stabilizing method (Papadimitriou et al., 2008).

Table 22: TCLP for SSA pastes at 7 days of curing.

Metal	SSA	Paste			TCLP Limit (mg/l)
		0% SSA	20% SSA	40% SSA	
Al	0.631 (0.08)	0.015 (0.04)	0.0597 (0.09)	0.836 (0.07)	-
As	0.040 (0.03)	0.031 (0.02)	0.026 (0.03)	0.029 (0.008)	5
Ba	0.220 (0.05)	0.051 (0.01)	0.142 (0.07)	0.212 (0.128)	100
Cd	0.0046 (0.001)	0.003 LD	0.003 LD	0.003 LD	1
Cr	0.209 (0.18)	2.98 (0.37)	1.55 (0.74)	1.17 (0.79)	5
Cu	0.017 (0.011)	0.008 (0.0012)	0.015 (0.010)	0.014 (0.006)	-
Fe	0.117 (0.041)	0.067 (0.052)	0.038 (0.05)	0.009 (0.010)	-
Mg	122.2 (3.07)	0.550 (0.29)	0.231 (0.077)	0.869 (1.16)	-
Mn	0.015 (0.004)	0.0004 LD	0.002 LD	0.002 LD	-
Pb	0.055 (0.08)	0.011 LD	0.011 LD	0.011 LD	5
Sr	3.11 (0.07)	2.14 (0.51)	2.21 (0.23)	2.42 (0.33)	-
V	0.132 (0.03)	0.036 (0.01)	0.008 (0.002)	0.018 (0.02)	-
Zn	0.04 (0.008)	0.03 LD	0.02 LD	0.03 LD	-

\*Values in parenthesis are the standard deviation in mg/l / LD= Low detect.



Table 23: TCLP for SSA pastes at 28 days of curing.

Metal	SSA	Paste			TCLP Limit(mg/l)
		0% SSA	20% SSA	40% SSA	
Al	0.631 (0.08)	0.213 (0.07)	0.175 (0.078)	0.15 (0.033)	-
As	0.040 (0.03)	0.07 (0.008)	0.036 (0.02)	0.026 (0.03)	5
Ba	0.220 (0.05)	0.275 (0.03)	0.449 (0.01)	0.875 (0.037)	100
Cd	0.0046 (0.001)	0.003 LD	0.004 LD	0.003 LD	1
Cr	0.209 (0.18)	2.08 (0.13)	2.36 (0.20)	1.52 (0.37)	5
Cu	0.017 (0.011)	0.008 (0.007)	0.020 (0.008)	0.007 LD	-
Fe	0.117 (0.041)	0.04 (0.05)	0.066 (0.05)	0.069 (0.05)	-
Mg	122.2 (3.07)	0.03 (0.03)	0.016 (0.02)	0.05 (0.06)	-
Mn	0.015 (0.004)	0.003 LD	0.0022 (0.001)	0.003 LD	-
Pb	0.055 (0.08)	0.054 (0.03)	0.017 (0.01)	0.011 LD	5
Sr	3.11 (0.07)	6.81 (0.61)	6.15 (0.49)	6.65 (0.78)	-
V	0.132 (0.03)	0.001 LD	0.001 LD	0.001 LD	-
Zn	0.04 (0.008)	0.032 (0.01)	0.04 (0.009)	0.03 (0.005)	-

\* Values in parenthesis are the standard deviation in mg/l / LD = Low detect.

#### 4.11 PI for SSA Selection

The performance index approach was used to select the optimum incineration temperature and duration for SSA samples based on several tests. Table 24 and Table 25 show the weighted ranks and numeric indices for all SSA samples. The individual performance criteria are presented in Table 24, while the multifunctional performance criteria are presented in Table 25. The shaded cells indicate the incineration

temperature and duration that has the highest value with the required performance criteria. Except for the energy consumption; where the lowest is the better.

The pozzolanic activity was assessed by three different criteria (i.e. XRD analysis, SAI, and CH consumption). From Table 24, it can be seen that the highest content of  $\text{SiO}_2+\text{Al}_2\text{O}_3+\text{Fe}_2\text{O}_3$  was detected in SSA11-4. However, the SAI results indicated that SSA7-2 had the highest SAI, while SSA9-2 showed the highest CH consumption. SSA11-4 showed the highest workability, and workability retention values. The energy consumption increased with increasing the incineration temperature and duration, and hence, the lowest energy consumption value was observed for SSA7-2.

In order to select the optimum incineration temperature and duration that satisfies all the selected criteria, multifunctional performance criteria were used (Table 25). It can be seen that SSA9-2 had the highest PI value, followed by SSA11-2. Therefore, SSA incinerated at 900°C for 2 hours will be utilized in phase 2 to produce SCC.

Table 24: Performance indices for individual criteria.

Concrete Mixtures	Individual performance criterion											
	SiO <sub>2</sub> +Al <sub>2</sub> O <sub>3</sub> +Fe <sub>2</sub> O <sub>3</sub>		SAI		CH consumption		Workability		Workability retention (30 mins)		Energy consumption	
	W <sub>i</sub>	R <sub>i</sub>	W <sub>i</sub>	R <sub>i</sub>	W <sub>i</sub>	R <sub>i</sub>	W <sub>i</sub>	R <sub>i</sub>	W <sub>i</sub>	R <sub>i</sub>	W <sub>i</sub>	R <sub>i</sub>
SSA7-2	0.89	4.46	1.00	5.00	0.05	0.27	0.78	3.90	0.78	3.91	1.00	5.00
SSA7-4	0.94	4.70	0.93	4.63	0.39	1.95	0.85	4.23	0.79	4.33	0.50	2.52
SSA7-6	0.90	4.50	0.67	3.37	0.91	4.56	0.79	3.93	0.70	3.91	0.33	1.69
SSA9-2	0.87	4.34	0.82	4.11	1.00	5.00	0.76	3.82	0.75	3.94	0.99	4.97
SSA9-4	0.92	4.59	0.81	4.05	0.69	3.43	0.80	4.01	0.80	3.85	0.50	2.52
SSA9-6	0.92	4.59	0.59	2.95	0.90	4.50	0.80	3.98	0.80	4.00	0.33	1.69
SSA11-2	0.99	4.96	0.65	3.26	0.80	4.02	0.87	4.37	0.87	4.67	0.989	4.95
SSA11-4	1.00	5.00	0.74	3.68	0.79	3.95	1.00	5.00	1.00	5.00	0.50	2.51
SSA11-6	0.89	4.47	0.53	2.63	0.98	4.92	0.99	4.95	0.84	4.52	0.33	1.68

Table 25: Performance indices for multifunctional criteria.

Concrete Mixtures	Multiple Performance Criterion
SSA7-2	6.93
SSA7-4	29.4
SSA7-6	26.89
SSA9-2	100
SSA9-4	37.16
SSA9-6	24.48
SSA11-2	98.26
SSA11-4	68.56
SSA11-6	32.93

#### 4.12 Concluding Remarks

- The major constituents of all SSA samples were SiO<sub>2</sub>, CaO, and P<sub>2</sub>O<sub>5</sub>. However, other oxides such as Al<sub>2</sub>O<sub>3</sub>, Fe<sub>2</sub>O<sub>3</sub>, MgO, SO<sub>3</sub>, and K<sub>2</sub>O were present in a lesser amount.
- As the incineration temperature and time increases, the formation of quartz (SiO<sub>2</sub>) increased. XRD analysis indicated the occurrence of some amorphous phases in the SSA which suggested that SSA could exhibit pozzolanic activities and the potential to be used as a partial substitution of cement.
- SEM examination indicated that SSA particles were irregular with a rough surface. Nevertheless, the pore structure of the particles became more compact as a result of increasing the incineration temperature.

- Based on the Frattini test results, all SSA samples exhibited a late pozzolanic activity (i.e. at 28 days of curing), yet the highest CaO removal was observed when SSA was incinerated at 900°C for 2 hours
- SAI results showed that all mortars contained incinerated SSA for 6 hours didn't exhibit any pozzolanic activity. Also, it was concluded that as the incineration temperature increases, the SAI value decreases.
- SSA particles had a similar average particle size compared to OPC ~ 156 μm, the specific surface area of SSA particles was very close to that of OPC (1.0491 m<sup>2</sup>/g) falling in the range of 0.7 to 1.2 m<sup>2</sup>/g; indicating suitability for use as a supplementary cementing material.
- Due to the porous nature of SSA particles, incorporating SSA increased the total porosity of the paste at early ages. Yet, at late ages, an improvement in the microstructure for all the pastes was observed. Also, using 20% of SSA as cement replacement slightly reduced the total porosity and therefore enhanced the microstructure of the paste.
- SSA didn't affect the median pore size of the paste; where median pore diameter for all samples ranged from 2.51 to 2.73 μm. However, the highest pore diameter was found when pastes incorporated 40% of SSA. While, incorporating 20% of SSA in cement paste reduced the pore size diameter by 5% compared to the control mix.
- SSA addition reduced the consistency of the mortar due to high water absorption, irregular morphology and rough surface texture of SSA particles.

However, as the incineration temperature increased, particles became more compact. The highest workability was achieved when SSA was incinerated at 1100°C. This is due to the low SSA particles  $D_{50}$  and mean diameter compared to other SSA particles, in addition to the better compaction of materials as observed in SEM images. The inclusion of SSA improved the workability retention of cement paste.

- The addition of SSA in cement paste reduced the heat of hydration. Replacing 20% and 40% of OPC by SSA significantly reduced the heat of hydration by 10.87 and 31.5%, respectively.
- When using SSA in making concrete, it is very essential to examine the leachability of heavy metals due to their hazardous behavior to the environment. All tested metals had leaching concentration lower than the allowed TCLP limits; indicating that there was no toxicity issue with the produced material and can be considered as a non-hazardous material.
- SSA produced by incineration at 900°C for 2 hours showed the highest PI value in terms of pozzolanic activity, workability, and energy consumption. Therefore, it was selected for examination as partial cement replacement in SCC mixture.

## **Chapter 5: Results and Discussion – Phase 2 : Reusing Sewage Sludge Ash in Producing SCC**

### **5.1 Introduction**

After examining SSA characteristics in phase 1 and their potential to be used as a partial replacement of OPC, the feasibility of incorporating SSA in SCC mixtures as partial replacement of cement was judged by investigating the performance of the produced SCC mixtures. The performance of concrete mixtures was studied in both fresh and hardened stages. In this thesis, the fresh concrete properties were examined by performing the following tests: slump flow,  $T_{50\text{ cm}}$ , J-ring, and V-funnel. Regarding the hardened concrete, the mechanical performance of SCC was evaluated through conducting compressive strength test at different ages. Furthermore, the durability characteristics of SCC was judged based on the bulk electrical resistivity, permeable pore percentage, water permeability, initial rate of absorption, and drying shrinkage. The following sections in this chapter present and discuss the results of each test for the SCC mixtures incorporating SSA (0%, 20%, and 40%) as partial replacement of cement.

### **5.2 Fresh Concrete Tests**

In this section, the results obtained from the fresh concrete are presented, interpreted, and discussed. Three important properties were evaluated including flowability, passing ability, and cohesiveness of the produced SCC mixtures. All of the fresh concrete tests took place after mixing directly.

### 5.2.1 Slump Flow

The flowability of the produced SCC mixtures was evaluated by the slump flow test and results are presented in Table 26. It was obvious that without any further modifications to the control mix, the increase of incorporation percentage of SSA from 0 to 40% resulted in a significant decrease of workability as illustrated in Figure 48 and Figure 49 (b, d, and e). According to EFNARC specification in Table 27, R-20T was classified as SF1, yet R-40T1 and R-40T2 were dry enough not to fall in any of the SCC classifications. This huge reduction of workability could be explained by the high porosity and water absorption of SSA as well as the irregular shape and rough microstructure as observed in the SEM. This was also observed by Pan et al. (2002); when OPC was replaced by SSA in conventionally vibrated cement mortars. Besides, several researchers declared that the water demand in SSA mortars was higher than that in 100% OPC mortars (Monzó et al., 1996; Bhatti and Reid, 1989; Tay et al., 1991). Other solid waste products showed similar behavior in terms of workability when incorporated in SCC. Taha (2016) observed a reduction in the slump flow diameter as the ceramic waste powder (CWP) replacement level increased. Similar results were obtained by Chopra and Siddique (2015) when using rice husk ash (RHA) as cement replacement. Also, a study of replacing cement with metakaolin that is characterized with a higher specific area compared to cement with irregular particle shape was conducted by Sfikas et al. (2014). Results showed that as the replacement level increased, the slump flow values decreased. On the other hand, some supplementary cementing materials such as FA, which is characterized with spherical particles was found to reduce the need of superplasticizer necessary to obtain a similar



slump flow compared with the concrete containing only cement as binder (Bartos et al., 2002).

As mentioned above, to overcome this noticeable reduction in flowability resulted from incorporating SSA in the concrete mixtures, modifications to the control mix was done such as increasing the dosage of the admixture used and reducing the dune sand-to-fine aggregate ratio. Figure 49 (c and f) represents a modified SCC mixture introducing 20% and 40% SSA as a partial replacement of OPC, respectively. It was clear that increasing the admixtures dosage and modifying the mixture proportions when introducing SSA in SCC mixtures contributed to the enhancement of the flowability behavior of the mix. The slump value of was higher compared to the control mix. R-20 showed tendency to move from slump flow one to slump flow class three, and R-40 jumped to class flow two.

Table 26: Slump flow of mixtures with SSA as cement replacement.

<b>Mixtures</b>	<b>Slump flow diameter (mm)</b>
R-0	720
R-20T	588
R-20	760
R-40T1	320
R-40T2	478
R-40	735

Table 27: Classification of slump flow values. (EFNARC, 2005).

<b>Class</b>	<b>Slump-flow in mm</b>
SF1	550 to 650
SF2	660 to 750
SF3	760 to 850

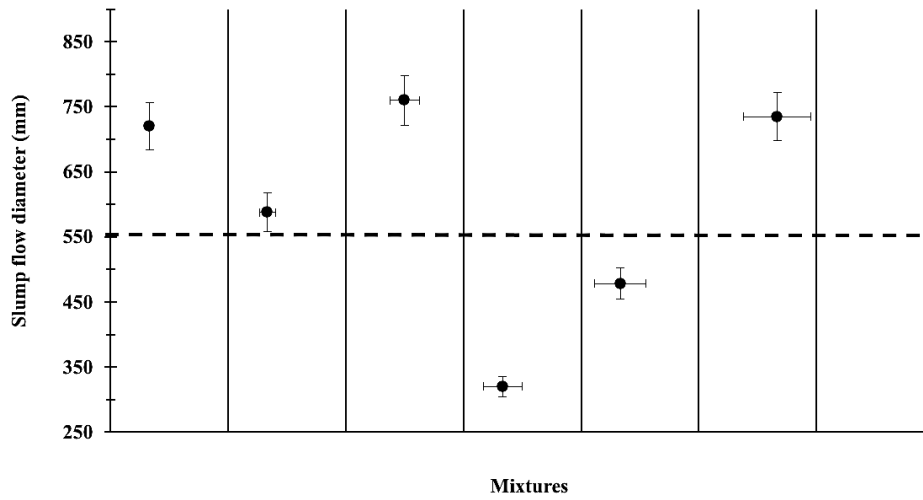


Figure 48: Slump flow results of mixtures with SSA as cement replacement.



Figure 49: Flowability behavior for produced SCC mixtures.

In addition to the measurement of the slump flow diameter, the time taken for the concrete to completely fill the 500 mm circle on the steel base plate was measured and results are presented in Table 28. Without any further addition of SP and VMA, all trials showed an increase in the  $T_{50}$  cm time and didn't satisfy EFNARC guidelines,

which agreed with the results obtained from the slump flow tests, indicating a significant decrease in the flowability. However, after modifications were done on these trials, a reduction of  $T_{50}$  flow time from 4.32 seconds in the control mix to 2.09 seconds in R-20 and 3.19 seconds was detected for R-40. All modified mixtures were less than 5 s and all SCC mixtures showed flow time values in the range of 2–5 s. Both the slump-flow values and the  $T_{50}$  times are in good agreement with the EFNAC specifications.

Table 28:  $T_{50}$  results for mixtures with SSA as cement replacement.

<b>Mixtures</b>	<b><math>T_{50}</math> (seconds)*</b>
R-0	4.32 (0.32)
R-20T	7.48 (0.29)
R-20	2.09 (0.43)
R-40T1	26 (0.38)
R-40T2	11.32 (0.65)
R-40	3.19 (0.41)

\*Values in parentheses are the standard deviation in seconds

### 5.2.2 J-Ring Test

Since all the previous trials (i.e. R-20T, R-40T1, ad R-40T2) failed to achieve the requirements of SCC suggested by EFNARC, J-ring test was performed on three SCC mixtures including R-0, R-20, and R-40. The test results will give indications on the passing ability of the produced SCC mixtures. In other words, how the SCC mixtures would function in a restricted environment resembled by the reinforcing bars of the J-ring. The values of the J-ring test and the result of subtracting the obtained J-ring lateral flow diameter from the slump flow diameters obtained previously are presented in Table 29 and Figure 50. Figure 50 represents the passing ability of mixtures classified as high, moderate and low as per ASTM C1621. The increments

of SP and VMA dosages obviously participated in enhancing the passing ability of the mixture as shown in Figure 51 (b and c). R-20 and R-40 exhibited no visible blocking, suggesting that it would perform very well in highly congested reinforced concrete structures or small size sections.

Table 29: J-ring diameter values and passing ability of mixtures with SSA as cement replacement.

Mixtures	Slump flow diameter (mm)	J-ring diameter (mm)	Passing ability (mm)*
R-0	720	730	10
R-20	760	745	15
R-40	735	730	5

\*Passing ability (mm) = Slump flow diameter – J-ring diameter

Investigators studied the effect of other waste materials on the passing ability of SCC. Taha (2016) reported that an improvement in the passing ability was observed as the CWP replacement level increased. Boukendakdji et al. (2009) suggested that to have a good passing ability, the maximum replacement percentage of slag is 20%. Moreover, using limestone powder (LSP) and silpazz as SCM in SCC satisfied the passing ability guideline suggested by EFNARC (2005).

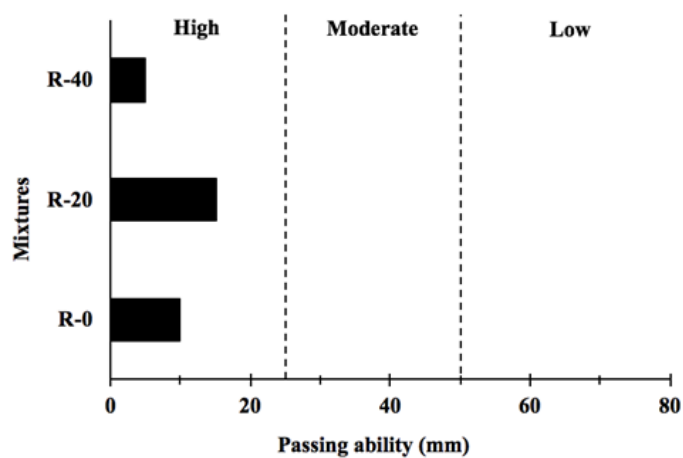


Figure 50: Passing ability of mixtures with SSA as cement replacement.



Figure 51: J-ring test for SCC mixtures.

### 5.2.3 V-Funnel Test

V-funnel test allows the freshly mixed concrete to flow through small cross sections and bounded spaces, and hence the viscosity and filling characteristics of the mixture being tested could be judged. The EFNARC (2005) specifications are shown in Table 30. VS represents the viscosity classes expressed by the  $T_{50}$ , while VF represents the viscosity classes expressed by the V-funnel time.

V-funnel test was conducted on the three mixtures (R-0, R20, and R-40) and results are presented in Table 31. The recorded V-funnel times show an increasing trend, indicating a higher viscosity in the replacement mixtures. Although R-20 and R-40 contained a higher VMA dosage than the control mix, an increase of the produced SCC mix viscosity was noted; as the V-funnel time increased from 7.6 seconds in the control to 12.2 seconds in R-40. Yet, it is within the acceptable range as per EFNARC. From Table 30 and Figure 52, the control mix (R-0) corresponded to the first viscosity class, while the other two mixtures incorporating SSA as a partial replacement of cement were classified according to the second viscosity class according to EFNARC

specifications. This implies that the inclusion of SSA led to more viscous concrete, thus improving the segregation resistance properties of concrete.

Table 30: Viscosity classes. (EFNARC, 2005).

<b>Class</b>	<b>T50 (seconds)</b>	<b>V-funnel time (seconds)</b>
VS1/VF1	$\leq 2$	$\leq 8$
VS2/VF1	$>2$	9 to 25

The effect of several SCM on the V-funnel times was investigated by Uysal and Sumer (2011). Similar to SSA, as the replacement percentage of FA increased from 15 to 35%, the V-funnel time increased as well. However, increasing the percentage replacement of MP from 10 to 30% resulted in a decrease of the V-funnel time. The optimal replacement percentage of GGBS in terms of V-funnel time, was found to be 60% and 20% for both limestone powder (LP) and blast powder (BP), respectively.

Table 31: Recorded V-funnel times for mixtures with SSA as cement replacement.

<b>Mixtures</b>	<b>V-funnel (seconds)</b>
R-0	7.59
R-20	10.54
R-40	12.20

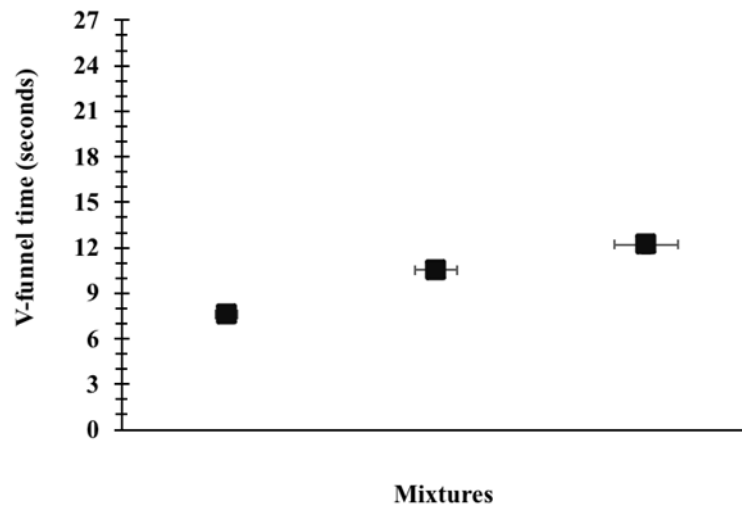


Figure 52: V-funnel time for mixtures with SSA as cement replacement.

#### 5.2.4 Concluding Remarks

- Incorporating SSA in the control mix at 20% and 40% partial replacement of cement resulted in a significant decrease of the slump flow and  $T_{50}$  cm values due to its rough surface texture and irregular morphology, in addition to the high absorption characteristics of SSA particles.
- When reusing SSA in producing SCC, it is mandatory to modify the mixture. The fine aggregate content should be reduced and adjusting the SP and VMA dosages.
- Reducing the dune sand-to-total fine aggregate ratio in R-20 and R-40 by 10% and 24% respectively and increasing the admixture dosages caused a better flowability of the mixture than that of the control mix; where both R-20 and R-40 were classified as SF2 according to EFNARC specifications. In addition, a reduction in  $T_{50}$  cm time was recorded.

- The J-ring test results of R-20 and R-40 were under 0-25 mm and satisfied EFNARC guidelines. Both mixtures exhibited a high passing ability, therefore could be used in congested reinforcement elements.
- Although the VMA dosages were increased, the V-funnel time values increased as the replacement level of SSA increased from 0% to 40% and both mixtures incorporating SSA as a partial replacement of OPC were classified as VF2 according to EFNARC specifications.
- The increment of V-funnel time indicates that the addition of SSA in SCC mixture increased its viscosity, and therefore improved the segregation resistance of the mixture.
- In terms of fresh properties, using SSA as a partial replacement of OPC to produce SCC was feasible. However, to achieve a concrete mixture with the addition of SSA that satisfies all three requirements of SCC; flowability, passing ability, and cohesiveness, the mix design should be modified to have less dune sand – to – crushed stone sand ratio, and high admixture dosages.

### **5.3 Hardened Concrete Properties**

In this section, the mechanical properties such as compressive strength, and drying shrinkage, besides durability characteristics such as pore size distribution, electrical resistivity, sorptivity, percent permeable pores, and water permeability were evaluated. All outcomes are presented, interpreted, and discussed in the coming subsections.



### 5.3.1 Compressive Strength

The compressive strength of concrete is an essential property for construction. It is the most valued by designers and engineers; where it is the main criteria used to determine whether a given concrete mixture will meet the needs of a specific application. The compressive strength of concrete is mainly affected by the cement hydration process and the production of C-S-H since it is the responsible for strength and other mechanical properties of cement-based material (Shahrin and Bobko, 2017). Strength is measured at four different test ages (7, 28, and 90 days) in order to account for the changes in the concrete structure and therefore, its strength development with age. These changes happen due to variations in the hydrated cement paste and the transition zone that are prone to alterations with time and different ambient conditions (Mehta and Monteiro, 1994).

The strength values presented were obtained by calculating the average of three specimens for each concrete mixture at the test age. The variation in the measured values in the three replicates can be attributed to the quality control followed during the casting and testing of the mixtures. With regards to “Specifications for structural concrete –ACI 301-05”, the coefficient of variation (COV) within the test results for batches cast in the laboratory with a “good” class of operation should not exceed 4%. The COV is simply the standard deviation divided by the mean as a percentage, and it is a measure of the relative variability for a given data set. It helps to judge the reproducibility of measurements on replicates in any test results. The calculated COV of the three strength values is presented in Table 32. The COV values showed good quality control of the mixtures.

The mean values of the compressive strength ( $F_c$ ) of hardened SCC control mix and SCC incorporated 20% and 40% of SSA at 7, 28, and 56 days of curing were measured, and results are summarized in Table 33 and Figure 53. The control mix (R-0) developed compressive strength of 57.4, 66.7, and 71.2 MPa at the age of 7, 28 and 56 days, respectively. It was observed that, the compressive strength of SCC mixtures decreased with the addition of SSA as a partial replacement of OPC. However, for all the mixes the compressive strength increased with time. The reduction of strength caused by the addition of 20% SSA at early age (7 days) was approximately 9.4%, whereas at late ages (28 and 58 days), the compressive strength obtained for R-20 was comparable to the control mix with a reduction of 2%. Yet, as the replacement ratio of SSA increased, SCC mixtures exhibited a notable decrease in strength. In agreement with Goh et al. (2003), adding 40% of SSA, reduced the compressive strength up to 50%. Similar to R-20, this reduction became less with time at about 30.9%, and 22% for 28 and 56 days, respectively. This notable decrease in strength could be explained by the slow pozzolanic activity that SSA exhibits at early ages (Pan et al., 2002), and the changes in the content of pozzolanic active matter in the sewage sludge. In addition, it was obvious from the calculated strength gain of SCC mixtures illustrated in Figure 54 that SSA participates in improving strength at later ages. As the replacement percentage of SSA increased, the strength development with age increased as well. From 7 to 28 days, replacing up to 40% of OPC with SSA, resulted in a strength gain of about 50%, followed by R-20 and R-0 with values of 16.2, and 25.7%. From 28 to 56 days, R-40 improved the strength by 20%. Therefore, it is obvious that the pozzolanic reaction is continued for a long period; which implies that SSA particles exhibited pozzolanic reactivity at late ages, which might have in turn delayed early strength gain.

Hence, it can be reported that SSA plays an important active role in late compressive strength development and a positive strength gain with age. In addition, in terms of compressive strength, and to avoid strength reduction, it is recommended to produce SCC mixtures with SSA replacement ratios of the range of 20%. The same conclusion was also reached by Kappel et al. (2017) when SSA replaced 20% of OPC in conventionally vibrated mortars.

Table 32: COV of compressive strength values for mixtures with SSA as OPC replacement.

Mixtures	Coefficient of variance (%)		
	7 days	28 days	56 days
R-0	3.6	2.1	1.9
R-20	2.4	0.9	2.0
R-40	3.1	1.1	3.2

Table 33: Average compressive strength for mixtures with SSA as OPC replacement

Compressive Strength (MPa)	Test age	Mixtures		
		R-0	R-20	R-40
	7 Days	57.4	52	30.1
	% change at 7D from control	-	- 9.4	- 47.7
	28 Days	66.7	65.4	46.0
	% change at 28D from control	-	- 1.94	- 31.0
	% change at 28D from 7D	16.20	25.77	52.8
	56 Days	71.23	69.5	55.2
	% change at 56D from control	-	- 2.43	- 22.5
	% change at 56D from 28D	6.79	6.27	20

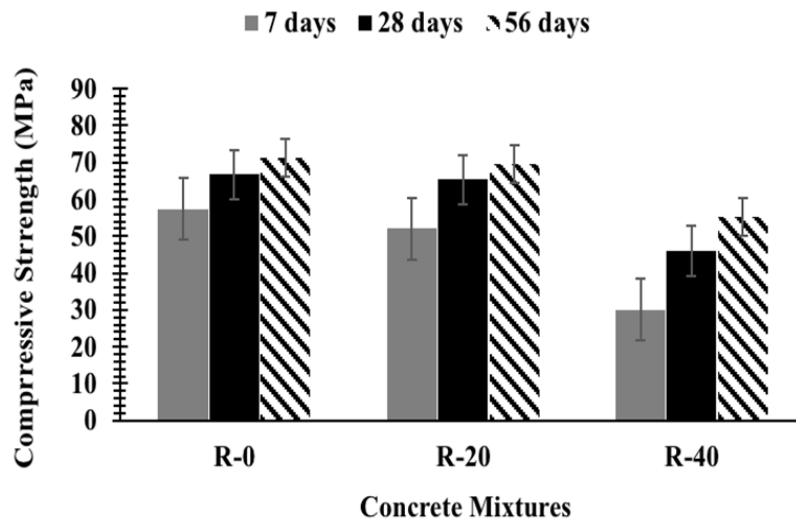


Figure 53: Compressive strength for mixtures with SSA as OPC replacement.

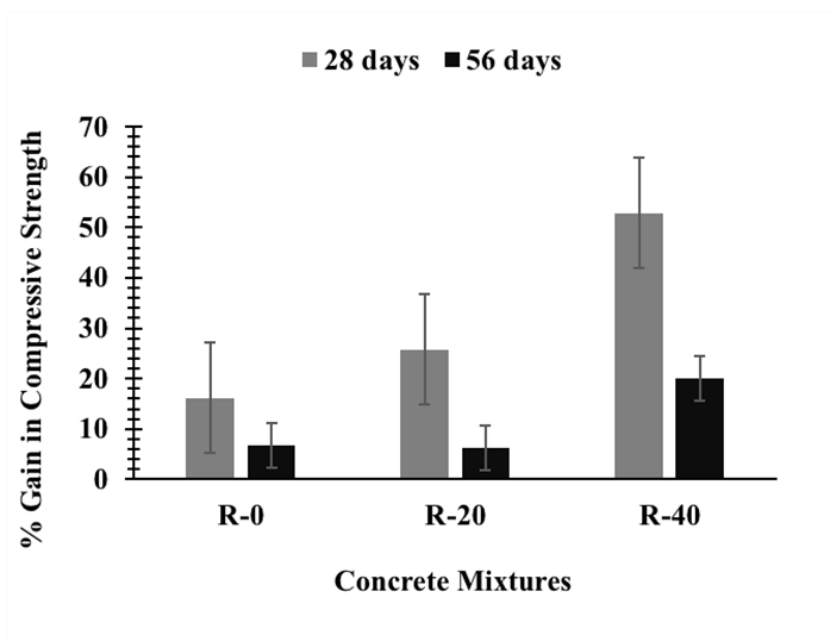


Figure 54: Percentage gain in compressive strength.

### 5.3.2 Pore Size Distribution

The hydration reaction taking part in cement results in a product consisting of solid and a pore system. Therefore, the matrix consists of aggregates, the solid cement

hydrates, unhydrated cement, etc., and the pore system. (Nagraj and Zahida, 1996). The pore system is responsible of the most properties of concrete mixes, notably strength and durability. The most important characteristics of pore system are porosity and pore size distribution, which can be determined through mercury intrusion porosimetry (MIP).

The pore size distribution is illustrated in Figure 55. Average results of the total porosity and the median pore diameter are shown Table 34. It can be observed that at 56 days of curing, the total porosity of pastes contained 20 and 40% SSA slightly increased from about 22 to 25%. Yet, increasing the replacement ratio from 20% to 40%, showed a negligible increase of the porosity. The median pore diameter results shows that there was no significant difference between R-0 and R-20 in the median pore diameter. Yet, replacing up to 40% of OPC by SSA, resulted in a slight increase of about 11.6% in the median pore diameter compared to the control mix. As reported in literature, this slight increase in the median pore diameter was mainly due to the porous nature observed in SSA particles (Chen and Poon, 2017); which in turn decreased the interconnectivity of the pores in the mix. Dense pore structure limits the penetrability through concrete matrix, and therefore improve the strength and durability of concrete when subjected to aggressive environment. Hence, the pore diameter is an indirect measure of the strength and durability of the produced concrete. As a result, it can be concluded that the observed increment in median pore diameter for R-40; would slightly decrease the durability of the produced SCC.

Table 34: Total porosity for concrete with SSA as cement replacement.

Mortars	Total Porosity (%)*	Median pore diameter ( $\mu\text{m}$ )*
	56 days	56 days
R-0	22.404	2.8944
R-20	25.745	2.8981
R-40	25.349	3.0111

\*Values are the mean in % for the total porosity and in  $\mu\text{m}$  for the median pore diameter

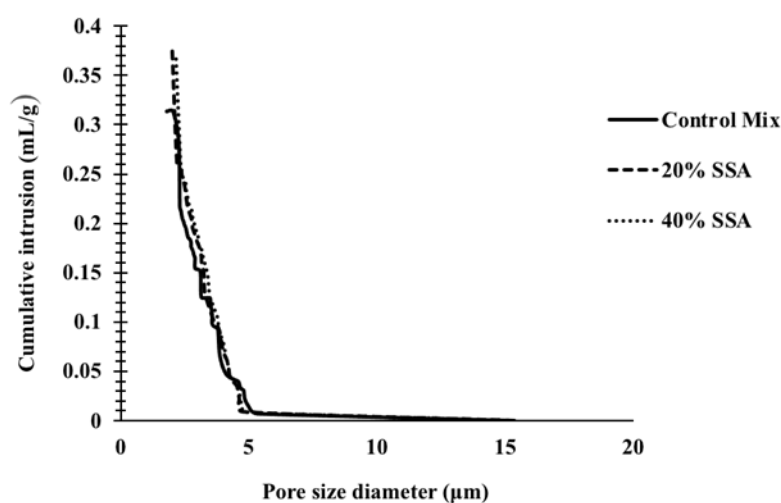


Figure 55: Pore size distribution of concrete mixtures with SSA as cement replacement.

### 5.3.3 Bulk Electrical Resistivity

Bulk electrical resistivity of the concrete mixtures at each age were measured as the average resistivity of three tested specimens. Several factors such as porosity, pore size distribution, connectivity, concrete's moisture content, and ionic mobility in pore solution affect the resistivity of concrete (Shahroodi, 2010). The resistivity test was conducted to assess the possibility of steel corrosion in concrete. According to ACI 222R-01 (2010), the corrosion protection level is divided into four categories based on the resistivity value and are presented in Table 35.

Table 35: Corrosion protection classification based on concrete resistivity. (ACI 222R01, 2008).

<b>Resistivity (k<math>\Omega</math>.cm)</b>	<b>Corrosion protection</b>
<5	Low
5 – 10	Moderate – Low
10 – 20	High
>20	Very High

Figure 56 and Table 36 represent the total bulk resistivity for all SCC mixtures at 28 and 56 days of curing. Observing the results, R-0 and R-20 mixes had very close resistivity values of 10.7 and 10.9 k $\Omega$ .cm, respectively; showing high corrosion protection for steel bars embedded in concrete with regards to ACI 222R-01 (2010). As the replacement level increased to 40% (R-40), the bulk resistivity value dropped notably to 4.87 k $\Omega$ .cm, and therefore had a low corrosion protection. Based on the non-linear relationship between moisture content and bulk electrical resistivity, the reason behind this decrease might be due the excess moisture content which was not yet consumed by hydration, due to the reduction in the cement content. In addition, it could be attributed to the high median pore diameter for R-40. As the replacement ratio of SSA increases, the metal oxides level increases in the mix. From Table 37, it can be reported that the total metal oxide of SSA was 25.36%, while 7.44% was only detected in OPC. Additionally, both CuO, and NiO which are highly conductive metals were significantly higher in SSA compared to OPC. This could be another reason for the significant decrease in the electrical resistivity for SCC mix with 40% SSA replacement. However, at late ages, all SCC mixtures showed a high corrosion protection. The bulk resistivity of R-40 considerably increased by more than half with a value of 10.22 k $\Omega$ .cm. Results indicated that SSA tended to consume calcium hydroxide over time, producing more C-S-H gel in the concrete due to possible

pozzolanic reactions; this decreased the amount of OH<sup>-</sup> in the pore solution, and refirming the pore structure, therefore reducing the conductivity of the concrete, and consequently contributing to the increase in the electrical resistivity.

Reusing SSA as lightweight aggregate to produced light weight concrete resulted in increasing the resistivity of the concrete, and therefore it was reported that SSA can be used to produce LWC with a good corrosion endurance (Tuan et al., 2013).

Table 36: Resistivity results for mixtures with SSA as OPC replacement.

Average Resistivity (kΩ.cm)	Test age	Mixtures		
		R-0	R-20	R-40
	28 days	10.7 (0.077)	10.87 (0.41)	4.87 (0.84)
	% change at 28 d from control	-	1.59	-54.49
	56 Days	12.85 (0.25)	11.42 (0.40)	10.22 (1.13)
	% change at 56 d from control	-	-11.13	-20.47
	% change at 56 d from 28 d	20.09	5.06	109.86

\* Values in parentheses represent the standard deviation in kΩ.cm.

Table 37: Metal oxides concentration in OPC and SSA9-2.

Oxide (wt%)	OPC	SSA9-2
Alumina (Al <sub>2</sub> O <sub>3</sub> )	1.97	9.63
Iron oxide (Fe <sub>2</sub> O <sub>3</sub> )	4.25	6.17
Magnesium oxide (MgO)	-	7.02
Potassium oxide (K <sub>2</sub> O)	0.66	1.20
Titanium oxide (TiO <sub>2</sub> )	0.27	0.70
Zinc oxide (ZnO)	0.06	0.25
Strontium oxide (SrO)	0.12	0.15
Manganese oxide (MnO)	0.09	0.13
Copper oxide (CuO)	0.019	0.10
Nickel oxide (NiO)	0.003	0.018
Total metal oxides	7.44	25.36



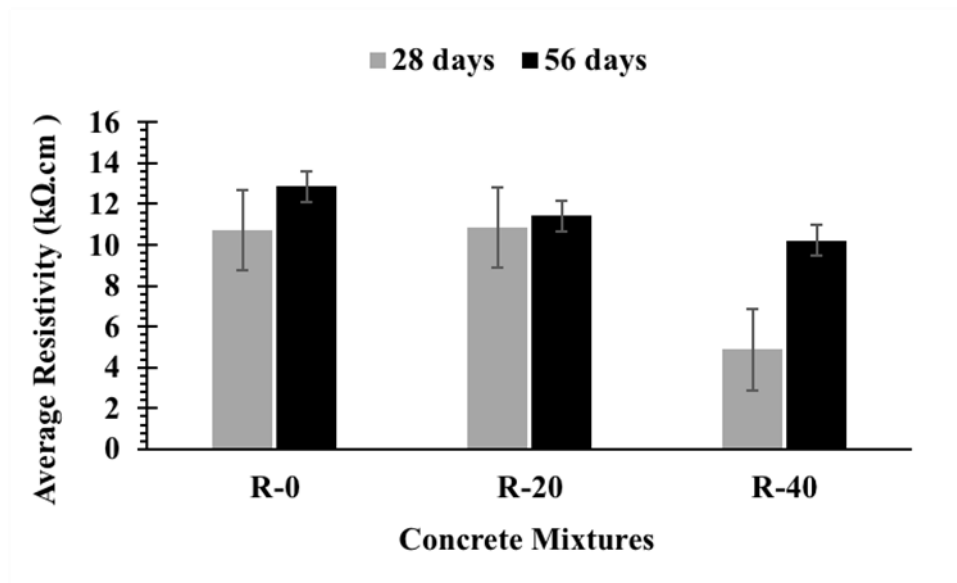


Figure 56: Bulk resistivity for mixtures with SSA as OPC replacement.

### 5.3.4 Initial Rate of Absorption

Initial rate of absorption (i.e. sorptivity) was also referred to as the rate of capillary absorption. The capillary pores are present in hardened concrete as a result of excess water leaving the concrete after the cement hydration process stops, resulting in the formation of the pore system. Capillary absorption (sorptivity) is primarily the transport mechanism for water in the tiny pores in concrete due to surface interactions between the water and the pore wall. It depends on the properties and composition of concrete constitute materials, initial curing condition and duration, age of concrete and environmental exposure during drying and conditioning of concrete (Singh et al., 2018).

Table 38 and Figure 57 present the initial rate of absorption of SCC mixtures at two test ages i.e.: 28 and 56 days. It was clear that as the curing age increased the initial rate of absorption for all the mixes decreased. At 28 days of curing, it was

observed that the control mix had the lowest initial rate of absorption with a value of  $0.15 \text{ mm/min}^{1/2}$ . Incorporating 20, and 40% of SSA as a partial replacement of cement increased the initial rate of absorption by 13% and 6%, respectively. At late ages (56 days) it was noted that the lowest initial rate of absorption was detected for R-20 with a value of  $0.10 \text{ mm/min}^{1/2}$  with 50% decrease in the sorptivity value, followed by control mix and R-40; which verifies that previously observed results that implied the late pozzolanic activity of SSA particles and the reduction in permeable pores percentage. At late ages, the SSA reaction with cement by binding CH with its free silica results in the production of non-soluble C-S-H structure. Thus, producing densely packed concrete with reduced water infiltration. Jamshidi et al. (2012) found that using SSA content of 5% or even 10% does not change the concrete capillary network. However, increasing the ash content to 20% almost doubled the initial rate of absorption. Torgal and Castro-Gomes (2006) obtained capillary water absorption coefficients between  $0.85$  and  $2.6 \text{ kg/m}^2 \text{ h}^{0.5}$  for a plain C20/25 strength class concrete, the most used strength class in Europe (ERMCO, 2009). Therefore, it can be concluded that the addition of 20% SSA with further modifications in the mix design, could produce SCC with a satisfactory water absorption rate, and thus good durability.

Table 38: Initial rate of absorption for mixtures with SSA as OPC replacement.

Initial rate of absorption ( $\text{mm/min}^{1/2}$ )	Test age	Mixtures		
		R-0	R-20	R-40
	28 Days	0.15 (3.15)	0.17 (3.17)	0.16 (7.53)
	% change at 28d from control	-	13.3	6.2
	56 Days	0.14 (16.62)	0.10 (8.18)	0.15 (9.46)
	% change at 56d from control	-	-28.57	7.14
	% change at 56d from 28d	-6.67	-50	-6.25

\*Values in parentheses are the standard deviation in  $\text{mm/min}^{1/2}$

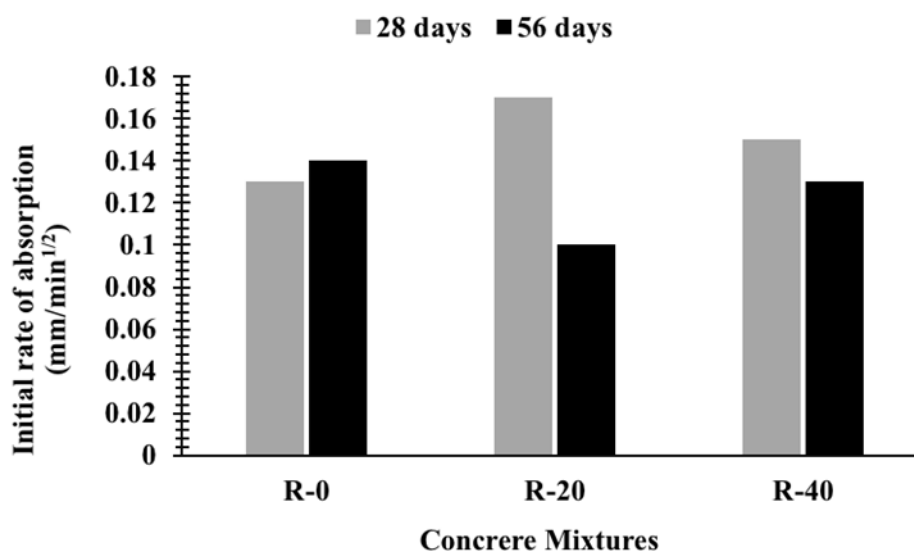


Figure 57: Initial rate of absorption for mixtures with SSA as OPC replacement.

### 5.3.5 Permeable Pore Percentage

Besides initial rate of absorption test, permeable pore percentage was also evaluated. The difference is that the initial rate of absorption uses specimens partially in contact with water from only one side, while the permeable pores test requires the sample to be fully submerged. Hence, it was expected that permeable pores test will give indication on the average value rather than only the surface pores.

The development of the microstructure could be assessed by measuring the permeable pores of the concrete mixtures. The results of the permeable pores at 28 and 56 days of age are shown in Table 39. Overall, there was no considerable effect of incorporating SSA on the volume of voids. However, at 28 days of curing, the highest permeable pore percentage was found when OPC was replaced by 20% SSA (R-20) with a value of 12%, followed by R-0 and R-40 with 11.4 and 11%, respectively. As the curing age increased, the permeable pores percentage for R-20 dropped to 7.3% to have the lowest percent of permeable pore; which is reflected on reducing the initial

water absorption of R-20. Both R-0 and R-40 had a very similar permeable pore percentage with values of 7.8 and 7.9% respectively; indicating that as the replacement percentage increases, the effectiveness of SSA to minimize the permeable pore fraction is reduced. Hence, it can be concluded that incorporating 20% of SSA in SCC mixtures improved the durability characteristics of SSA mixture, while replacing 40% would result in SCC mixture relatively similar to the control mix in terms of microstructure's development.

Table 39: Permeable pore test results for mixtures with SSA as OPC replacement.

Concrete Mixtures	Average permeable pores (%)*	
	28 days	56 days
R-0	11.4 (0.08)	7.8 (0.12)
R-20	12 (0.32)	7.3(0.54)
R-40	11 (0.1)	7.9 (0.64)

\*Values in parenthesis are the standard deviation in %.

### 5.3.6 Water Permeability

Durability can be connected to the ease with which both liquids and gasses can flow through concrete, in another term “permeability” (Mohammed et al., 2019). Permeability is a measure of flow of water under pressure in a saturated porous medium. The permeability of cementitious materials depends mostly on their porosity, tortuosity, and continuity of pores aligned with size, shape and pore distribution.

The water permeability and permeable pores in SCC mixtures cured at 28 and 56 days was measured, and results are shown in Table 40. Results obtained showed that as the replacement percentage of SSA increased, the water permeability coefficient increased. Yet, it became lower with late ages. The ability of water

penetrating SCC mixes made of SSA is mainly due to the porous nature of SSA particles, and the porosity between the pores which was previously observed in the pore size distribution analysis. R-20 had 10 and 100 times higher water permeability compared to the control mix at 28 and 56 days respectively, while R-40 showed an even higher water permeability by 100 and 1000 times at 28 and 56 days. However, by observing the results, it was found that the water permeability coefficient was low for all SCC mixtures. Since water permeability is one of the main factors affecting the durability of concrete (Ramezani-pour and Tarighat, 2001), it can be concluded that all SCC mixtures included SSA as partial replacement of cement tended to have a high durability.

Table 40: Water permeability test results for mixtures with SSA as OPC replacement.

Concrete Mixtures	Average water permeability (m/sec)	
	28 days	56 days
R-0	8.33E-12	8.75E-13
R-20	8.47E-11	7.24E-11
R-40	4.53E-10	1.62E-10

### 5.3.7 Drying Shrinkage

Shrinkage can be defined as volumetric time dependent change in concrete due to loss in moisture conditions (Bhattacharya, 2008) or the withdrawal of water from concrete stored in air (Neville, 1995). Emptying of the capillaries causes a loss of water without shrinkage but, once the capillary water has been lost, the removal of adsorbed water takes place and causes shrinkage (Neville, 1995). Concrete usually undergoes shrinkage when there is a difference in the relative humidity of the voids in the concrete pore structure and the surrounding environment the concrete is placed in. As this difference increases, an evaporation process starts taking place. The evaporation

process depends on several factors: external (i.e. relative humidity and temperature) and internal (i.e. amount of mixing water, size of aggregate, and quantity of cementitious material used) that can affect both the rate and magnitude of shrinkage (Ates, 2010). The temperature and relative humidity readings were monitored throughout the test period and they ranged from 25°C to 35°C and from 40% to 60%, respectively.

The drying shrinkage strain for the three SCC mixtures was measured over 110 days as shown in Figure 58. It can be seen that up to 10 days, the highest drying shrinkage value was obtained for the control mix. This might be due the high heat of hydration of the control mix. After 10 days, the drying shrinkage values of the control mix and R-20 became relatively close; indicating that replacing up to 20% of SSA, had no effect on the drying shrinkage values. At 40% SSA replacement, drying shrinkage measurements between 56 and 76 days were not recorded and illustrated in Figure 58 as a gap. Yet, it can be seen that increasing the replacement ratio up to 40% (R-40) increased the drying shrinkage of the mix which might be related to the increase in free water content in the mix (Pittman and Ragan, 1998). Water absorbed by the pores of SSA particles creates additional free water in addition to the water in the cement paste. Upon drying, the free water in the pores of SSA particles might evaporate before being consumed by the cement hydration. The drying shrinkage of SSC mixtures containing 0% SSA, 20% SSA, and 40% SSA was 0.053%, 0.494% and 0.050% of the initial length respectively at the end of 56 days; meeting the requirement of BS ISO 1920 (2009) which specifies a drying shrinkage limit of 0.075% at 56 days. This indicates that replacing SSA as partial replacement of OPC would not negatively affect the performance of SCC in terms on drying shrinkage.

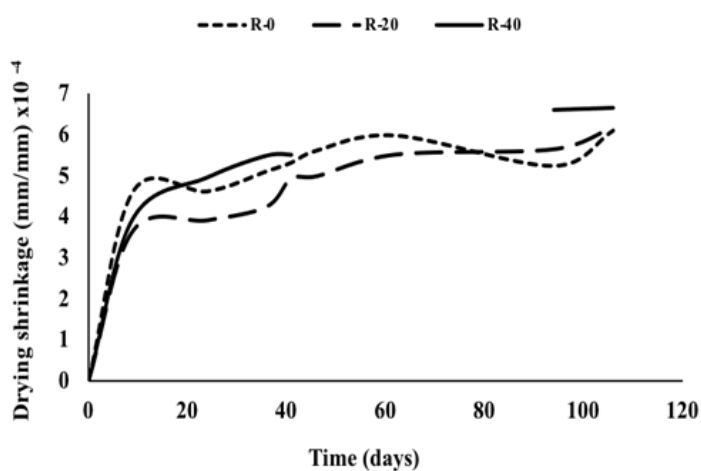


Figure 58: Drying shrinkage strain for mixtures with SSA as OPC replacement.

#### 5.4 Performance Index for SCC mixtures

According to EFNARC (2005) guidelines, the concrete purchaser should only select those fresh concrete characteristics necessary for the special SCC application and over specification of both the concrete characteristics and class should be avoided. However, slump flow will usually be required for all SCC mixtures. When good surface finish is required in addition to the existence of highly congested reinforcement such as non-structural elements, viscosity becomes essential (PI-1).

Table 42 and Table 43 show the weighted ranks and numeric indices for all SCC mixtures. The individual performance criteria are presented in Table 41, while the multifunctional performance criteria are presented in Table 42. The shaded cells indicate the mixtures that best suits the application with the required performance criteria.

Table 41 shows the selected SCC mixtures for different performance criteria. R-40 had the optimal fresh concrete properties. Therefore, reusing 40% of SSA could

be used to produce SCC for low-strength but high flowability and viscosity applications. For certain applications, the flowability and compressive strength are very important to meet construction and design requirements. Therefore, it is needed to select the mixture with optimum flowability and compressive strength. The use of 20% SSA will satisfy this performance criteria (PI-3). For applications that require strength and durability (PI-6), it was found that SCC mixtures without any addition of SSA would produce a mixture with desired performance, and increasing the addition of SSA in the mixture would not be recommended in terms of strength and durability. If flowability and durability are the required properties (PI-4), then, the use of 20% SSA mixtures would achieve the desired properties. For applications that require all properties (PI-7), flowability, viscosity, strength and durability, the use of 20% SSA will satisfy the requirement. It can be concluded that the most suitable SSA replacement level for required performance criteria is 20%; where it had the highest PI in all performance criteria except for the strength and durability (PI-6), yet the difference between the control mix and R-20 was observed to be minor and therefore negligible.

The results of the PI approach showed that SSA can be used as a partial cement replacement to produce concrete mixtures with desired performance criteria. However, the SSA content will vary and will depend mainly on the required performance criteria of the mixture that will be application related. The PI approach is a very useful tool that can help combining several data values in just one metric in order to facilitate the selection process. The PI approach can be modified to include other performance criteria such as cost and possible others.



Table 41: Selected SCC mixtures for different performance criteria.

<b>Performance Criteria</b>	<b>SCC Mixtures</b>
Flowability + Viscosity	R-40
Flowability + Strength	R-20
Viscosity + Strength	R-20
Flowability + Durability	R-20
Viscosity + Durability	R-20
Strength + Durability	R-0
Workability + Viscosity + Strength + Durability	R-20

Table 42: Performance indices for individual criteria.

Concrete Mixtures	Individual performance criterion							
	Flowability		Viscosity		Strength (28 days)		Durability (28 days)	
	W <sub>i</sub>	R <sub>i</sub>	W <sub>i</sub>	R <sub>i</sub>	W <sub>i</sub>	R <sub>i</sub>	W <sub>i</sub>	R <sub>i</sub>
R-0	0.95	4.74	0.62	3.11	1	5	0.98	4.90
R-20	1	5	0.86	4.31	0.98	4.90	1	5
R-40	0.97	4.84	1	5	0.69	3.45	0.45	2.24

Table 43: Performance indices for multifunctional criteria.

Concrete Mixtures	Multiple Performance Criterion						
	PI-1	PI-2	PI-3	PI-4	PI-5	PI-6	PI-7
R-0	68	96	73	92	71	100	68
R-20	89	100	100	100	100	98	100
R-40	100	68	81	44	52	32	35

Table 44: Required performance criterion.

Performance Index (PI)	Required Performance Criterion
PI-1	Flowability + Viscosity
PI-2	Flowability + Strength
PI-3	Viscosity + Strength
PI-4	Flowability + Durability
PI-5	Viscosity + Durability
PI-6	Strength + Durability
PI-7	Workability + Viscosity + Strength + Durability

## 5.5 Concluding Remarks

Several conclusions were drawn on the performance of SCC utilizing SSA at the hardened stage. The findings are summarized below based on the test results discussed earlier:

- At early ages (i.e. 7 days), incorporating 20% and 40% of SSA as a partial replacement of OPC resulted in a decrease of SCC compressive strength by 9.7 and 47.7%, respectively. However, at late ages (i.e. 28 and 56 days), the compressive strength value of SCC mix incorporating 20% of SSA was comparable to the control mix with a reduction percentage of only 1.94 and 2.43%, respectively. Although the compressive strength increased at late age (i.e. 28, and 56 days) for R-40, yet it was lower than the control mix (R-0) by 31% and 22.5%, respectively.
- SCC mixes incorporated SSA as partial replacement showed a very good strength gain with age. At 28 days, the strength gain of R-0 (0% SSA) was 16.20%, while mixes incorporated 20% of SSA had a strength gain around 25%. Additionally, the strength developed was found to increase as the replacement ratio increased; where mixes incorporate 40% of SSA had a strength gain more than triple the control mix with 0% SSA. At late ages, the strength development of SSA incorporated 20% was comparable to the control mix. However, R-40 had a high strength gain with a value of 20%. Therefore, SSA was found to exhibit late pozzolanic activity, suggesting that using SSA in concrete mixtures improves late strength development.

- Incorporating 20% and 40% of SSA in concrete slightly increased the total porosity of the mix. However, the effect of incorporating 20% of SSA on the pore size distribution was negligible, while at 40% replacement level a minor increase was observed which might in turn slightly decrease the durability of the mixtures.
- At 28 days, both R-0 and R-20 showed high bulk resistivity, hence resulted in a “high” corrosion protection, while the bulk resistivity for 40% SSA had a very low corrosion protection due to excess moisture content which was not hydrated due to the decrease in cement content, and the total conductive metal oxides detected in SSA particles. However, at 56 days all SCC mixtures showed high electrical resistivity and therefore high corrosion protection.
- From the calculated percentage reduction of the initial rate of absorption (i.e. sorptivity), it was observed that SSA addition increased the rate of absorption at 28 days. However, at late ages and due to the pozzolanic activity of SSA, the rate of absorption decreased for all SCC mixtures, and the lowest was found when 20% of SSA replaced OPC.
- The general trend for the results of the permeable pores test was similar to all SCC mixtures. Yet, there was a slight increase in SCC mix incorporating 20% SSA as cement replacement. With age, the permeable pores of R-20 were found to decrease having the lowest permeable pore percentage compared to both R-0 and R-40.
- The water permeability of the mixtures was found to increase with increasing the replacement ratio of SSA. R-20 had 10 and 100 times higher water

permeability compared to the control mix at 28 and 56 days, respectively, while R-40 showed an even higher water permeability by 100, and 1000 times at 28 and 56 days, respectively. Despite of the observed increment of the water permeability as SSA content increase, all SCC mixtures had a very low water permeability value.

- The volumetric change (i.e. drying shrinkage) results showed that adding up to 40% of SSA resulted in increasing the drying shrinkage of the mix compared to the control mix and R-20. However, at 110 days all mixtures followed similar trend; suggesting that SSA addition had no considerable effects on the shrinkage of concrete.
- In general, it is feasible to utilize SSA in producing SCC with good strength and durability characteristics at a replacement ratio of 20%. However, at higher replacement ratios (i.e. 40%), SSA could be utilized to produce SCC mixtures with acceptable strength and durability.
- SCC mixture R-40 meets fresh properties in terms of flowability (i.e. slump flow), and viscosity (i.e. V-funnel). Therefore, R-40 could be used in the construction that does not require high strength.
- Mixture R-20 was found to satisfy all fresh properties, strength, and durability. Therefore, it could be used in most of the construction applications.
- SSA can replace cement up to 40% by mass in applications that do not require high strength. Yet, the optimal replacement percentage was found to be 20%

by mass; where it can be used in many applications requiring workable concrete, cohesive with high strength and longer service life.

## Chapter 6: Conclusions and Recommendations

### 6.1 General

The main aim of the proposed thesis is to investigate the potential of reusing solid waste materials as a concrete constituent to produce green and sustainable concrete, therefore taking a further step towards sustainable development. Disposal of solid waste material such as sewage sludge ash (SSA) is a serious environmental concern. Hence, this study could offer alternative route for disposing SSA in an environmentally friendly way, besides to enhancing the awareness of individuals and communities about the availability of such waste materials and attracting them towards developing new ways and ideas for reusing and utilizing SSA in the construction sector.

This experimental work focused on choosing the optimal incineration temperature and time to produce SSA with suitable characteristics to be incorporated as partial replacement of OPC in making SCC. Therefore, as a first step (phase 1), the effect of different incineration temperature and time on SSA characteristics (i.e. chemical, and mineral composition, morphology, particle and pore size distribution, pozzolanic reactivity, heat of hydration, and leachability of heavy metals) was investigated. In the second step, SSA replaced 20, and 40% of OPC, and the produced SCC mixtures were evaluated for their performance in the fresh and the hardened stages using multiple tests for each stage. Slump flow, J-ring, and V-funnel tests were conducted to assess the fresh stage characteristics. While compressive strength, pore size distribution, electrical bulk resistivity, initial rate of absorption, permeable pores, water permeability and drying shrinkage tests were performed to evaluate the

properties of the SCC mixtures in their hardened stage. Finally, a performance index evaluation approach was used to aid the identification of the best suitable mixture for a certain performance criterion or multifunctional performance criteria.

The main outcomes of the thesis beside recommendation for future work on the employment of SSA in the production of SCC are mentioned in the following subsections.

## **6.2 Conclusions**

### **6.2.1 Sewage Sludge Ash (SSA) Characteristics**

Several findings were observed on the characteristics of SSA incinerated at different temperature and time. The outcomes are listed below based on the test results discussed earlier:

- The major constituents of SSA samples were  $\text{SiO}_2$ ,  $\text{CaO}$ , and  $\text{P}_2\text{O}_5$ . However, other oxides such as  $\text{Al}_2\text{O}_3$ ,  $\text{Fe}_2\text{O}_3$ ,  $\text{MgO}$ ,  $\text{SO}_3$ , and  $\text{K}_2\text{O}$  were present in lesser proportions.
- As the incineration temperature and time increases, the formation of quartz ( $\text{SiO}_2$ ) increased. XRD analysis indicated the occurrence of some amorphous phases in the SSA which suggested that SSA could exhibit pozzolanic activities and has a potential to be used as a partial substitution of cement.
- SEM examination indicated that SSA particles were irregular with a rough surface. Nevertheless, the pore structure of the particles became more compact as a result of increasing the incineration temperature.



- Based on the Frattini test results, SSA samples exhibited a late pozzolanic activity (i.e. at 28 days of curing), yet the highest CaO removal was observed when SSA was incinerated at 900°C for 2 hours
- SAI results showed that mortars contained incinerated SSA for 6 hours didn't exhibit any pozzolanic activity. Also, it was concluded that as the incineration temperature increases, the SAI value decreases.
- SSA particles had a similar average particle size compared to OPC ~ 156 μm. The specific surface area of SSA particles was very close to that of OPC (1.0491 m<sup>2</sup>/g) falling in the range of 0.7 to 1.2 m<sup>2</sup>/g; indicating suitability for use as a supplementary cementing material.
- Due to the porous nature of SSA particles, incorporating SSA increased the total porosity of the paste at early ages. Yet, at late ages, an improvement in the microstructure for all the pastes was observed. Also, using 20% of SSA as cement replacement slightly reduced the total porosity and therefore enhanced the microstructure of the paste.
- SSA didn't affect the median pore size of the paste; where median pore diameter for all samples ranged from 2.51 to 2.73 μm. However, the highest pore diameter was found when pastes incorporated 40% of SSA. Incorporating 20% of SSA in cement paste reduced the pore size diameter by 5% compared to the control mix.
- SSA addition reduced the consistency of the mortar due to high water absorption, irregular morphology and rough surface texture of SSA particles.

However, as the incineration temperature increased, particles became more compact. The highest workability was achieved when SSA was incinerated at 1100°C due to the low SSA particles  $D_{50}$  and mean diameter compared to other SSA particles, in addition to the better compaction of materials as observed in SEM images. The inclusion of SSA improved the workability retention of cement paste.

- The addition of SSA in cement paste reduced the heat of hydration. Replacing 20% and 40% of OPC by SSA reduced the heat of hydration by 10.87 and 31.5%, respectively.
- The level of leaching of all tested metals was lower than their corresponding TCLP limit; indicating that there was no toxicity issue with the produced material and can be considered as a non-hazardous material.
- Based on the performance index approach, SSA produced by incineration at 900°C for 2 hours was selected to be examined as partial cement replacement in SCC mixture.

### **6.2.2 Fresh Concrete Properties**

Multiple concluding remarks could be drawn regarding the performance of SCC with SSA at the fresh stage. The main outcomes are summarized below based on the test results discussed earlier:

- Incorporating SSA in the control mix as 20% and 40% partial replacement of cement resulted in a significant decrease of the slump flow and  $T_{50\text{cm}}$  values

due to its rough surface texture and irregular morphology, in addition to the high absorption characteristics of SSA particles.

- When reusing SSA in producing SCC, it is mandatory to modify the mixture. The fine aggregate content should be reduced and adjusting the superplasticizer and viscosity enhancing admixture dosages.
- Reducing the dune sand-to-total fine aggregate ratio in R-20 and R-40 by 10% and 24% respectively and increasing the admixture dosages resulted in producing a concrete mixture with a better flowability than the control mix; where both R-20 and R-40 were classified as SF2 according to EFNARC specifications.
- The J-ring test results of R-20 and R-40 were under 0-25 mm and satisfied EFNARC guidelines. Both mixtures exhibited a high passing ability, therefore could be used in congested reinforcement elements.
- Although the VMA dosages were increased, the V-funnel time values increased as the replacement level of SSA increased from 0% to 40% and both mixtures incorporating SSA as a partial replacement of OPC were classified as VF2 according to EFNARC specifications.
- The increment of V-funnel time indicates that the addition of SSA in SCC mixture increased its viscosity, and therefore improved the segregation resistance of the mixture.
- In terms of fresh properties, using SSA as a partial replacement of OPC to produce SCC was feasible. However, to achieve a concrete mixture with the addition of SSA that satisfies all three requirements of SCC; flowability,

passing ability, and cohesiveness, the mix design should be modified to have less dune sand–to–crushed stone sand ratio, and high admixture dosages.

### 6.2.3 Hardened Concrete Properties

The hardened properties of SCC containing SSA as cement replacement were evaluated at 28 and 56 days. The main conclusions are summarized as follows:

- At early ages (i.e. 7 days), incorporating 20% and 40% of SSA as a partial replacement of OPC resulted in a decrease of SCC compressive strength by 9.7 and 47.7 %, respectively. However, at late ages (i.e. 28 and 56 days), the compressive strength value of SCC mix incorporating 20% of SSA was comparable to the control mix with a reduction percentage of only 1.94 and 2.43%, respectively. Although the compressive strength increased at late age (i.e. 28, and 56 days) for R-40, yet it was lower than the control mix (R-0) by 31% and 22.5%, respectively.
- SCC mixes incorporated SSA as partial replacement showed a very good strength gain with age. At 28 days, the strength gain of R-0 (0% SSA) was 16.20%, while mixes incorporated 20% of SSA had a strength gain around 25%. Additionally, the strength developed was found to increase as the replacement ratio increased; where mixes incorporate 40% of SSA had a strength gain more than triple the control mix with 0% SSA addition. At late ages, the strength development of SSA incorporated 20% was comparable to the control mix. However, R-40 had a high strength gain with a value of 20%. Therefore, SSA was found to exhibit late pozzolanic activity, suggesting that using SSA in concrete mixtures improves late strength development.

- Incorporating 20% and 40% of SSA in concrete slightly increased the total porosity of the mix. However, the effect of incorporating 20% of SSA on the pore size distribution was negligible, while at 40% replacement level a minor increase was observed which might in turn slightly decrease the durability of the mixtures.
- At 28 days, both R-0 and R-20 showed high bulk resistivity, hence resulted in a “high” corrosion protection, while the bulk resistivity for 40% SSA had a very low corrosion protection due to excess moisture content which was not hydrated due to the decrease in cement content, and the total conductive metal oxides detected in SSA particles. However, at 56 days all SCC mixtures showed high electrical resistivity and therefore high corrosion protection.
- From the calculated percentage reduction of the initial rate of absorption (i.e. sorptivity), it was observed that SSA addition increased the rate of absorption at 28 days. However, at late ages and due to the pozzolanic activity of SSA, the rate of absorption decreased for all SCC mixtures, and the lowest was found when 20% of SSA replaced OPC.
- The general trend for the results of the permeable pores test was similar to all SCC mixtures. Yet, there was a slight increase in SCC mix incorporating 20% SSA as cement replacement. With age, the permeable pores of R-20 were found to decrease having the lowest permeable pore percentage compared to both R-0 and R-40.
- The water permeability of the mixtures was found to increase with increasing the replacement ratio of SSA. R-20 had 10 and 100 times higher water permeability compared to the control mix at 28 and 56 days, respectively, while R-40 showed an even higher water permeability by 100, and 1000 times at 28

and 56 days. Despite of the observed increment of the water permeability as SSA content increased, all SCC mixtures had a very low water permeability value.

- The volumetric change (i.e. drying shrinkage) results showed that adding up to 40% of SSA resulted in increasing the drying shrinkage of the mix compared to the control mix and R-20. However, at 110 days all mixtures followed similar trend; suggesting that SSA addition had no considerable effects on the shrinkage of concrete.
- In general, it is feasible to utilize SSA in producing SCC with good strength and durability characteristics at a replacement ratio of 20%. However, at higher replacement ratios (i.e. 40%), SSA could be utilized to produce SCC mixtures with acceptable strength and durability.
- SCC mixture R-40 meets fresh properties in terms of flowability (i.e. slump flow), and viscosity (i.e. V-funnel). Therefore, R-40 could be used in the construction that does not require high strength.
- Mixture R-20 was found to satisfy all fresh properties, strength, and durability. Therefore, it could be used in most of the construction applications.
- SSA can replace cement up to 40% by mass in applications that do not require high strength. Yet, the optimal replacement percentage was found to be 20% by mass; where it can be used in many applications requiring workable concrete, cohesive with high strength and longer service life.

### 6.3 Recommendations

Based on the conducted investigation and the above conclusions, a number of recommendations are suggested for future studies as a continuation for the use of SSA in SCC industry.

- Full-scale testing (i.e. other mechanical properties) for SCC produced by utilizing SSA.
- Further work is needed to study the relation between SSA and admixtures.
- Study the concentration and leachability of heavy metals from concrete monolith.
- The microstructure of SCC mixtures after replacing SSA with OPC was not investigated in this thesis. Therefore, it is important to examine the development of microstructure in details.
- Study the performance of SSA when combined with other supplementary cementing materials (SCMs) by ternary and quaternary blends.
- Examining the effect of increasing the fineness of the SSA and the performance of SCC mixtures.
- Investigate the influence of SSA on the concrete mixtures' thermal stability and characteristics.

## References

- Ai-sharif, M. M., & Attom, M. F. (2014). A geoenvironmental application of burned wastewater sludge ash in soil stabilization. *Environmental Earth Sciences*, 71(5), 2453-2463.
- Aksu, Z. (2005). Application of biosorption for the removal of organic pollutants: A review. *Process Biochemistry*, 40(3-4), 997-1026.
- Alshankiti, A., Degefa, B.A., Gill, S., & Akhand, N. (2018). Sludge valorization feasibility study in United Arab Emirates. *International Center for Biosaline Agriculture*, Poster. Retrieved from [http://www.biosaline.org/sites/default/files/scientific\\_poster\\_12-sludge\\_valorization\\_feasibility\\_study\\_in\\_united\\_arab\\_emirates.pdf](http://www.biosaline.org/sites/default/files/scientific_poster_12-sludge_valorization_feasibility_study_in_united_arab_emirates.pdf) (Accessed 22nd December, 2018).
- Al-Shmaisani, S., Kalina, R., Rung, M., Ferron, R., & Juenger, M. (2018). *Implementation of a Testing Protocol for Approving Alternative Supplementary Cementitious Materials (SCMs): Natural Minerals and Reclaimed and Remediated Fly Ashes*. University of Texas at Austin. Center for Transportation Research.
- Alyamac, K. E., Ghafari, E., & Ince, R. (2017). Development of eco-efficient self-compacting concrete with waste marble powder using the response surface method. *Journal of Cleaner Production*, 144, 192-202.
- Anderson, M., & Skerratt, R. G. (2003). Variability study of incinerated sewage sludge ash in relation to future use in ceramic brick manufacture. *British Ceramic Transactions*, 102(3), 109-113.
- Aprianti, E., Shafigh, P., Bahri, S., & Farahani, J. N. (2015). Supplementary cementitious materials origin from agricultural wastes—A review. *Construction and Building Materials*, 74, 176-187.
- Ashish, D. K., & Verma, S. K. (2019). An overview on mixture design of self-compacting concrete. *Structural Concrete*, 20(1), 371-395.
- Ashtiani, M. S., Scott, A. N., & Dhakal, R. P. (2013). Mechanical and fresh properties of high-strength self-compacting concrete containing class C fly ash. *Construction and Building Materials*, 47, 1217-1224.
- Ates, U. (2010). *Effect of pozzolanic material on the restrained shrinkage behavior of self-consolidating concrete*. PhD, Rutgers University. New Jersey, United States.
- Atis, C. D. (2002). Heat evolution of high-volume fly ash concrete. *Cement and Concrete Research*, 32(5), 751-756.



- Azarsa, P., & Gupta, R. (2017). Electrical resistivity of concrete for durability evaluation: A review. *Advances in Materials Science and Engineering*, 2017. <https://doi.org/10.1155/2017/8453095>.
- ACI 237R-07. (2008). Self-Consolidating Concrete. American Concrete Institute, ISBN: 9780870312441, 34.
- ACI 301-89. (1989). Specifications for Structural Concrete for Buildings. American Concrete Institute, 34.
- ACI 222R-01. (2010). Protection of Metals in Concrete Against Corrosion. American Concrete Institute, 41.
- ASTM C109/C109M. (2012). Standard Test Method for Compressive Strength of Hydraulic Cement Mortars. *ASTM International, West Conshohocken, Pennsylvania*.
- ASTM C1107/C1107M. (2012). Standard Specification for Packaged Dry, Hydraulic-Cement Grout (Nonshrink). *ASTM International, West Conshohocken, Pennsylvania*.
- ASTM C1437-15. (2019). Standard test method for flow of hydraulic cement mortar. *ASTM International, West Conshohocken, Pennsylvania*.
- ASTM C150/C150M-17. (2019). Standard specification for Portland cement. *ASTM International, West Conshohocken, Pennsylvania*.
- ASTM C157. (2006). Standard test method for length change of hardened hydraulic-cement mortar and concrete. *ASTM International, West Conshohocken, Pennsylvania*.
- ASTM C1585-13. (2013). Standard Test Method for Measurement of Rate of Absorption of Water by Hydraulic-Cement Concretes. *ASTM International, West Conshohocken, Pennsylvania*.
- ASTM C1602. (2006). Specification for Mixing Water Used in the Production of Hydraulic Cement Concrete. *ASTM International, West Conshohocken, Pennsylvania*.
- ASTM C1611/C1611M. (2018). Standard Test Method for Slump Flow of Self-Consolidating Concrete. *ASTM International, West Conshohocken, Pennsylvania*.
- ASTM C1621/C1621M – 17. (2019). Standard Test Method for Passing Ability of Self-Consolidating Concrete by J-Ring. *ASTM International, West Conshohocken, Pennsylvania*.

- ASTM C1679. (2017). Standard Practice for Measuring Hydration Kinetics of Hydraulic Cementitious Mixtures Using Isothermal Calorimetry. *ASTM International, West Conshohocken, Pennsylvania.*
- ASTM C230/C230M. (1998). Standard specification for flow table for use in tests of hydraulic cement. *ASTM International, West Conshohocken, Pennsylvania.*
- ASTM C311/C311M-13. (2012). Standard test methods for sampling and testing fly ash or natural pozzolans for use in Portland-cement concrete. *ASTM International, West Conshohocken, Pennsylvania.*
- ASTM C494. (2013). Standard specification for chemical admixtures for concrete. Annual book of ASTM standards. *ASTM International, West Conshohocken, Pennsylvania.*
- ASTM C618-12a. (2012). Standard specification for coal fly ash and raw or calcined natural pozzolan for use in concrete. *ASTM International, West Conshohocken, Pennsylvania.*
- ASTM C642-13. (2013). Standard Test Method for Density, Absorption, and Voids in Hardened Concrete. *ASTM International, West Conshohocken, Pennsylvania.*
- Baeza, F., Payá, J., Galao, O., Saval, J. M., & Garcés, P. (2014). Blending of industrial waste from different sources as partial substitution of Portland cement in pastes and mortars. *Construction and Building Materials, 66*, 645-653.
- Baeza-Brotons, F., Garcés, P., Payá, J., & Saval, J. M. (2014). Portland cement systems with addition of sewage sludge ash. Application in concretes for the manufacture of blocks. *Journal of Cleaner Production, 82*, 112-124.
- Bapat, J. D. (2012). *Mineral admixtures in cement and concrete*. CRC Press.
- Bartos, P. J., Sonebi, M., & Tamimi, A. K. (2002). *Report 24: Workability and rheology of fresh concrete: compendium of tests—report of RILEM Technical Committee TC 145-WSM (Vol. 24)*. RILEM publications.
- Bhattacharya, A. (2008). *Effects of aggregate grading and admixtures/fillers on fresh and hardened properties of self-consolidating concrete* [MSc Thesis].
- Bhatty, J. I., & Reid, K. J. (1989). Compressive strength of municipal sludge ash mortars. *Materials Journal, 86*(4), 394-400.
- Bhatty, J. I., & Reid, K. J. (1989). Lightweight aggregates from incinerated sludge ash. *Waste Management & Research, 7*(4), 363–376.
- Białecka, B., Adamczyk, Z., & Grabowski, J. (2001). Utilization of sewage sludge for the production of selected ceramic construction materials. *Ceramics Material, 53*, 26-30.

- Bialowiec, A., Janczukowicz, W., & Krzemieniewski, M. (2009). Possibilities of management of waste fly ashes from sewage sludge thermal treatment in the aspect of legal regulations. *Rocznik Ochrona Srodowiska*, *11*, 959-971.
- Boukendakdji, O., Kenai, S., Kadri, E. H., & Rouis, F. (2009). Effect of slag on the rheology of fresh self-compacted concrete. *Construction and Building Materials*, *23*(7), 2593–2598.
- Boulay, N., & Edwards, M. (2000). Copper in the urban water cycle. *Critical Reviews in Environmental Science and Technology*, *30*(3), 297–326.
- Bouziani, T. (2013). Assessment of fresh properties and compressive strength of self-compacting concrete made with different sand types by mixture design modelling approach. *Construction and Building Materials*, *49*, 308–314.
- Brouwers, H. J. H., & Radix, H. J. (2005). Self-compacting concrete: Theoretical and experimental study. *Cement and Concrete Research*, *35*(11), 2116–2136.
- BS EN 12390-3 (2009). Testing hardened concrete. Compressive Strength of Test Specimens. *British Standard Institution, London, UK*.
- BS EN 196-5. (2011). Methods of testing cement - Part 5: Pozzolanicity test for pozzolanic cement. *British Standards Institution, London, UK*.
- BS EN 197-1. (2011). Cement, Part 1: composition, specifications and conformity criteria for common cements. *British Standards Institution, London, UK*.
- BS EN 450-1. (2012). Fly Ash for Concrete—Definition, Specifications and Conformity Criteria. *British Standards Institution, London, UK*.
- BS EN 7591-1. (1992). Porosity and pore size distribution of materials—Method of evaluation by mercury porosimetry. *British Standards Institution, London, UK*.
- BS ISO 1920-8. (2009). Testing of concrete. Determination of the drying shrinkage of concrete for samples prepared in the field or in the laboratory.
- Burris, L. E., & Juenger, M. C. (2016). Milling as a pretreatment method for increasing the reactivity of natural zeolites for use as supplementary cementitious materials. *Cement and Concrete Composites*, *65*, 163-170.
- Cepuritis, R., Jacobsen, S., Pedersen, B., & Mørtzell, E. (2016). Crushed sand in concrete—effect of particle shape in different fractions and filler properties on rheology. *Cement and Concrete Composites*, *71*, 26–41.
- Cheeseman, C. R., & Viridi, G. S. (2005). Properties and microstructure of lightweight aggregate produced from sintered sewage sludge ash. *Conservation and Recycling*, *45*(1), 18-30

- Cheeseman, C. R., Sollars, C. J., & McEntee, S. (2003). Properties, microstructure and leaching of sintered sewage sludge ash. *Resources, Conservation and Recycling*, 40(1), 13–25.
- Chen, C. H., Chiou, J., & Wang, K. S. (2006). Sintering effect on cement bonded sewage sludge ash. *Cement and Concrete Composites*, 28(1), 26-32.
- Chen, M., Blanc, D., Gautier, M., Mehu, J., & Gourdon, R. (2013). Environmental and technical assessments of the potential utilization of sewage sludge ashes (SSAs) as secondary raw materials in construction. *Waste Management*, 33(5), 1268-1275.
- Chen, Z., & Poon, C.S. (2017). Comparative studies on the effects of sewage sludge ash and fly ash on cement hydration and properties of cement mortars. *Construction and Building Materials*, 154, 791-803.
- Chen, Z., Li, J. S., & Poon, C. S. (2018). Combined use of sewage sludge ash and recycled glass cullet for the production of concrete blocks. *Journal of Cleaner Production*, 171, 1447-1459.
- Chiou, J., Wang, K. S., Chen, C. H., & Lin, Y. T. (2006). Lightweight aggregate made from sewage sludge and incinerated ash. *Waste Management*, 26(12), 1453-1461.
- Chipasa, K. B. (2003). Accumulation and fate of selected heavy metals in a biological wastewater treatment system. *Waste Management*, 23(2), 135-143.
- Chopra, D., & Siddique, R. (2015). Strength, permeability and microstructure of self-compacting concrete containing rice husk ash. *Biosystems Engineering*, 130, 72-80.
- Collins, F., & Sanjayan, J. (2000). Effect of pore size distribution on drying shrinking of alkali-activated slag concrete. *Cement and Concrete Research*, 30(9), 1401–1406.
- Commission, M. W. C. (1990). Sewage sludge ash use in bituminous paving. *Minnesota Department of Transportation, Minnesota Pollution Control Agency, St. Paul, MN*, 325.
- Corinaldesi, V., & Moriconi, G. (2011). The role of industrial by-products in self-compacting concrete. *Construction and Building Materials*, 25(8), 3181–3186.
- Coutand, M., Cyr, M., & Clastres, P. (2006). Use of sewage sludge ash as mineral admixture in mortars. *Proceedings of the Institution of Civil Engineers-Construction Materials*, 159(4), 153-162.

- Cyr, M., Coutand, M., & Clastres, P. (2007). Technological and environmental behavior of sewage sludge ash (SSA) in cement-based materials. *Cement and Concrete Research*, 37(8), 1278-1289.
- Daczko, J. (2019). *Self-consolidating concrete: Applying what we know*. CRC press.
- Danner, T., Norden, G., & Justnes, H. (2018). Characterisation of calcined raw clays suitable as supplementary cementitious materials. *Applied Clay Science*, 162, 391-402.
- Day, R., Gaimster, R., & Gibbs, J. (2005). Self-compacting concrete. *Concrete*, 39(10), 40-42.
- De Rojas, M. S., & Frías, M. (1996). The pozzolanic activity of different materials, its influence on the hydration heat in mortars. *Cement and Concrete Research*, 26(2), 203-213.
- De Rojas, M. S., Luxán, M. P. D., Frías, M., & Garcia, N. (1993). The influence of different additions on portland cement hydration heat. *Cement and Concrete Research*, 23(1), 46-54.
- Deeb, R., & Karihaloo, B. L. (2013). Mix proportioning of self-compacting normal and high-strength concretes. *Magazine of Concrete Research*, 65(9), 546–556.
- Dehn, F., Holschemacher, K., & Weiße, D. (2000). Self-compacting concrete (SCC) time development of the material properties and the bond behaviour. *Selbstverdichtendem Beton*, 5, 115–124.
- Diamond, S. (1976). Cement paste microstructure-an overview at several levels. *Proceeding Conference Held at University of SheffieldHydraulic Cement Paste-Their Structure and Properties*, 5–31.
- Diamond, S. (1986). The microstructure of cement paste in concrete. *In Proceedings of the 8th International Congress on the Chemistry of Cement*, 1, 113-121.
- Diamond, S. (2000). Mercury porosimetry: an inappropriate method for the measurement of pore size distributions in cement-based materials. *Cement and Concrete Research*, 30(10), 1517-1525.
- Diaz-Loya, I., Juenger, M., Seraj, S., & Minkara, R. (2019). Extending supplementary cementitious material resources: Reclaimed and remediated fly ash and natural pozzolans. *Cement and Concrete Composites*, 101, 44-51.
- Dinakar, P. (2012). Design of self-compacting concrete with fly ash. *Magazine of Concrete Research*, 64(5), 401–409.
- Dinakar, P., & Manu, S. N. (2014). Concrete mix design for high strength self-compacting concrete using metakaolin. *Materials & Design*, 60, 661–668.

- Dinakar, P., Sethy, K. P., & Sahoo, U. C. (2013). Design of self-compacting concrete with ground granulated blast furnace slag. *Materials & Design*, *43*, 161–169.
- Domone, P. (2009). *Proportioning of self-compacting concrete—the UCL method*. Retrieved from <https://discovery.ucl.ac.uk/id/eprint/1340073> (Accessed 15th April, 2019)
- Donatello, S., & Cheeseman, C. R. (2013). Recycling and recovery routes for incinerated sewage sludge ash (ISSA): A review. *Waste Management*, *33*(11), 2328–2340.
- Donatello, S., Freeman-Pask, A., Tyrer, M., & Cheeseman, C. R. (2010). Effect of milling and acid washing on the pozzolanic activity of incinerator sewage sludge ash. *Cement and Concrete Composites*, *32*(1), 54–61.
- Edamatsu, Y., Sugamata, T., & Ouchi, M. (2003). A mix-design method for self-compacting concrete based on mortar flow and funnel tests. *International RILEM Symposium on Self-Compacting Concrete*, 345–354.
- Edwin, R. S., De Schepper, M., Gruyaert, E., & De Belie, N. (2016). Effect of secondary copper slag as cementitious material in ultra-high performance mortar. *Construction and Building Materials*, *119*, 31–44.
- EFNARC (European Federation of National Trade Associations Representing Producers and Applicators of Specialist Building Products). (2005). *The European guidelines for self-compacting concrete: Specification, production and use*. Hampshire, U.K. Retrieved from <http://www.efnarc.org/pdf/SCCGuidelinesMay2005.pdf> (Accessed 24th November, 2020).
- EPA, U. (1992). Method 1311 Toxicity characteristic leaching procedure (TCLP). *Agency EP, editor*. Washington DC, USA.
- ERMCO (2009). European ready-mixed concrete industry statistics. Retrieved from <https://www.thbb.org/media/1944/ermco-2009.pdf> (Accessed 26th November, 2020).
- Esmailkhanian, B., Khayat, K. H., & Wallevik, O. H. (2017). Mix design approach for low-powder self-consolidating concrete: Eco-SCC—content optimization and performance. *Materials and Structures*, *50*(2), 1–18.
- Felekoglu, B. (2007). Utilisation of high volumes of limestone quarry wastes in concrete industry (self-compacting concrete case). *Resources, Conservation and Recycling*, *51*(4), 770–791.
- Felix, F., Fraaij, A. L. A., & Hendriks, C. F. (1997). Inorganic immobilisation of waste materials. *In Studies in Environmental Science*, *71*, 769–780.

- Ferrara, L., Park, Y. D., & Shah, S. P. (2007). A method for mix-design of fiber-reinforced self-compacting concrete. *Cement and Concrete Research*, 37(6), 957–971.
- Forth, J. P., Zoorob, S. E., & Thanaya, I. N. A. (2006). Development of bitumen-bound waste aggregate building blocks. *Proceedings of the Institution of Civil Engineers-Construction Materials*, 159(1), 23-32.
- Franz, M. (2008). Phosphate fertilizer from sewage sludge ash (SSA). *Waste Management*, 28(10), 1809-1818.
- Frías, M., De Rojas, M. S., & Cabrera, J. (2000). The effect that the pozzolanic reaction of metakaolin has on the heat evolution in metakaolin-cement mortars. *Cement and Concrete Research*, 30(2), 209-216.
- Frigione, G., & Marra, S. (1976). Relationship between particle size distribution and compressive strength in Portland cement. *Cement and Concrete Research*, 6(1), 113-127.
- Fuentes, A., Lloréns, M., Sáez, J., Soler, A., Aguilar, M. I., Ortuño, J. F., & Meseguer, V. F. (2004). Simple and sequential extractions of heavy metals from different sewage sludges. *Chemosphere*, 54(8), 1039-1047.
- Gesoğlu, M., Güneyisi, E., Kocabağ, M. E., Bayram, V., & Mermerdaş, K. (2012). Fresh and hardened characteristics of self-compacting concretes made with combined use of marble powder, limestone filler, and fly ash. *Construction and Building Materials*, 37, 160-170.
- Ghafari, E., Feys, D., & Khayat, K. (2016). Feasibility of using natural SCMs in concrete for infrastructure applications. *Construction and Building Materials*, 127, 724–732.
- Goh, C. C., Show, K. Y., & Cheong, H. K. (2003). Municipal solid waste fly ash as a blended cement material. *Journal of Materials in Civil Engineering*, 15(6), 513-523.
- Goldstone, M. E., Kirk, P. W. W., & Lester, J. N. (1990). The behaviour of heavy metals during wastewater treatment I. Cadmium, chromium and copper. *Science of the Total Environment*, 95, 233-252.
- Gray, D. H., & Penessis, C. (1972). Engineering properties of sludge ash. *Journal (Water Pollution Control Federation)*, 847–858.
- Güneyisi, E., Gesoğlu, M., & Özbay, E. (2009). Effects of marble powder and slag on the properties of self compacting mortars. *Materials and Structures*, 42(6), 813–826.

- Güneysi, E., Gesoğlu, M., Al-Rawi, S., & Mermerdaş, K. (2014). Effect of volcanic pumice powder on the fresh properties of self-compacting concretes with and without silica fume. *Materials and Structures*, 47(11), 1857-1865.
- Gupta, P., Chatterji, S., & Jeffery, J. W. (1970). Studies on the Effect of Various Additives on the Hydration Reaction of Tricalcium Aluminate. *Cement Technology, Part 1*, 1:3-10
- Hall, C. (1977). Water movement in porous building materials—I. Unsaturated flow theory and its applications. *Building and Environment*, 12(2), 117-125
- Halliday, J. E., Jones, M. R., Dyer, T. D., & Dhir, R. K. (2012). Potential use of UK sewage sludge ash in cement-based concrete. *Proceedings of the Institution of Civil Engineers-Waste and Resource Management*, 165(2), 57–66.
- Hamood, A., Khatib, J. M., & Williams, C. (2017). The effectiveness of using Raw Sewage Sludge (RSS) as a water replacement in cement mortar mixes containing Unprocessed Fly Ash (u-FA). *Construction and Building Materials*, 147, 27-34.
- Hemalatha, T., Ramaswamy, A., & Kishen, J. C. (2015). Simplified mixture design for production of self-consolidating concrete. *ACI Materials Journal*, 112(2), 277.
- Hewlett, P., & Liska, M. (2019). *Lea's chemistry of cement and concrete*. Butterworth-Heinemann.
- Ho, D. W. S., Sheinn, A. M. M., Ng, C. C., & Tam, C. T. (2002). The use of quarry dust for SCC applications. *Cement and Concrete Research*, 32(4), 505-511.
- Hollanders, S., Adriaens, R., Skibsted, J., Cizer, Ö., & Elsen, J. (2016). Pozzolanic reactivity of pure calcined clays. *Applied Clay Science*, 132, 552–560.
- Hou, J., Liu, Q., Liu, J., & Wu, Q. (2018). Material properties of steel slag-cement binding materials prepared by precarbonated steel slag. *Journal of Materials in Civil Engineering*, 30(9), 04018208.
- Hu, J., Ge, Z., & Wang, K. (2014). Influence of cement fineness and water-to-cement ratio on mortar early-age heat of hydration and set times. *Construction and Building Materials*, 50, 657–663.
- Huang, S. C., Chang, F. C., Lo, S. L., Lee, M. Y., Wang, C. F., & Lin, J. D. (2007). Production of lightweight aggregates from mining residues, heavy metal sludge, and incinerator fly ash. *Journal of Hazardous Materials*, 144(1-2), 52-58.



- Hwang, C. L., & Hung, M. F. (2005). Durability design and performance of self-consolidating lightweight concrete. *Construction and Building Materials*, 19(8), 619–626.
- Hwang, C., & Tsai, C. T. (2005). The effect of aggregate packing types on engineering properties of self-consolidating concrete. In SCC'2005-China: *1st International Symposium on Design, Performance and Use of Self-Consolidating Concrete* (pp. 337-345). RILEM Publications SARL.
- Ingunza, M. del P. D., Camarini, G., & da Costa, F. M. S. (2018). Performance of mortars with the addition of septic tank sludge ash. *Construction and Building Materials*, 160, 308–315.
- Istuque, D. B., Reig, L., Moraes, J. C. B., Akasaki, J. L., Borrachero, M. V., Soriano, L., & Tashima, M. M. (2016). Behaviour of metakaolin-based geopolymers incorporating sewage sludge ash (SSA). *Materials Letters*, 180, 192-195.
- Jamshidi, M., Jamshidi, A., Mehrdadi, N., & Pacheco-Torgal, F. (2012). Mechanical performance and capillary water absorption of sewage sludge ash concrete (SSAC). *International Journal of Sustainable Engineering*, 5(3), 228-234.
- Jordan, G., Prevette, S., & Woodward, S. (2001). The Performance-Based Management Handbook: Analyzing, Reviewing and Reporting Performance Data. *Training Resources and Data Exchange Performance-Based Management Special Interest Group*. Retrieved from [http://qiroadmap.org/?wpfb\\_dl=19](http://qiroadmap.org/?wpfb_dl=19) (Accessed 11st October, 2018).
- Joseph, A. M., Snellings, R., Van den Heede, P., Matthys, S., & De Belie, N. (2018). The use of municipal solid waste incineration ash in various building materials: A Belgian point of view. *Materials*, 11(1), 141.
- Kapoor, A., & Viraraghavan, T. (1995). Fungal biosorption—an alternative treatment option for heavy metal bearing wastewaters: a review. *Bioresource Technology*, 53(3), 195-206.
- Kappel, A., Ottosen, L. M., & Kirkelund, G. M. (2017). Colour, compressive strength and workability of mortars with an iron rich sewage sludge ash. *Construction and Building Materials*, 157, 1199–1205.
- Karvelas, M., Katsoyiannis, A., & Samara, C. (2003). Occurrence and fate of heavy metals in the wastewater treatment process. *Chemosphere*, 53(10), 1201-1210.
- Katsioti, M., Katsiotis, N., Rouni, G., Bakirtzis, D., & Loizidou, M. (2008). The effect of bentonite/cement mortar for the stabilization/solidification of sewage sludge containing heavy metals. *Cement and Concrete Composites*, 30(10), 1013-1019.

- Khaleel, O. R., & Razak, H. A. (2014). Mix design method for self compacting metakaolin concrete with different properties of coarse aggregate. *Materials & Design*, 53, 691–700.
- Khanbiluardi, R. M. (1994). Ash use from suffolk county wastewater treatment plant. *Sewer, District*, 3.
- Khanbilvardi, R., & Afshari, S. (1995). Sludge ash as fine aggregate for concrete mix. *Journal of Environmental Engineering*, 121(9), 633-638.
- Khatib, J. M. (2008). Performance of self-compacting concrete containing fly ash. *Construction and Building Materials*, 22(9), 1963–1971.
- Khatib, J. M., & Hibbert, J. J. (2005). Selected engineering properties of concrete incorporating slag and metakaolin. *Construction and Building Materials*, 19(6), 460-472.
- Khayat, K. H., Bickley, J., & Lessard, M. (2000). Performance of self-consolidating concrete for casting basement and foundation walls. *Materials Journal*, 97(3), 374–380.
- Kjersgaard, D., Jacobsen, B. N., Rindel, K., Andreasen, L., Larsen, F., Nyegaard, P., Pade, C., & Bodker, J. (2007). The reuse of bio ash for the production of concrete, A Danish case study. *IWA Specialist Conference on Wastewater Biosolids*, 24–27.
- Kosior-Kazberuk, M. (2011). Application of SSA as partial replacement of aggregate in concrete. *Polish Journal of Environmental Studies*, 20(2), 365-370.
- Krejcirikova, B., Ottosen, L. M., Kirkelund, G. M., Rode, C., & Peuhkuri, R. (2019). Characterization of sewage sludge ash and its effect on moisture physics of mortar. *Journal of Building Engineering*, 21, 396-403.
- Kroiss, H., Rechberger, H., & Egle, L. (2011). Phosphorus in water quality and waste management. In *Integrated Waste Management-Volume II* (pp. 181–214). IntechOpen.
- Krüger, O., Grabner, A., & Adam, C. (2014). Complete survey of German sewage sludge ash. *Environmental Science & Technology*, 48(20), 11811-11818.
- Lester, J. N. (1983). Significance and behaviour of heavy metals in waste water treatment processes I. Sewage treatment and effluent discharge. *Science of the Total Environment*, 30, 1-44.
- Li, J., Yin, J., Zhou, S., & Li, Y. (2005). Mix proportion calculation method of self-compacting high performance concrete. *SCC'2005-China: 1st International*

*Symposium on Design, Performance and Use of Self-Consolidating Concrete*, 199–205.

- Lin, C. F., Wu, C. H., & Ho, H. M. (2006). Recovery of municipal waste incineration bottom ash and water treatment sludge to water permeable pavement materials. *Waste Management*, 26(9), 970-978.
- Lin, D. F., & Tsai, M. C. (2006). The effects of nanomaterials on microstructures of sludge ash cement paste. *Journal of the Air & Waste Management Association*, 56(8), 1146-1154.
- Lin, D. F., & Weng, C. H. (2001). Use of sewage sludge ash as brick material. *Journal of Environmental Engineering*, 127(10), 922-927.
- Lin, D. F., Lin, K. L., & Luo, H. L. (2007). A comparison between sludge ash and fly ash on the improvement in soft soil. *Journal of the Air & Waste Management Association*, 57(1), 59-64.
- Lin, K. L., & Lin, C. Y. (2004). Hydration properties of eco-cement pastes from waste sludge ash clinkers. *Journal of the Air & Waste Management Association*, 54(12), 1534-1542.
- Lin, K. L., & Lin, C. Y. (2005). Hydration characteristics of waste sludge ash utilized as raw cement material. *Cement and Concrete Research*, 35(10), 1999-2007.
- Lin, K. L., Chang, W. C., Lin, D. F., Luo, H. L., & Tsai, M. C. (2008). Effects of nano-SiO<sub>2</sub> and different ash particle sizes on sludge ash–cement mortar. *Journal of Environmental Management*, 88(4), 708-714.
- Lin, Y., Zhou, S., Li, F., & Lin, Y. (2012). Utilization of municipal sewage sludge as additives for the production of eco-cement. *Journal of Hazardous Materials*, 213, 457-465.
- Liu, M. (2010). Self-compacting concrete with different levels of pulverized fuel ash. *Construction and Building Materials*, 24(7), 1245-1252.
- Lind, B.B., Norrman, J., Larsson, L.B., Ohlsson, S.-A., & Bristav, H. (2008). Geochemical anomalies from bottom ash in a road construction e comparison of the leaching potential between an ash road and the surroundings. *Waste Management*. 28,170- 180
- Long, G., Gao, Y., & Xie, Y. (2015). Designing more sustainable and greener self-compacting concrete. *Construction and Building Materials*, 84, 301–306.
- Lv, Y., Ye, G., & De Schutter, G. (2019). Investigation on the potential utilization of zeolite as an internal curing agent for autogenous shrinkage mitigation and the effect of modification. *Construction and Building Materials*, 198, 669-676.

- Lynn, C. J., Dhir, R. K., Ghataora, G. S., & West, R. P. (2015). Sewage sludge ash characteristics and potential for use in concrete. *Construction and Building Materials*, 98, 767–779.
- Malherbe, J. S. (2015). *Self-compacting concrete versus normal compacting concrete: A techno-economic analysis*. PhD, Stellenbosch University. Stellenbosch, South Africa.
- Malhotra, V. M., & Mehta, P. K. (2004). *Pozzolanic and cementitious materials*. CRC Press.
- Mamlouk, M. S., & Zaniewski, J. P. (2006). *Materials for civil and construction engineers*. Pearson Prentice Hall Upper Saddle River, NJ.
- Mandanoust, R., & Mousavi, S. (2012). Fresh and Hardened Properties of Self-Compacting Concrete Containing Metakaolin. *Construction and Building Materials*, 35, 752-760.
- Marani, D., Braguglia, C. M., Mininni, G., & Maccioni, F. (2003). Behaviour of Cd, Cr, Mn, Ni, Pb, and Zn in sewage sludge incineration by fluidised bed furnace. *Waste Management*, 23(2), 117-124.
- Marsh, B. (2003). High volume fly ash concrete. *Concrete (London)*, 37(4), 54–55.
- Massazza, F. (1998). Pozzolana and pozzolanic cements. *Lea's Chemistry of Cement and Concrete*, 4, 471-631.
- Mehta, P. K., & Monteiro, P. J. M. (1994). *Concrete: Structures, properties and materials*. São Paulo: Pini, 572.
- Merino, I., Arévalo, L. F., & Romero, F. (2005). Characterization and possible uses of ashes from wastewater treatment plants. *Waste Management*, 25(10), 1046-1054.
- Mindess, S., Young, J. F., & Darwin, D. (2003). *Concrete*. Prentice Hall.
- Misture, S. T., & Snyder, R. L. (2001). Encyclopedia of Materials. *Science and Technology*, 10, 9799-9809.
- Mohammed, A., Sanjayan, J. G., Nazari, A., & Al-Saadi, N. T. (2019). The impact of graphene oxide on cementitious composites. *In Nanotechnology in Eco-efficient Construction* (pp. 69–95). Elsevier.
- Monzó, J., Paya, J., Borrachero, M. V., & Córcoles, A. (1996). Use of sewage sludge ash (SSA)-cement admixtures in mortars. *Cement and Concrete Research*, 26(9), 1389-1398.

- Monzó, J., Payá, J., Borrachero, M. V., & Girbés, I. (2003). Reuse of sewage sludge ashes (SSA) in cement mixtures: the effect of SSA on the workability of cement mortars. *Waste Management*, 23(4), 373-381.
- Monzó, J., Paya, J., Borrachero, M. V., & Peris-Mora, E. (1999). Mechanical behavior of mortars containing sewage sludge ash (SSA) and Portland cements with different tricalcium aluminate content. *Cement and Concrete Research*, 29(1), 87-94.
- Morais, L. C., Dweck, J., Gonçalves, E. M., & Büchler, P. M. (2006). An experimental study of sewage sludge incineration. *Environmental Technology*, 27(9), 1047-1051.
- Nagraj, T. S., & Zahida, B. (1996). Generalization of Abrams' laws. *Cement and Concrete Research*, 26(6), 933-942.
- Naik, T. R., Kumar, R., Ramme, B. W., & Canpolat, F. (2012). Development of high-strength, economical self-consolidating concrete. *Construction and Building Materials*, 30, 463-469.
- Nakic, D. (2018). Environmental evaluation of concrete with sewage sludge ash based on LCA. *Sustainable Production and Consumption*, 16, 193-201.
- Nehdi, M., Pardhan, M., & Koshowski, S. (2004). Durability of self-consolidating concrete incorporating high-volume replacement composite cements. *Cement and Concrete Research*, 34(11), 2103-2112.
- Nepomuceno, M., Oliveira, L., & Lopes, S. M. R. (2012). Methodology for mix design of the mortar phase of self-compacting concrete using different mineral additions in binary blends of powders. *Construction and Building Materials*, 26(1), 317-326.
- Neville, A. M. (1995). *Properties of concrete* (Vol. 4). Longman London. Retrieved from <https://www.scribd.com/document/350943966/Properties-of-Concrete-by-a-m-Neville> (Accessed 20th January, 2020).
- Nielsen, J. S., & Hruday, S. E. (1983). Metal loadings and removal at a municipal activated sludge plant. *Water Research*, 17(9), 1041-1052.
- Nuruddin, M. F., Demie, S., & Shafiq, N. (2011). Effect of mix composition on workability and compressive strength of self-compacting geopolymer concrete. *Canadian Journal of Civil Engineering*, 38(11), 1196-1203.
- O'hara, R., Buchanan, F., & Dunne, N. (2014). Injectable calcium phosphate cements for spinal bone repair. In *Biomaterials for Bone Regeneration* (pp. 26-61). Elsevier.

- Okah, J. C., & Godwin, O. (2016). The Effect of Time on the Workability of Different Fresh Concrete Mixtures in Different Management Conditions. *International Journal of Applied Science and Mathematical Theory*, 2(1), 49-58
- Okamura, H., & Ouchi, M. (2003). Self-compacting concrete. *Journal of Advanced Concrete Technology*, 1(1), 5–15.
- Okamura, H., & Ozawa, K. (1995). Mix design for self-compacting concrete. *Concrete Library of JSCE*, 25(6), 107-120.
- Omran, A., Soliman, N., Zidol, A., & Tagnit-Hamou, A. (2018). Performance of ground-glass pozzolan as a cementitious material—a review. *Advances in Civil Engineering Materials*, 7(1), 237-270.
- Ottosen, L. M., Jensen, P. E., & Kirkelund, G. M. (2014). Electrodialytic separation of phosphorus and heavy metals from two types of sewage sludge ash. *Science and Technology*, 49(12), 1910-1920.
- Ozbay, E., Oztas, A., Baykasoglu, A., & Ozbebek, H. (2009). Investigating mix proportions of high strength self compacting concrete by using Taguchi method. *Construction and Building Materials*, 23(2), 694–702.
- Pan, S.C., Tseng, D.H., & Lee, C. (2002). Use of sewage sludge ash as fine aggregate. *Journal of Solid Waste Technology and Management*, 28(3), 121-130.
- Pan, S.-C., Tseng, D.-H., Lee, C.-C., & Lee, C. (2003). Influence of the fineness of sewage sludge ash on the mortar properties. *Cement and Concrete Research*, 33(11), 1749–1754.
- Papadimitriou, C. A., Haritou, I., Samaras, P., & Zouboulis, A. I. (2008). Evaluation of leaching and ecotoxicological properties of sewage sludge–fly ash mixtures. *Environmental Research*, 106(3), 340-348.
- Paris, J. M., Roessler, J. G., Ferraro, C. C., DeFord, H. D., & Townsend, T. G. (2016). A review of waste products utilized as supplements to Portland cement in concrete. *Journal of Cleaner Production*, 121, 1–18.
- Parra, C., Valcuende, M., & Gómez, F. (2011). Splitting tensile strength and modulus of elasticity of self-compacting concrete. *Construction and Building Materials*, 25(1), 201–207.
- Payá, J., Monzó, J., Borrachero, M. V., Amahjour, F., Girbés, I., Velázquez, S., & Ordóñez, L. M. (2002). Advantages in the use of fly ashes in cements containing pozzolanic combustion residues: silica fume, sewage sludge ash, spent fluidized bed catalyst and rice husk ash. *Environmental & Clean Technology*, 77(3), 331-335.

- Pekmezci, B.Y., & Akyüz, S. (2004). Optimum usage of a natural pozzolan for the maximum compressive strength of concrete. *Cement and Concrete Research*, 34(12), 2175-2179.
- Pelisser, F., Vieira, A., & Bernardin, A. M. (2018). Efficient self-compacting concrete with low cement consumption. *Journal of Cleaner Production*, 175, 324-332.
- Petersson, O., Billberg, P., & Van, B. K. (2004). A model for self-compacting concrete. *In Production methods and workability of concrete* (pp. 495–504). CRC Press.
- Pinarli, V. (2000). Sustainable Waste Management-Studies on the use of sewage sludge ash in the construction industry as concrete material. *In Sustainable Construction: Use of Incinerator Ash* (pp. 415–425). Thomas Telford Publishing.
- Pinarli, V., & Kaymal, G. (1994). An innovative sludge disposal option-reuse of sludge ash by incorporation in construction materials. *Environmental technology*, 15(9), 843-852.
- Pittman, D. W., & Ragan, S. A. (1998). Drying shrinkage of roller-compacted concrete for pavement applications. *Materials Journal*, 95(1), 19-26.
- Prajapati, J., & Karanjit, S. (2019). Effect of Coarse Aggregate Sources on the Compressive Strength of Various Grade of Nominal Mixed Concrete. *Journal of Science and Engineering*, 7, 52-60.
- Rahman, M. A., Sarker, P. K., Shaikh, F. U. A., & Saha, A. K. (2017). Soundness and compressive strength of Portland cement blended with ground granulated ferronickel slag. *Construction and Building Materials*, 140, 194-202.
- Rajeshkumar, S., Bharath, L. V., & Geetha, R. (2019). Broad spectrum antibacterial silver nanoparticle green synthesis: Characterization, and mechanism of action. *In Green synthesis, characterization and applications of nanoparticles* (pp. 429–444). Elsevier.
- Ramachandran, V. S. (1996). *Concrete admixtures handbook: Properties, science and technology*. William Andrew.
- Ramezaniapour, A. A., & Tarighat, A. (2001). Neural Network Modeling of Concrete Carbonation. *Special Publication*, 199, 899-916.
- Ranjbar, M. M., Madandoust, R., Mousavi, S. Y., & Yosefi, S. (2013). Effects of natural zeolite on the fresh and hardened properties of self-compacted concrete. *Construction and Building Materials*, 47, 806-813.

- Ravina, D (1980). Optimized determination of PFA (fly ash) fineness with reference to pozzolanic activity. *Cement and Concrete Research*, 10(4), 573-580.
- Rissanen, J., Ohenoja, K., Kinnunen, P., & Illikainen, M. (2017). Partial replacement of Portland-composite cement by fluidized bed combustion fly ash. *Journal of Materials in Civil Engineering*, 29(8), 401-706.
- Rodríguez, N. H., Martínez-Ramírez, S., Blanco-Varela, M. T., Donatello, S., Guillem, M., Puig, J., & Flores, J. (2013). The effect of using thermally dried sewage sludge as an alternative fuel on Portland cement clinker production. *Journal of Cleaner Production*, 52, 94-102.
- Saak, A. W., Jennings, H. M., & Shah, S. P. (2001). New methodology for designing self-compacting concrete. *Materials Journal*, 98(6), 429–439.
- Sadek, D. M., Amin, S. K., & Youssef, N. F. (2014). Blended cement utilizing ceramic wall tiles waste. *Construction Materials and Structures*, 152–161. <https://doi.org/10.3233/978-1-61499-466-4-152>
- Şahmaran, M., Yaman, İ. Ö., & Tokyay, M. (2009). Transport and mechanical properties of self consolidating concrete with high volume fly ash. *Cement and Concrete Composites*, 31(2), 99–106.
- Scrivener, K., Martirena, F., Bishnoi, S., & Maity, S. (2018). Calcined clay limestone cements (LC3). *Cement and Concrete Research*, 114, 49-56.
- Sedran, T., & De Larrard, F. (1999). Optimization of self-compacting concrete thanks to packing model. *Proceedings 1st SCC Symp, CBI Sweden, RILEM PRO7*, 321–332.
- Seraj, S., Ferron, R. D., & Juenger, M. C. (2016). Calcining natural zeolites to improve their effect on cementitious mixture workability. *Cement and Concrete Research*, 85, 102–110.
- Sfikas, I. P., Badogiannis, E. G., & Trezos, K. G. (2014). Rheology and Mechanical Characteristics of Self-Compacting Concrete Mixtures Containing Metakaolin. *Construction and Building Materials*, 64, 121-129.
- Shahrin, R., & Bobko, C. P. (2017). Characterizing strength and failure of calcium silicate hydrate aggregates in cement paste under micropillar compression. *Journal of Nanomechanics and Micromechanics*, 7(4), 601-7002.
- Shahroodi, A. (2010). *Development of test methods for assessment of concrete durability for use in performance-based specifications*. PhD, University of Toronto. Toronto, Canada.



- Sheen, Y.-N., Le, D. H., & Sun, T. H. (2015). Greener Self-Compacting Concrete Using Stainless Steel Reducing Slag. *Construction and Building Materials*, 82, 341-350.
- Shi, C., Wu, Z., Lv, K., & Wu, L. (2015). A review on mixture design methods for self-compacting concrete. *Construction and Building Materials*, 84, 387–398.
- Shi, H.-S., & Kan, L.-L. (2009). Leaching behavior of heavy metals from municipal solid wastes incineration (MSWI) fly ash used in concrete. *Journal of Hazardous Materials*, 164(2–3), 750–754.
- Shirodkar, P., Sonpal, K., Norton, A., Weaver, R., Tomlinson, C., Nolan, A., & Jahan, K. (2011). Evaluation of fatigue and rutting performance of sewage sludge ash (SSA) in asphalt Concrete. *The Journal of Solid Waste Technology and Management*, 37(1), 55-60.
- Siddique, R. & Kunal. (2015). Design and development of self-compacting concrete made with coal bottom ash. *Journal of Sustainable Cement-Based Materials*, 4(3–4), 225–237.
- Singh, B., Kumar, R., & Asati, A. K. (2018). Influence of parameters on performance of earth air heat exchanger in hot-dry climate. *Journal of Mechanical Science and Technology*, 32(11), 5457-5463
- Smol, M., Kulczycka, J., Henclik, A., Gorazda, K., & Wzorek, Z. (2015). The possible use of sewage sludge ash (SSA) in the construction industry as a way towards a circular economy. *Journal of Cleaner Production*, 95, 45–54.
- Snellings, R., Horckmans, L., Van Bunderen, C., Vandewalle, L., & Cizer, Ö. (2017). Flash-calcined dredging sediment blended cements: effect on cement hydration and properties. *Materials and Structures*, 50(6), 241-244.
- Solis, G. J., Alonso, E., & Riesco, P. (2002). Distribution of metal extractable fractions during anaerobic sludge treatment in southern Spain WWTPs. *Water, Air, and Soil Pollution*, 140(1-4), 139-156.
- Sonebi, M. (2004). Medium strength self-compacting concrete containing fly ash: Modelling using factorial experimental plans. *Cement and Concrete Research*, 34(7), 1199–1208.
- Stones, T. (1977). A Study on the Loading and Performance of Sewage Treatment Plants. *Effluent and Water Treatment Journal*, 17(7).
- Stumm, W. (1992). Chemistry of the solid-water interface: *Processes at the mineral-water and particle-water interface in natural systems*. John Wiley & Son Inc.

- Su, N., Hsu, K. C., & Chai, H. W. (2001). A simple mix design method for self-compacting concrete. *Cement and Concrete Research*, 31(12), 1799–1807.
- Sukumar, B., Nagamani, K., & Raghavan, R. S. (2008). Evaluation of strength at early ages of self-compacting concrete with high volume fly ash. *Construction and Building Materials*, 22(7), 1394-1401.
- Taha, S. T. S. (2016). *Using Ceramic Waste Powder in Producing Self-Compacting Concrete*. PhD, The UAE University, Al-Ain, UAE.
- Tay, J. H. (1987). Sludge ash as filler for Portland cement concrete. *Journal of Environmental Engineering*, 113(2), 345-351.
- Tay, J. H., & Show, K. Y. (1994). Municipal wastewater sludge as cementitious and blended cement materials. *Cement and Concrete Composites*, 16(1), 39-48.
- Tay, J. H., & Yip, W. K. (1989). Sludge ash as lightweight concrete material. *Journal of Environmental Engineering*, 115(1), 56-64.
- Tay, J. H., Yip, W. K., & Show, K. Y. (1991). Clay-blended sludge as lightweight aggregate concrete material. *Journal of Environmental Engineering*, 117(6), 834-844.
- Taylor-Lange, S. C., Lamon, E. L., Riding, K. A., & Juenger, M. C. (2015). Calcined kaolinite–bentonite clay blends as supplementary cementitious materials. *Applied Clay Science*, 108, 84–93.
- Tchobanoglous, G., Burton, F. L., & Stensel, H. D. (1991). *Wastewater engineering. Management*, 7(1), 4.
- Tenza-Abril, A. J., Saval, J. M., & Cuenca, A. (2015). Using sewage-sludge ash as filler in bituminous mixes. *Journal of Materials in Civil Engineering*, 27(4), 401-414.
- Torgal, F. P., & Castro-Gomes, J. P. (2006). Influence of physical and geometrical properties of granite and limestone aggregates on the durability of a C20/25 strength class concrete. *Construction and Building Materials*, 20(10), 1079-1088.
- Toumi, A., Nejmeddine, A., & Belkoura, M. (2003). The fate of heavy metals (Zn, Cu, Pb, Cd and Cr) in an integrated wastewater treatment plant: Two phase anaerobic reactor (RAP)-high rate algal pond (HRAP). *Environmental Technology*, 24(2), 153-159.
- Tsai, C. C., Wang, K. S., & Chiou, J. (2006). Effect of SiO<sub>2</sub>–Al<sub>2</sub>O<sub>3</sub>–flux ratio change on the bloating characteristics of lightweight aggregate material produced from recycled sewage sludge. *Journal of Hazardous Materials*, 134(1-3), 87-93.

- Tseng, D. H., Pan, S. C., & Lee, C. (2000). Enhancement of pozzolanic activity and morphology of sewage sludge ash by calcination. *Journal of the Chinese Institute of Environmental Engineering*, 10(4), 261-270.
- Tuan, B. L. A., Hwang, C. L., Lin, K. L., Chen, Y. Y., & Young, M. P. (2013). Development of lightweight aggregate from sewage sludge and waste glass powder for concrete. *Construction and Building Materials*, 47, 334-339.
- Tyagi, R. D., & Couillard, D. (1987). Bacterial leaching of metals from digested sewage sludge. *Process Biochemistry*, 22(4), 114-117.
- Uyarra, E., & Gee, S. (2013). Transforming urban waste into sustainable material and energy usage: The case of Greater Manchester (UK). *Journal of Cleaner Production*, 50, 101-110.
- Uysal, M., & Sumer, M. (2011). Performance of self-compacting concrete containing different mineral admixtures. *Construction and Building Materials*, 25(11), 4112-4120.
- Uysal, M., & Yilmaz, K. (2011). Effect of mineral admixtures on properties of self-compacting concrete. *Cement and Concrete Composites*, 33(7), 771-776.
- Wang, F., Kovler, K., Provis, J. L., Buchwald, A., Cyr, M., Patapy, C., Kamali-Bernard, S., Courard, L., & Sideris, K. (2018). Metakaolin. In *Properties of Fresh and Hardened Concrete Containing Supplementary Cementitious Materials* (pp. 153-179). Springer.
- Wang, K. S., Tseng, C. J., Chiou, J., & Shih, M. H. (2005). The thermal conductivity mechanism of sewage sludge ash lightweight materials. *Cement and Concrete Research*, 35(4), 803-809.
- Wang, X., Jin, Y., Wang, Z., Mahar, R. B., & Nie, Y. (2008). A research on sintering characteristics and mechanisms of dried sewage sludge. *Journal of Hazardous Materials*, 160(2-3), 489-494.
- Wegman, D. E., & Young, D. S. (1988). Testing and evaluating sewage sludge ash in asphalt paving mixtures. *67th Annual Transportation Research Board Meeting, Washington, DC*, 23.
- Wu, J., Yang, Y. S., & Lin, J. (2005). Advanced tertiary treatment of municipal wastewater using raw and modified diatomite. *Journal of Hazardous Materials*, 127(1-3), 196-203.
- Wu, Q., & An, X. (2014). Development of a mix design method for SCC based on the rheological characteristics of paste. *Construction and Building Materials*, 53, 642-651.

- Wu, Z., Zhang, Y., Zheng, J., & Ding, Y. (2009). An experimental study on the workability of self-compacting lightweight concrete. *Construction and Building Materials*, 23(5), 2087–2092.
- Xie, Y., Liu, B., Yin, J., & Zhou, S. (2002). Optimum mix parameters of high-strength self-compacting concrete with ultrapulverized fly ash. *Cement and Concrete Research*, 32(3), 477-480.
- Xu, G. R., Zou, J. L., & Li, G. B. (2008). Effect of sintering temperature on the characteristics of sludge ceramsite. *Journal of Hazardous Materials*, 150(2), 394-400.
- Yip, W. K., & Tay, J. H. (1990). Aggregate made from incinerated sludge residue. *Journal of Materials in Civil Engineering*, 2(2), 84-93.
- Yusuf, R. O., Noor, Z. Z., Din, M. D. F. M. D., & Abba, A. H. (2012). Use of sewage sludge ash (SSA) in the production of cement and concrete—a review. *International Journal of Global Environmental Issues*, 12(2-4), 214- 228.
- Zhou, H.-B., Liu, Y.-L., Jin, S., Zhang, Y., Luo, G.-N., & Lu, G.-H. (2010). Investigating behaviours of hydrogen in a tungsten grain boundary by first principles: From dissolution and diffusion to a trapping mechanism. *Nuclear Fusion*, 50(2), 025016.

## List of Publications

1. S. Al Shanti, A.S. El-Dieb, M.A. Maraqa, “*Potential Reuse of Sewage Sludge Ash in the Production of Self-Compacted Concrete*”, Accepted in the 6th International Conference on Construction Materials (ConMat’20), Fukuoka International Congress Center, Fukuoka, Japan, 27-29 August. 2020. <https://core.ac.uk/download/pdf/185486959.pdf>
2. S. Al Shanti, A.S. El-Dieb, M.A. Maraqa, “*Characterization of Sewage Sludge Ash as affected by different Temperature and Time*”, Accepted in the 5th International Conference on Sustainable Construction Materials and Technologies (SCMT5), Kingston University, London, UK , 14-17 July 2019, DOI: 10.18552/2019/IDSCMT5183

